# Fakultät für Physik und Astronomie

## Ruprecht-Karls-Universität Heidelberg

Diplomarbeit

Im Studiengang Physik

vorgelegt von

Dominik Scala

geboren in Bochum

2013

# Radiative Symmetriebrechung

# in Links-Rechts Symmetrischen Modellen

# mit einer Shiftsymmetrie an der Planckskala

Die Diplomarbeit wurde von Dominik Scala

ausgeführt am

Max-Planck-Institut für Kernphysik in Heidelberg

unter der Betreuung von

Herrn Prof. Dr. Manfred Lindner

# Department of Physics and Astronomy

## University of Heidelberg

Diploma thesis

in Physics

submitted by

Dominik Scala

born in Bochum

2013

# Radiative Symmetry Breaking

# in Left-Right Symmetric Models

# with a Shift Symmetry at the Planck Scale

This diploma thesis has been carried out by Dominik Scala

at the

Max-Planck-Institut für Kernphysik in Heidelberg

under the supervision of

Herrn Prof. Dr. Manfred Lindner

**Radiative Symmetriebrechung in Links-Rechts-Symmetrischen Modellen mit einer Shiftsymmetrie an der Planckskala:**

Unter der Annahme, dass das Standard Modell bis zur Planckskala $\Lambda_{Pl} \sim 10^{19}$ GeV gültig ist, zeigt die Higgs Selbstkopplung einen Wert, der nahe $\Lambda_{Pl}$ erstaunlich klein ist. Es ist verlockend anzunehmen, dass dies von der einbettenden Theorie der Gravitation erzwungen wird. In einem stringtheoretischen Kontext wurde diese Beobachtung kürzlich interpretiert als die Invarianz des Skalarpotentials an der Planckskala unter konstanter Verschiebung des Higgsfeldes.

Im Allgemeinen sind solche Randwertbedingungen von besonderem Interesse für die Untersuchung von radiativer Symmetriebrechung in Modellen mit klassischer konformer Invarianz, denn die Planckskala ist mit der Brechungsskala über das Laufen der Skalarkopplungen verbunden.

In dieser Arbeit wird die Coleman-Weinberg Symmetriebrechung im links-rechts-symmetrischen Modell diskutiert bei Anwesenheit einer solchen *Shift-Symmetry*, die für den besonderen Fall der Links-Rechts-Symmetrie verallgemeinert ist. Im reduzierten Parameterraum gelingt es, eine große Hierarchie zwischen der Planckskala und der Links-Rechts-Brechungsskala zu generieren. Um auch die elektroschwache Skala zu stabilisieren, wird das Modell um zwei Fermionen erweitert, die zum Laufen der Skalarkopplungen beitragen.

**Radiative Symmetry Breaking of Left-Right Symmetric Models with a Shift Symmetry at the Planck Scale:**

Under the assumption that the Standard Model is valid up to the Planck scale $\Lambda_{Pl} \sim 10^{19}$ GeV, the quartic Higgs coupling exhibits near $\Lambda_{Pl}$ a value remarkably close to zero. It is tempting to consider this feature as a manifestation of boundary conditions imposed by the embedding theory of gravity. In a stringy context this observation has recently been interpreted in terms of the scalar potential being invariant under a constant shift of the Higgs field at the Planck scale.

In general, such boundary conditions are of special interest in the study of radiatively induced symmetry breaking in models with classical conformal invariance, as the Planck scale is connected to the breaking scale via the running of the scalar couplings.

In this thesis, the Coleman-Weinberg symmetry breaking of the minimal classically conformally invariant left-right (LR) symmetric model is reconsidered in the presence of a shift symmetry which is generalized to the case of the LR symmetry. Within the restricted parameter space imposed by the shift symmetry, a large hierarchy between the LR breaking scale and the Planck scale can be generated. In order to stabalize the electroweak-scale as well, the model is extended by two fermionic representations, which contribute to the running of the scalar couplings.

# Contents

*Contents*

# Chapter 1

# Introduction

For many years the Standard Model (SM) of particle physics has been in perfect agreement with experimental observations. With the recent discovery of a $\sim 125\,\text{GeV}$ Higgs boson [1, 2], even the last fundamental particle predicted by the SM seems to be found. At the same time, however, neutrino oscillations[1] represent the most striking hint to new physics beyond the SM. In contradiction to the SM prediction, neutrinos are massive. Thus, the SM needs to be extended. While there are many non-minimal proposals to obtain neutrino masses (see *e.g.* Ref. [4]), the most famous approach is the introduction of right-handed (sterile) neutrinos to the SM [5].

Besides experimental requirements, also from a theoretical perspective, an alternative to the SM is desirable due to its inherent problems of naturalness. One of the most severe is the so-called hierarchy problem. It states that, in the process of renormalization, the quadratically divergent corrections to the Higgs mass term have to be canceled to unnaturally high precision in order to explain the smallness of the Higgs mass. A solution to the hierarchy problem has been proposed by Bardeen.[2] He argued that in the classically conformal limit of the SM,[3] these divergences would turn out to be unphysical. For this argument to be applicable, no intermediate theory is allowed up to the embedding at the Planck scale,

$$\Lambda_{\text{Pl}} \sim 1.22 \cdot 10^{19}\,\text{GeV}. \qquad (1.1)$$

For the SM, classical conformal invariance has however been excluded, since it predicts a too low Higgs mass (for a review see [7]). Motivated by the work of Nicolai and Meissner [8–10], who showed that classical conformal symmetry might be entailed

---

[1]See the Particle Data Group review [3].
[2]See Ref. [6] and references therein.
[3]This corresponds to scale-invariance, thus to a vanishing Higgs mass term $\mu^2 \phi^2 \subset \mathcal{L}$.

by the embedding theory including gravity, Holthausen et al. [6] considered classical conformal invariance in the minimal left-right (LR) symmetric model [11–13]. The LR symmetric model extends the SM gauge group to

$$SU(3)_C \times SU(2)_L \times SU(2)_R \times U(1)_{B-L}. \tag{1.2}$$

The LR symmetric model is attractive from a theoretical point of view as it restores parity to be a symmetry of nature. Furthermore, by generalization of the Gell-Mann Nishijima relation, in the LR symmetric model the generator of the $U(1)$ can be expressed by the difference of baryon and lepton numbers, which within the SM are conserved quantities at the classical level. With regard to neutrino masses, it naturally provides the introduction of right-handed neutrinos which in the minimal model allows for Dirac mass terms via the Higgs mechanism.[4]

As the gauge sector of the model is enlarged with respect to the SM, spontaneous symmetry breaking has to be performed minimally in two steps. Using the approximate analytical method by Gildener and Weinberg (GW) [15], which generalizes the Coleman-Weinberg breaking mechanism [16], Holthausen et al. showed that the minimal LR symmetry can successfully be broken by radiative corrections. They found that in a large fraction of parameter space the right-handed scale $v_R$ could be stabilized at $v_R =$ against $\Lambda_{\text{Pl}}$.[5] The separation of these scales has been called *big hierachy*. However, in order to stabilize the electroweak scale against $v_R$, which is referred to as the *little hierarchy*, a certain amount of fine-tuning was needed. This fine-tuning problem is adressed in the present thesis.

In the framework of the GW-method, the radiative symmetry breaking is triggered by the running of the scalar couplings. Since, in a given model, the running is fixed by initial conditions, the symmetry breaking scenario is completely determined by the choice of these conditions. Thus, the fine-tuning problem can be transfered to the question of conditions imposed on the values of the scalar couplings at $\Lambda_{\text{Pl}}$.

Assuming that the SM is valid up to the Planck scale, the observed Higgs mass corresponds to a quartic coupling $\lambda$ which is remarkably close to zero at the Planck

---

[4]The *minimal model* refers to a scalar sector containing one bidoublet, as well as right- and left-handed doublets. Note, however, that since it has been noticed that the model containing triplets instead of doublets allows for neutrino Majorana masses, this triplet model is often referred to as the minimal model (for a review see [14]), although it contains more degrees of freedom.

[5]Current limits on the right-handed scale suggest that $v_R$ has to be at least in the multi-TeV regime [17–20]. Throughout this diploma-thesis, it will assumed that $v_R = 10\,\text{TeV}$. However, the results will not depend much on this particular choice.
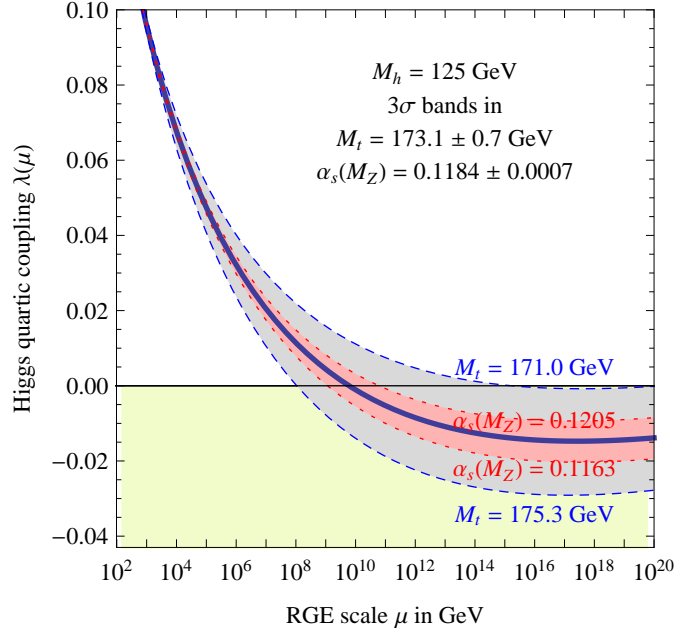
Figure 1.1: The renormalization group running of the SM Higgs quartic coupling with $m_h = 125\,\mathrm{GeV}$ at two-loop order [21]. Under the assumption that the SM is valid up to the Planck scale $\Lambda_{\mathrm{Pl}}$, the observed Higgs mass predicts a quartic coupling $\lambda$ which is very close to zero at $\mu = \Lambda_{\mathrm{Pl}}$. This might be considered as a consequence of boundary conditions imposed by the embedding theory including gravity.

scale (see figure 1.1).[6] It is tempting to consider this to be non-accidental, but instead to be imposed by Planck scale physics. In a string theoretical context, the observation $\lambda(\Lambda_{\mathrm{Pl}}) \approx 0$ has recently been interpreted as the manifestation of a *shift symmetry* [24] which, at the Planck scale, leaves the scalar potential invariant under a constant shift of the Higgs field,

$$\phi \to \phi + \alpha. \tag{1.3}$$

Here, this assumption will be generalized to the context of the LR symmetric model. As in the minimal LR symmetric model, the role of the SM Higgs is played by a bidoublet field $\Phi$, the shift symmetry will be defined with respect to $\Phi$, rather than to the left-handed doublet. This will drastically reduce the allowed parameter space of possible initial conditions for the scalar couplings at $\Lambda_{\mathrm{Pl}}$ to the two dimensional

---

[6]The presumable introduction of three heavy right-handed neutrinos might modify the running of $\lambda$ and change this picture [22, 23].

subspace of doublet self-couplings. The remaining couplings, namely the bidoublet self-couplings as well as the intermediate doublet-bidoublet couplings are then purely generated by quantum corrections being not present at the Planck scale.

The outline of this thesis is as follows. In chapter 2, the GW-method in the minimal LR symmetric model will be reviewed. Subsequently, in chapter 3 the shift symmetry is introduced and it is analyzed, if within the reduced parameter space the desired symmetry breaking pattern, given by the big and little hierachies, can be obtained. In chapters 4 and 5, the minimal model is extended by additional fermionic representations. As these couple to the scalar sector by Yukawa type interactions, the running of the scalar couplings is modified and thus the process of symmetry breaking affected. In particular, it is studied if the presence of these representations leads to a stabilization of the little hierarchy. For this purpose, the contributions to the beta-functions of the model are calculated. All numerical calculations are performed with the computational software program Mathematica.

# Chapter 2

# Radiative Breaking of the Minimal Scale Invariant LR Symmetric Model

## 2.1 The Minimal Scale Invariant Left-Right Symmetric Model

### 2.1.1 Fermionic Representations

The Left-Right (LR) Symmetric Model [11–13], including parity, is based on the gauge group

$$SU(3)_C \times SU(2)_L \times SU(2)_R \times U(1)_{B-L} \times P, \qquad (2.1)$$

which extends the Standard Model of particle physics (SM) by the additional subgroup $SU(2)_R$. [1] It represents the minimal extension of the SM that allows for parity being a symmetry of nature. While the SM is a chiral gauge theory, organizing left- and right-handed fermions as

$$Q_L^i = \begin{pmatrix} u_L^i \\ d_L \end{pmatrix}, \quad L_L = \begin{pmatrix} \nu_L^i \\ e_{L,} \end{pmatrix}, \quad u_R, \quad d_R, \quad e_R^i \qquad (2.2)$$

the LR symmetric model treats left- and right-handed (fermion) representations in a completely symmetric way. The left-handed fields are associated to the fundamental representation of the $SU(2)_L$

$$Q_L^i = \begin{pmatrix} u_L^i \\ d_L^i \end{pmatrix} : [(\tfrac{\mathbf{1}}{\mathbf{2}}, \mathbf{0})](\mathbf{3}, \mathbf{2}, \mathbf{1}, \tfrac{1}{3}), \quad L_L^i \begin{pmatrix} \nu_L^i \\ e_L^i \end{pmatrix} : \quad [(\tfrac{\mathbf{1}}{\mathbf{2}}, \mathbf{0})](\mathbf{1}, \mathbf{2}, \mathbf{1}, -\mathbf{1}) \qquad (2.3)$$

---

[1]The corresponding gauge couplings are as usual denoted by $g_3$, $g_2$ and $g_1$.

while the right-handed fermions are represented by $SU(2)_R$ doublets

$$Q_R^i = \begin{pmatrix} u_R^i \\ d_R^i \end{pmatrix} : [(\mathbf{0}, \tfrac{\mathbf{1}}{\mathbf{2}})](\mathbf{3}, \mathbf{1}, \mathbf{2}, \tfrac{1}{3}), \quad L_R^i \begin{pmatrix} \nu_R^i \\ e_R^i \end{pmatrix} : \quad [(\mathbf{0}, \tfrac{\mathbf{1}}{\mathbf{2}})](\mathbf{1}, \mathbf{1}, \mathbf{2}, -1) \tag{2.4}$$

Here, the representations are denoted in the usual way according to the complete symmetry group, including the Lorentz group,

$$[\text{Spin}(1,3)] \times (SU(3)_C \times SU(2)_L \times SU(2)_R \times U(1)_{B-L}). \tag{2.5}$$

This requires the (natural) introduction of right-handed neutrinos to theory, which are not present in the standard picture of the SM.

In Ref. [6], the isomorphism $SU(2) \times SU(2) \simeq \text{Spin}(4)$ was used to express the $SU(2)_L \times SU(2)_R$ representations in a more compact way. For computational simplicity and for consistency, this notation will be adopted here. While the main features are presented here briefly, for a more detailed treatment the reader is referred to references [6] and [25]. Noticing that the $\text{Spin}(4)$ is the double covering group of the $SO(4)$ one can use the familiar $SO(4)$ spinor representations in order to merge the above doublets into four-component multiplets, $\underline{Q}$ and $\underline{L}$, which are given by

$$\underline{Q}^i = \begin{pmatrix} Q_L^i \\ -iQ_R^i \end{pmatrix} : [(\tfrac{\mathbf{1}}{\mathbf{2}}, \mathbf{0})(\mathbf{2}, \mathbf{1}) \oplus (\mathbf{0}, \tfrac{\mathbf{1}}{\mathbf{2}})(\mathbf{1}, \mathbf{2})](\mathbf{3}, \tfrac{1}{3}), \tag{2.6}$$

$$\underline{L}^i = \begin{pmatrix} L_L^i \\ -iL_R^i \end{pmatrix} : [(\tfrac{\mathbf{1}}{\mathbf{2}}, \mathbf{0})(\mathbf{2}, \mathbf{1}) \oplus (\mathbf{0}, \tfrac{\mathbf{1}}{\mathbf{2}})(\mathbf{1}, \mathbf{2})](\mathbf{1}, -1). \tag{2.7}$$

with the representations denoted by

$$\text{Spin}(1,3) \times (SU(2)_L \times SU(2)_R) \times (SU(3)_C \times U(1)_{B-L}). \tag{2.8}$$

To gain the transformation properties of these $SO(4)$ representations, one introduces, in complete analogy to the Lorentz group, a set of gamma matrices $\Gamma_{ab}^A$ which satisfy the Clifford algebra

$$\{\Gamma^A, \Gamma^B\} = 2\delta^{AB}. \tag{2.9}$$

The generators $\Sigma^{AB}$ of the $SO(4)$ are then given by the commutators

$$\Sigma^{AB} = \frac{1}{4} \left[ \Gamma^A, \Gamma^B \right] \tag{2.10}$$

and one has

$$\underline{Q}^i \rightarrow S(A)\underline{Q}^i \quad \text{and} \quad \underline{L}^i \rightarrow S(A)\underline{L}^i \tag{2.11}$$

with

$$S(A) := \exp\left(\frac{1}{2}\alpha_{AB}\Sigma^{AB}\right), \tag{2.12}$$

while the transformation properties with respect to the $SU(3)_C \times U(1)_{B-L}$ remain as in the standard notation (for a good review see *e.g.* [14]). Note that, in order to make the notation clear, the $\Gamma^A$ are indicated by latin capitals and their components by small letters while the usual $\gamma^\mu$ are indicated by greek letters. In Ref. [6], for the gamma matrices $\Gamma^A$ it is used the hermitian representation

$$\Gamma^A = \begin{pmatrix} 0 & \sigma^A \\ \bar{\sigma}^A & 0 \end{pmatrix}, \tag{2.13}$$

where $\sigma^A = (\vec{\sigma}, \mathrm{i}\mathbb{1})$, $\bar{\sigma}^A = (\vec{\sigma}, -\mathrm{i}\mathbb{1})$ and the $\vec{\sigma} = (\sigma_1, \sigma_2, \sigma_3)$ represent the Pauli matrices. In this basis the chirality operator is given by

$$\Gamma = \Gamma^1\Gamma^2\Gamma^3\Gamma^4 = \begin{pmatrix} 1 & 0 \\ 0 & -1 \end{pmatrix} \tag{2.14}$$

and one defines the projection operators

$$\mathbb{P}_L = \frac{1 + \Gamma}{2} = \begin{pmatrix} 1 & 0 \\ 0 & 0 \end{pmatrix} \quad \text{and} \quad \mathbb{P}_L = \frac{1 - \Gamma}{2} = \begin{pmatrix} 0 & 0 \\ 0 & 1 \end{pmatrix}, \tag{2.15}$$

which project the spinors (2.11) to the left- and right-handed doublets, (2.3) and (2.4), respectively. Furthermore, using the $SO(4)$ notation, the parity transformation which interchanges right- and left-handed fields,

$$Q^i_L \leftrightarrow Q^i_R, \quad L^i_L \leftrightarrow L^i_R, \tag{2.16}$$

is given by

$$\mathbb{P}: \quad \underline{Q} \to \Gamma^4 \underline{Q}, \quad \underline{L} \to \Gamma^4 \underline{L}. \tag{2.17}$$

The section is concluded giving the covariant derivatives for the spinor representations.

For the quarks one has

$$D_{\underline{\mu}}^Q = \partial_\mu + \mathrm{i}\frac{1}{2} g_1 B_\mu (B-L) + \frac{1}{2}\frac{g_2}{\sqrt{2}} W_\mu^{AB} \Sigma^{AB} + \mathrm{i}\frac{g_3}{2} G_\mu^m \lambda^m, \tag{2.18}$$

and for the leptons

$$D_{\underline{\mu}}^L = \partial_\mu + \mathrm{i}\frac{1}{2} g_1 B_\mu (B-L) + \frac{1}{2}\frac{g_2}{\sqrt{2}} W_\mu^{AB} \Sigma^{AB}, \tag{2.19}$$

where in **(??)** the $\lambda_m$ represent the Gell-Mann matrices and the $B_\mu$, $W_\mu^{AB}$ and $G_\mu^m$ are the gauge bosons of the left-right symmetric model. The generator of the $U(1)$,

$$B - L = \begin{cases} \frac{1}{3} & \text{for quarks} \\ -1 & \text{for leptons} \end{cases}, \tag{2.20}$$

is the difference of baryon and lepton numbers and thus, in contrast to the SM, given by physical quantities.

## 2.1.2 Scalar Sector and Potential

The scalar sector of the minimal model contains the right- and left-handed doublets

$$\chi_L = \begin{pmatrix} \chi_L^0 \\ \chi_L^- \end{pmatrix} : [(\mathbf{0},\mathbf{0})](\mathbf{1},\mathbf{2},\mathbf{1},-1), \quad \chi_R = \begin{pmatrix} \chi_R^0 \\ \chi_R^- \end{pmatrix} : [(\mathbf{0},\mathbf{0})](\mathbf{1},\mathbf{1},\mathbf{2},-1), \tag{2.21}$$

as well as a bidoublet representation

$$\Phi = \frac{1}{\sqrt{2}} \begin{pmatrix} \phi_1^0 & \phi_1^+ \\ \phi_1^- & \phi_2^0 \end{pmatrix} : [(\mathbf{0},\mathbf{0})](\mathbf{1},\mathbf{2},\mathbf{2},0). \tag{2.22}$$

With this scalar content, as in the SM, the double purpose of giving masses to both gauge bosons and fermions by means of spontaneous symmetry breaking is served.

For the latter, the fermions are coupled to the bidoublet via the Yukawa couplings

$$\mathcal{L}_{\text{Yuk}} = -Y_Q^{+ij}\bar{Q}_{Li}\Phi Q_{Rj} - Y_Q^{-ij}\bar{Q}_{Li}\tilde{\Phi}Q_{Rj}$$
$$-Y_L^{+ij}\bar{L}_{Li}\Phi L_{Rj} - Y_L^{-ij}\bar{L}_{Li}\tilde{\Phi}L_{Rj} + H.c., \tag{2.23}$$

where $\tilde{\Phi} = \sigma_2\Phi^*\sigma_2$. Note that there is no such coupling between scalar doublets fermions.

As in the preceding section, one can use the $SO(4)$ notation for the scalar representations. Just as the fermions, the scalar doublets are then given by spinor representations, combining the right- and left-handed doublets to

$$\underline{\Psi} = \begin{pmatrix} \chi_L \\ \chi_R \end{pmatrix}: \quad (\mathbf{0},\mathbf{0})[(\mathbf{2},\mathbf{1}) \oplus (\mathbf{1},\mathbf{2})](\mathbf{1},-1). \tag{2.24}$$

The bidoublet instead, having four complex degrees of freedom, can be represented by a complex $SO(4)$ vector $\phi^A$, which can be contracted with the gamma matrices to give

$$\underline{\Phi} = \begin{pmatrix} 0 & \Phi \\ -\tilde{\Phi}^\dagger & 0 \end{pmatrix}: \quad (\mathbf{0},\mathbf{0})(\mathbf{2},\mathbf{2})(\mathbf{1},0). \tag{2.25}$$

In terms of (2.24) and (2.25) the scalar potential is given by

$$V = \frac{\kappa_1}{2}(\bar{\underline{\Psi}}\underline{\Psi})^2 + \frac{\kappa_2}{2}(\bar{\underline{\Psi}}\Gamma\underline{\Psi}) + \lambda_1(\text{Tr}\underline{\Phi}^\dagger\underline{\Phi})^2 + \lambda_2(\text{Tr}\underline{\Phi}\underline{\Phi} + \text{Tr}\underline{\Phi}^\dagger\underline{\Phi}^\dagger)^2 \tag{2.26}$$
$$+ \lambda_3(\text{Tr}\underline{\Phi}\underline{\Phi} - \text{Tr}\underline{\Phi}^\dagger\underline{\Phi}^\dagger)^2 + \lambda_4(\text{Tr}\underline{\Phi}\underline{\Phi}^\dagger)(\text{Tr}\underline{\Phi}\underline{\Phi} + \text{Tr}\underline{\Phi}^\dagger\underline{\Phi}^\dagger)$$
$$+ \beta_1\bar{\underline{\Psi}}\underline{\Psi}\text{Tr}\underline{\Phi}^\dagger\underline{\Phi} + \beta_2(\text{Tr}\underline{\Phi}\underline{\Phi} + \text{Tr}\underline{\Phi}^\dagger\underline{\Phi}^\dagger)\bar{\underline{\Psi}}\underline{\Psi}$$
$$+ i\beta_3(\text{Tr}\underline{\Phi}\underline{\Phi} - \text{Tr}\underline{\Phi}^\dagger\underline{\Phi}^\dagger)\bar{\underline{\Psi}}\Gamma\underline{\Psi} + f_1\underline{\Psi}[\underline{\Phi}^\dagger,\underline{\Phi}]\underline{\Psi}$$

and the Yukawa couplings (2.23) read

$$\mathcal{L}_{Yuk} = iY_Q^+\bar{\underline{Q}}\frac{1+\Gamma}{2}\underline{\Phi}\underline{Q} + iY_Q^-\bar{\underline{Q}}\frac{1-\Gamma}{2}\underline{\Phi}\underline{Q} + H.c.. \tag{2.27}$$

In chapters 4 and 5, it will be convenient to decompose the bidoublet further into its hermitian and anti-hermitian parts

$$\underline{\Phi} = \frac{1}{\sqrt{2}}(\underline{\Phi}_1 + i\underline{\Phi}_2) = \frac{1}{\sqrt{2}}\Gamma_A(\phi_1^A + \phi_2^A), \tag{2.28}$$

with $\underline{\Phi}_1$ and $\underline{\Phi}_2$ hermitian[2]. In order to make the scalar potential (2.26) more accessible to the analytical minimization method by Gildener and Weinberg, in Ref. [6] a discrete $\mathbb{Z}_4$ symmetry is additionally introduced. Under this symmetry the field representations transform as

$$L_R \to \mathrm{i}L_R, \quad Q_R \to -\mathrm{i}Q_R, \quad \underline{\Phi} \to \mathrm{i}\underline{\Phi}, \quad \underline{\Psi} \to -\mathrm{i}\underline{\Psi}. \tag{2.31}$$

The potential interactions then reduces to

$$V = \frac{\kappa_1}{2}(\bar{\underline{\Psi}}\underline{\Psi})^2 + \frac{\kappa_2}{2}(\bar{\underline{\Psi}}\Gamma\underline{\Psi}) + \lambda_1(\mathrm{Tr}\underline{\Phi}^\dagger\underline{\Phi})^2 + \lambda_2(\mathrm{Tr}\underline{\Phi}\underline{\Phi} + \mathrm{Tr}\underline{\Phi}^\dagger\underline{\Phi}^\dagger)^2 \tag{2.32}$$
$$+ \lambda_3(\mathrm{Tr}\underline{\Phi}\underline{\Phi} - \mathrm{Tr}\underline{\Phi}^\dagger\underline{\Phi}^\dagger)^2 + +\beta_1\bar{\underline{\Psi}}\underline{\Psi}\mathrm{Tr}\underline{\Phi}^\dagger\underline{\Phi} + +f_1\underline{\Psi}[\underline{\Phi}^\dagger, \underline{\Phi}]\underline{\Psi}$$

and the Yukawa couplings are exclusively given by

$$Y_{\underline{Q}}^+ \quad \text{and} \quad Y_{\underline{L}}^-. \tag{2.33}$$

In order to explain the fermion masses, small $\mathbb{Z}_4$-breaking Yukawa terms $Y_Q^-$ and $Y_L^+$ have to be reintroduced. The authors of Ref. [6], however argue that these terms are maximally of the order $\frac{m_b}{m_t} \sim \mathcal{O}(1\%)$ and therefore do not generate large $\mathbb{Z}_4$-breaking scalar couplings.

---

[2]For future use, the intermiediate doublet-bidoublet couplings and Yukawa couplings are given in terms of (2.28):

$$2\beta_1\underline{\Psi}_a^\dagger\underline{\Psi}_a\Phi_i^A\Phi_i^A - i4f_1\epsilon_{ij}(\Gamma\Sigma^{CD})_{ba}\underline{\Psi}_b^\dagger\underline{\Psi}_a\Phi_i^C\Phi_j^D$$
$$+4\beta_2\underline{\Psi}_a^\dagger\underline{\Psi}_a(\Phi_1^C\Phi_1^C - \Phi_2^C\Phi_2^C) - 8\beta_3\underline{\Psi}_b^\dagger\Gamma_{ba}\underline{\Psi}_a(\Phi_1^C\Phi_2^C + \Phi_2^C\Phi_1^C) \subset V \tag{2.29}$$

and

$$\mathcal{L}_{\mathrm{Yuk}} = -\frac{1}{2}\left(\bar{Y}_{\underline{Q}}^+ + \bar{Y}_{\underline{Q}}^-\right)\bar{Q}\underline{\Phi}_2 Q + \frac{i}{2}\left(\bar{Y}_{\underline{Q}}^+ - \bar{Y}_{\underline{Q}}^-\right)\bar{Q}\Gamma\underline{\Phi}_1 Q, \tag{2.30}$$

where in the last line it is used the definition $\bar{Y}_{\underline{Q}}^+ = \frac{1}{\sqrt{2}}(Y_{\underline{Q}}^+ + Y_{\underline{Q}}^{+\dagger}), \quad \bar{Y}_{\underline{Q}}^- = \frac{1}{\sqrt{2}}(Y_{\underline{Q}}^- + Y_{\underline{Q}}^{-\dagger}).$

## 2.2 Radiative Symmetry Breaking

### 2.2.1 The Gildener-Weinberg Method

The additional $SU(2)_R$ introduces new weak gauge interactions which are, if parity is assumed, described by the same coupling constant $g_2$ that already represents the strength of the $SU(2)_L$ gauge interactions. As, however, right-handed vector currents are not probed by experiment [17–20], the corresponding mediators of the right-handed weak interaction, denoted by $W_R^\pm$ and $Z_R$, have to be accordingly heavy. Just as in the standard model, this is achieved by the Higgs mechanism. For this purpose, in the minimal model, the gauge group (2.1) is spontaneously broken in two steps

$$SU(3)_C \times SU(2)_L \times SU(2)_R \times U(1)_{B-L} \times P$$

$$\Downarrow$$

$$SU(3)_C \times SU(2)_L \times U(1)_Y \qquad (2.34)$$

$$\Downarrow$$

$$SU(3)_C \times U(1)_Q,$$

corresponding to two distint breaking scales. In the first step, together with the gauge subgroup $SU(2)_R$ also parity is broken. The corresponding scale should, however, not be much greater than a few TeV as otherwise, except for providing a framework for neutrino masses, the model would not have many testable consequences. The second breaking step corresponds to the familiar breaking of the SM gauge group at the electroweak scale,

In Ref. [6], it was shown that in the classically conformally invariant model this pattern can be realized by radiatively induced symmetry breaking. For this purpose, the approximate minimization method by Gildener and Weinberg (GW) [15] was used.

The GW method generalizes the Coleman-Weinberg mechanism [16] of radiative symmetry breaking to cases which include potentials of arbitrarily many scalar fields. Using the renormalization group running of the scalar couplings it reduces the minimization of the effective potential to a one-dimensional problem which can be solved analytically. In this section, the ideas of GW will be reviewed briefly.

Under the assumption of conformal invariance, a tree-level scalar potential $V_0$ can

generally be written as

$$V_0 = f_{ijkl}\phi_i\phi_j\phi_k\phi_l, \tag{2.35}$$

which contains exclusively $\phi^4$-terms and the coefficients $f_{ijkl}$ represent the scalar couplings. Let the field space be spanned by

$$\phi_i = N_i\phi \tag{2.36}$$

where the $N_i$ are on a unit sphere, meaning $\sum_i N_i = 1$, and $\phi$ is the radial field component. Then (2.35) becomes

$$V_0 = f_{ijkl}N_iN_jN_kN_l\phi^4. \tag{2.37}$$

Gildener and Weinberg stated that using an appropriate renormalization point $\mu_{\mathrm{GW}}$ one can force the couplings $f_{ijkl}$ to satisfy

$$\min\left(f_{ijkl}(\mu_{GW})N_iN_jN_kN_l\phi^4\right)\Big|_{N_i=n_i} = 0 \tag{2.38}$$

for $\phi \neq 0$. Hence, at $\mu_{\mathrm{GW}}$ the minimum of the tree-level potential is degenerate along the field direction

$$\Phi_i = n_i\phi \qquad \text{with} \qquad \sum_i n_i = 1, \tag{2.39}$$

which is called a *flat direction*. The one-loop radiative corrections to the potential are then considered exclusively in this direction: As the minimum of the tree-level potential (2.38) is vanishing, radiative corrections are dominant in this field direction and are therefore neglected in all other directions. In this approximation, the minimization problem of the effective potential is thus reduced to the case of a single degree of freedom, given by the radial field component $\phi$.

For this purpose, however, the tree-level potential (2.37) has to be minimized under the additional constraint that the minimum is vanishing. This leads to the, so called, Gildener-Weinberg conditions

$$\frac{\partial}{\partial N_i}V|_{N_i=n_i} = 0, \quad V|_{N_i=n_i} = 0 \quad \text{and} \quad \sum_i n_i^2 = 1 \tag{2.40}$$

which have to be satisfied at the renormalization point $\mu_{\mathrm{GW}}$. The solutions to these conditions are generally expressed by a set of flat directions $\{n\}$ which individually

emerge once a corresponding condition

$$f^n(f_{ijkl}(\mu_{\text{GW}})) = 0 \tag{2.41}$$

is fulfilled at a scale $\mu_{\text{GW}}$, with $f^n$ a function of the scalar couplings. In practice, one sets boundary conditions to the scalar couplings at the highest scale for which the theory is supposed to be valid (here this scale is taken to be Planck scale) and then one lets these couplings evolve to lower scales. If then for a direction $n$ the condition (2.41) is fulfilled the direction $n$ becomes flat and symmetry breaking occurs[3].

As the tree-level potential is zero along the flat direction $\phi = n\phi$, the one-loop effective potential $V_{\text{eff}}$, in this direction (see Ref. [16]), is given by

$$V_{\text{eff}}(n\phi) = \delta V(n\phi) = A\phi^4 + B\phi^4 \ln\left(\frac{\phi^2}{\mu_{\text{GW}}^2}\right) \tag{2.42}$$

where $A$ and $B$ are the constants (see Ref. [15])

$$A = \frac{1}{64\pi^2 \langle\phi\rangle^4} \sum_i f_i M_i^4(n\langle\phi\rangle) \left(\ln\left(\frac{M_i^2(\langle\phi\rangle)}{\langle\phi\rangle^2} - c_i\right)\right) \tag{2.43a}$$

$$B = \frac{1}{64\pi^2 \langle\phi\rangle^4} \sum_i f_i M_i^4(n\langle\phi\rangle) \tag{2.43b}$$

with the $f_i$ being the (real-valued) degrees of freedom, $M_i$ the particle masses and the $c_i = \frac{3}{2}$ for scalars and fermions and $c_i = \frac{5}{6}$ for gauge bosons respectively. The vacuum expectation value ($VEV$) $\langle\phi\rangle$ of the radial field component is then obtained by the stationary condition

$$\left.\frac{\partial V_{\text{eff}}(\phi)}{\partial\phi}\right|_{\langle\phi\rangle} = 0, \tag{2.44}$$

which, using the general formula (2.42), leads to

$$\ln\frac{\langle\phi\rangle^2}{\mu_{\text{GW}}^2} = -\frac{1}{2} - \frac{A}{B}. \tag{2.45}$$

Note that the right-hand side of (2.45) is typically of order $\mathcal{O}(1)$ such that $\langle\phi\rangle$ and $\mu_{\text{GW}}$ usually do not differ by more than one order magnitude.

In the phenomenologically interesting minimum, which leaves the $U(1)_Q$ unbro-

---

[3]In section (2.2.3) it will accounted for the fact, that a given flat direction does not correspond to a minimum.

ken[4], the vacuum expectiation values ($VEV$) of the scalar fields in the minimal left-right symmetric model are given by

$$\langle \underline{\Psi} \rangle = \begin{pmatrix} v_L e^{i\theta} \\ 0 \\ v_R \\ 0 \end{pmatrix} = \frac{1}{\sqrt{2}} \begin{pmatrix} n_1 e^{i\theta} \\ 0 \\ n_2 \\ 0 \end{pmatrix} \langle \phi \rangle \tag{2.47}$$

and

$$\langle \Phi \rangle = \frac{1}{\sqrt{2}} \begin{pmatrix} n_3 & 0 \\ 0 & n_4 e^{i\alpha} \end{pmatrix} = \frac{1}{2} \begin{pmatrix} \kappa & 0 \\ 0 & \kappa' e^{i\alpha} \end{pmatrix} \langle \phi \rangle \,, \tag{2.48}$$

where the remaining phases have been set to zero making use of the gauge freedom (see *e.g.* Ref. [14]). In the next section, the solutions to the GW conditions in the minimal left-right symmetric model [6] are reviewed.

## 2.2.2 Flat Directions

The flat directions of the minimal conformally invariant left-right symmetric model, including a $\mathbb{Z}_4$ symmetry, have been calculated in Ref. [6] and are reproduced in table 2.1. The various flat directions have been characterized according to the GW condition which is obtained by deriving the potential with respect to the bidoublet phase $\alpha$ (*cf.* (2.47)):

$$0 = \frac{\partial V}{\partial \alpha}\bigg|_{N_i = n_i} = -8n_3^2 n_4^2 \sin \alpha \cos \alpha \tag{2.49}$$

This condition is satisfied if either $n_3 = 0$, $n_4 = 0$ or $\alpha = 0, \frac{\pi}{2}$. The solutions given by $n_3 \neq 0$ and $n_4 \neq 0$ are called solutions of type I. These type I solutions split further into the two subclasses corresponding to $\alpha = 0$ (Ia, Ic) and $\alpha = \frac{\pi}{2}$ (Ib, Id) respectively. Note that for the latter solutions $\kappa$ is imaginary. Hence, the solutions Ib and Ic are CP-breaking.

The solutions given by either $n_3 = 0$ or $n_4 = 0$ are of types IIa/e ,and IIb/d respectively, while the case that both $n_3$ and $n_4$ are vanishing is denoted by IIc.

---

[4]Using the $SO(4)$ notation, the electric charge $Q$ is related to the generators of the unbroken theory by the formula [25]

$$Q = -i\Sigma^{12} + \frac{1}{2}(B - L) \tag{2.46}$$

| | GW condition | | $\frac{n_1^2}{n_2^2}$ | $n_1^2 + n_2^2$ | $\frac{n_3^2}{n_4^2}$ | $n_3^2 + n_4^2$ | $\alpha$ | $\frac{n_3^2+n_4^2}{n_1^2+n_2^2}$ |
|---|---|---|---|---|---|---|---|---|
| Ia$\not{p}$ | $\kappa_+$ | $= \dfrac{\beta_1^2}{2(\lambda_1+4\lambda_2)} - \dfrac{f_1^2}{32\lambda_2}$ | 0 | $\dfrac{2(\lambda_1+4\lambda_2)}{2\lambda_1+8\lambda_2-\beta_1}$ | $\dfrac{4(2\beta_1+f_1)\lambda_2+f_1\lambda_1}{4(2\beta_1-f_1)\lambda_2-f_1\lambda_1}$ | $\dfrac{-\beta_1}{2\lambda_1+8\lambda_2-\beta_1}$ | 0 | $\dfrac{-\beta_1}{2\lambda_1+8\lambda_2}$ |
| Ia$P$ | $\kappa_1$ | | 1 | | | | | |
| Ib$\not{p}$ | $\kappa_+$ | $= \dfrac{\beta_1^2}{2(\lambda_1-4\lambda_3)} + \dfrac{f_1^2}{32\lambda_3}$ | 0 | $\dfrac{2(\lambda_1-4\lambda_3)}{2\lambda_1-8\lambda_3-\beta_1}$ | $\dfrac{4(2\beta_1+f_1)\lambda_3-f_1\lambda_1}{4(2\beta_1-f_1)\lambda_3+f_1\lambda_1}$ | $\dfrac{-\beta_1}{2\lambda_1-8\lambda_3-\beta_1}$ | $\dfrac{\pi}{2}$ | $\dfrac{-\beta_1}{2\lambda_1-8\lambda_3}$ |
| Ib$P$ | $\kappa_1$ | | 1 | | | | | |
| Ic | | $\lambda_1 = -4\lambda_2$ | $\frac{0}{0}$ | 0 | 1 | 1 | 0 | $\infty$ |
| Id | | $\lambda_1 = 4\lambda_3$ | $\frac{0}{0}$ | 0 | 1 | 1 | $\frac{\pi}{2}$ | $\infty$ |
| IIa$\not{p}$ | $\kappa_+$ | $= \dfrac{(2\beta_1-f_1)^2}{8\lambda_1}$ | 0 | $\dfrac{4\lambda_1}{-2\beta_1+f_1+4\lambda_1}$ | $\infty$ | $\dfrac{2\beta_1-f_1}{2\beta_1-f_1-4\lambda_1}$ | – | $\dfrac{f_1-2\beta_1}{4\lambda_1}$ |
| IIa$P$ | $\kappa_1$ | | 1 | | | | | |
| IIb$\not{p}$ | $\kappa_+$ | $= \dfrac{(2\beta_1+f_1)^2}{8\lambda_1}$ | 0 | $\dfrac{4\lambda_1}{-2\beta_1-f_1+4\lambda_1}$ | 0 | $\dfrac{2\beta_1+f_1}{2\beta_1+f_1-4\lambda_1}$ | – | $\dfrac{-f_1-2\beta_1}{4\lambda_1}$ |
| IIb$P$ | $\kappa_1$ | | 1 | | | | | |
| IIc$\not{p}$ | $\kappa_+$ | $= 0$ | 0 | 1 | $\frac{0}{0}$ | 0 | – | 0 |
| IIc$P$ | $\kappa_1$ | | 1 | | | | | |
| IId | | $\lambda_1 = 0$ | $\frac{0}{0}$ | 0 | 0 | 1 | – | $\infty$ |
| IIe | | $\lambda_1 = 0$ | $\frac{0}{0}$ | 0 | $\infty$ | 1 | – | $\infty$ |

Table 2.1: The flat directions of the minimal left-right symmetric doublet model, taken from Ref. [6]. The different solutions to the Gildener-Weinberg conditions are completely classified according to the two conditions (2.49) and (2.50), the resulting types are indicated in the first column. The second column gives the condition to the couplings which fixes the GW scale $\mu_{\mathrm{GW}}$ and was previously written as a function $f^n = 0$ with $f^n$ being a function of the running couplings. The remaining columns give the flat directions $n$.

The characterization due to (2.49) thus classifies the different flat directions with respect to their bidoublet $VEV$s, $\kappa$ and $\kappa'$. In order to introduce a distinction due to the doublet $VEV$s the following equation, which holds for non-vanishing $n_1$ and $n_2$, is used:

$$0 = \frac{1}{n_1}\frac{\partial V}{\partial N_1}\Big|_{N_i=n_i} - \frac{1}{n_2}\frac{\partial V}{\partial N_2}\Big|_{N_i=n_i} = \kappa_2\big(n_1^2 - n_2^2\big) \qquad (2.50)$$

Assuming $\kappa_2 \neq 0$, this equation is satisfied if $n_1 = n_2$. Thus, the different flat directions are either parity conserving for $n_1 = n_2$ or maximally parity breaking for one of the doublet VEVs being zero. The parity conserving solutions are denoted by the letter $p$ while $\not{p}$ denotes the parity breaking solutions. Those solutions for which $n_1 = n_2 = 0$ are given by types Ic, Id, IId and IIe.

The interesting solutions are of type Ia$\not{p}$, Ib$\not{p}$, IIa$\not{p}$ and IIb$\not{p}$, as phenomenology requires that on the one hand parity is broken and on the other hand the bidoublet

acquires at least one non-vanishing $VEV$ in order to satisfy the breaking pattern (2.34). It has, however, been noted in Ref. [6] that the solutions of types a and b are connected by the transformations $(\alpha, \lambda_2, \lambda_3) \rightarrow (\frac{\pi}{2} - \alpha, -\lambda_3, -\lambda_2)$ in the case of type I and by $(n_3^2, n_4^2, f_1) \rightarrow (n_4^2, n_3^2, -f_1)$ in the case of type II.

## 2.2.3 Second Derivatives: Scalar Mass Spectra

The Gildener-Weinberg conditions just reflect the fact that in a given flat direction the potential is stationary. They do not account for the possibility that such a stationary point may not be a minimum. In order to know if a flat direction corresponds to a minimum, it is therefore mandatory to check whether the second derivatives of the potential, evaluated at the stationary point, are greater than zero. This is equivalent to the mass matrix being positiv-definite, as it is

$$m_{ij}^2 = \frac{\partial^2 \mathrm{V}}{\partial \phi_i \partial \phi_j}\Big|_{N_i = n_i}, \tag{2.51}$$

where $\phi_i \in \{\sqrt{2}\mathrm{Re}(\underline{\Psi}_a), \sqrt{2}\mathrm{Im}(\underline{\Psi}_a), \underline{\Phi}_j^A\}$. Especially, if for given boundary conditions, more than one flat direction emerges, examining the mass matrix can provide a selection rule to decide in which flat direction the symmetry is broken. For this purpose, as required in the subsequent chapters, here the mass eigenvalues corresponding to the parity breaking flat directions Ib, IIa and IIc are collected. Note that at tree-level the particle which corresponds to the field exitation along the flat direction, the so-called *scalon s*, is massless. It acquires however a mass term at one loop order. which is given by

$$m_s^2 = \frac{\mathrm{d}^2}{\mathrm{d}\phi^2} V(n\phi)\big|_{\langle\phi\rangle} = 8B \langle\phi\rangle^2. \tag{2.52}$$

**Scalar Masses for Scenario IIa**

In the case of flat direction IIa these have already been calculated by [6]. There is one state orthogonal to the massless scalon $s$:

$$\begin{pmatrix} s \\ h \end{pmatrix} = \begin{pmatrix} n_2 & n_3 \\ -n_3 & n_2 \end{pmatrix} \cdot \begin{pmatrix} \chi_{Rr}^0 \\ \phi_{1r}^0 \end{pmatrix} = \begin{pmatrix} \cos\vartheta & \sin\vartheta \\ -\sin\vartheta & \cos\vartheta \end{pmatrix} \cdot \begin{pmatrix} \chi_{Rr}^0 \\ \phi_{1r}^0 \end{pmatrix} = O(\vartheta) \begin{pmatrix} \chi_{Rr}^0 \\ \phi_{1r}^0 \end{pmatrix}. \tag{2.53}$$

This state has been called $h$. It can be identified with the SM Higgs as it is the physical component of the field that transforms as the SM Higgs field and provides

fermion and left-handed gauge boson masses acquiring a vacuum expectation value. The mixing angle $\vartheta$ is given by

$$\tan^2 \vartheta = \frac{\kappa^2}{v_R^2} = \frac{f_1 - 2\beta_1}{4\lambda_1}. \tag{2.54}$$

Thus, given a little hierarchy that is not too large, the mixing is small and and $h$ can indeed be identified with the SM Higgs boson. Its mass is given by

$$m_h^2 = \frac{1}{2}(f_1 - 2\beta_1)\langle\phi\rangle^2, \tag{2.55}$$

which, again under the assumption of $\vartheta$ being small, can be approximated to

$$m_h^2 \approx 4\lambda_1 v_R^2 \tan^2 \vartheta = 4\lambda_1 \kappa^2. \tag{2.56}$$

The remaining masses are

$$m_{\sigma_1}^2 = m_{\sigma_2}^2 = \frac{f_1}{2}\langle\phi\rangle^2 \tag{2.57a}$$

$$m_{\chi_{Lr}^0}^2 = m_{\chi_{Li}^0}^2 = -\frac{4\kappa_2\lambda_1}{f_1 - 2\beta_1 + 4\lambda_1}\langle\phi\rangle^2 \tag{2.57b}$$

$$m_{\chi_{Lr}^-}^2 = m_{\chi_{Li}^-}^2 = \frac{-f_1^2 + 2f_1\beta_1 + 8\kappa_2\lambda_1}{-2f_1 + 4\beta_1 - 8\lambda_1}\langle\phi\rangle^2 = m_{\chi_{Lr}^0}^2 + f_1\kappa^2 \tag{2.57c}$$

$$m_{\phi_{2r}^0}^2 = \frac{2\left(-8\beta_1\lambda_2 + f_1\left(\lambda_1 + 4\lambda_2\right)\right)}{f_1 - 2\beta_1 + 4\lambda_1}\langle\phi\rangle^2 \tag{2.57d}$$

$$m_{\phi_{2i}^0}^2 = \frac{2\left(f_1\left(\lambda_1 - 4\lambda_3\right) + 8\beta_1\lambda_3\right)}{f_1 - 2\beta_1 + 4\lambda_1}\langle\phi\rangle^2 \tag{2.57e}$$

Additionally, there are six massless would-be-Nambu-Goldstone bosons (NGBs) $\pi_1$, $\pi_2$, $\phi_{2r}^-$, $\phi_{2i}^-$, $\phi_{1i}^0$ and $\chi_{Ri}^0$ corresponding to the six degrees of gauge freedom. The particle states $\pi_{1,2}$ and $\sigma_{1,2}$ are given by the superpositions

$$\begin{pmatrix} \pi_1 \\ \sigma_1 \end{pmatrix} = O(-\vartheta)\begin{pmatrix} \chi_{Ri}^- \\ \phi_{1i}^+ \end{pmatrix} \qquad \text{and} \qquad \begin{pmatrix} \pi_2 \\ \sigma_2 \end{pmatrix} = O(\vartheta)\begin{pmatrix} \chi_{Rr}^- \\ \phi_{1r}^+ \end{pmatrix}. \tag{2.58}$$

Given the scalar masses the one-loop scalon mass then yields

$$m_s^{\text{1-loop}} = \left(\frac{3g_1^4 + 6g_1^2 g_2^2 + 9g_2^4 + 64(\kappa_2^2 + \beta_1^2)}{64\pi^2} + \mathcal{O}\left(\frac{\kappa^2}{v_R^2}\right)\right)v_R^2. \tag{2.59}$$

**Scalar Masses for Scenario IIb**

As was already mentioned above the solution IIb is connected to the solutions of type IIa by the transformation $(f_1, n_3, n_4) \to (-f_1, n_4, n_3)$. Thus, the mass spectrum for the flat directions of type IIb can easily be obtained from the type IIa masses.

**Scalar Masses for Scenario IIc**

In the case of type IIc symmetry breaking the flat direction is along the neutral component of the right-handed doublet. Using the gauge freedom it can be chosen to be along its real part. Thus, the scalon is given by

$$s = \chi_{Rr}^0. \tag{2.60}$$

The tree-level mass spectrum reads

$$m^2_{\{\phi_{1r}^0, \phi_{1i}^0, \phi_{2r}^-, \phi_{2i}^-\}} = \frac{2\beta_1 - f_1}{4} \langle \phi \rangle^2 = \frac{2\beta_1 - f_1}{2} v_R^2 \tag{2.61a}$$

$$m^2_{\{\phi_{2r}^0, \phi_{2i}^0, \phi_{1r}^+, \phi_{1i}^+\}} = \frac{2\beta_1 + f_1}{4} \langle \phi \rangle^2 = \frac{2\beta_1 + f_1}{2} v_R^2 \tag{2.61b}$$

$$m^2_{\{\chi_{Lr}^0, \chi_{Li}^0, \chi_{Lr}^-, \chi_{Li}^-\}} = -\kappa_2 \langle \phi \rangle^2 = -2\kappa_2 v_R^2 \tag{2.61c}$$

$$\tag{2.61d}$$

Given these, the one-loop scalon mass yields

$$m_s^{\text{1-loop}} = \left( \frac{3g_1^4 + 6g_2^2 g_2^2 + 9g_2^4 + 48(8\kappa_2^2 + 4\beta_1^2 + f_1^2)}{64\pi^2} + \mathcal{O}\left( \frac{\kappa^2 + \kappa'^2}{v_R^2} \right) \right) v_R^2 \tag{2.62}$$

As the Standard Model gauge group is left unbroken in the case IIc, only three would-be-NGBs $\chi_{Rr}^-$, $\chi_{Ri}^-$ and $\chi_{Ri}^0$ emerge, which are eaten by the right-handed gauge bosons.

**Scalar Masses for Scenario Ia**

As already mentioned type Ia flat directions are connected to type Ib directions by the transformation $(\alpha, \lambda_2, \lambda_3) \leftrightarrow (\alpha, -\lambda_2, -\lambda_3)$. Since in the following chapters only type IIa and Ib flat directions will occur, here the type Ib mass spectrum will be given rather than that of type Ia.

**Scalar Masses for Scenario Ib**

For flat directions of type Ib the scalon is given by

$$s = n_2 \chi_{Rr}^0 + n_3 \phi_{1r}^0 + n_4 \phi_{2i}^0, \tag{2.63}$$

as both $\kappa$ and $\kappa'$ are non-vanishing and $\alpha$ is given by $\alpha = \pi/2$. The masses of its orthogonal complements, which will be called $\sigma_1$ and $\sigma_2$ are given by

$$m_{\sigma_1}^2 + m_{\sigma_2}^2 = \mathrm{Tr}[M^2] = \frac{-f_1^2 \lambda_1 - 16\beta_1^2 \lambda_3 + 4f_1^2 \lambda_3 + 32\beta_1 \lambda_1 \lambda_3}{32\lambda_3(\beta_1 - 2\lambda_1 + 8\lambda_3)} \tag{2.64}$$

$$= \frac{f_1^2 n_2^2}{32\lambda_3} - (\beta_1 - 2\lambda_1)(n_3^2 + n_4^2) \tag{2.65}$$

$$m_{\sigma_1}^2 - m_{\sigma_2}^2 = \frac{2}{32\lambda_3(\beta_1 - 2\lambda_1 + 8\lambda_3)} \Big[ \big( f_1^2(\lambda_1 - 4\lambda_3) + 16\beta_1(\beta_1 - 2\lambda_1)\lambda_3 \big)^2 \tag{2.66}$$

$$+ 128\lambda_3(\beta_1 - 2\lambda_1 + 8\lambda_3)\big( -f_1^2(\lambda_1 - 4\lambda_3)^2 + 64\beta_1^2 \lambda_3^2 \big) \Big]^{\frac{1}{2}}. \tag{2.67}$$

which may be approximated to

$$m_{\sigma_1}^2 - m_{\sigma_2}^2 = \frac{n_2^2}{16} \left( \left( \frac{f_1^2}{2\lambda_3} \right)^2 + 32(-\beta_1 + 2\lambda_1 + 8\lambda_3)\frac{f_1^2}{\lambda_3} \right)^{\frac{1}{2}} \left( 1 + \mathcal{O}\left( \frac{v_L^2}{v_R^2} \right) \right) \tag{2.68}$$

As the expressions of the mass eigenstates $\sigma_1$ and $\sigma_2$ in terms of superposed fields $\chi_{Rr}^0$, $\phi_{1r}^0$ and $\phi_{2i}^0$ are not easily accessed analytically, only the undiagonalized mass matrix will be given here:

$$-\mathcal{L} \supset \frac{1}{2}(\chi_{Rr}^0, \phi_{1i}^0, \phi_{2r}^0) M^2 \begin{pmatrix} \chi_{Rr}^0 \\ \phi_{1i}^0 \\ \phi_{2r}^0 \end{pmatrix} \tag{2.69}$$

with

$$M^2 = \begin{pmatrix} \frac{f_1^2 n_2^2}{32\lambda_3} - \beta_1(n_3^2 + n_4^2) & \frac{2\beta_1 - f_1)n_2 n_3}{2} & \frac{(2\beta_1 + f_1)n_2 n_4}{2} \\ \frac{(2\beta_1 - f_1)n_2 n_3}{2} & 2\lambda_1 n_3^2 & 2(\lambda_1 - 8\lambda_3)n_3 n_4 \\ \frac{2(\beta_1 + f_1)n_2 n_4}{2} & 2(\lambda_1 - 8\lambda_3)n_3 n_4 & 2\lambda_1 n_4^2 \end{pmatrix} \langle \phi \rangle^2. \tag{2.70}$$

The remaining scalar masses are

$$m_h = \frac{8\beta_1(\lambda_2 + \lambda_3)}{\beta_1 - 2\lambda_1 + 8\lambda_3}\langle\phi\rangle^2 \qquad\qquad = 16(\lambda_2 + \lambda_3)(\kappa^2 + \kappa'^2) \qquad (2.71a)$$

$$m^2_{\sigma_3} = m^2_{\sigma_4} = \frac{-f_1^2(\lambda_1 - 4\lambda_3) + 128\beta_1\lambda_3^2}{16\lambda_3(\beta_1 - 2\lambda_1 + 8\lambda_3)}\langle\phi\rangle^2 \qquad = \frac{f_1^2}{16\lambda_3}v_R^2 + 16\lambda_3(\kappa^2 + \kappa'^2) \quad (2.71b)$$

$$m^2_{\chi^0_{Lr}} = m^2_{\chi^0_{Li}} = \frac{2\kappa_2(\lambda_1 - 4\lambda_3)}{\beta_1 - 2\lambda_1 + 8\lambda_3}\langle\phi\rangle^2 \qquad\qquad = -2\kappa_2 v_R^2 \qquad\qquad (2.71c)$$

$$m^2_{\chi^-_{Lr}} = m^2_{\chi^-_{Li}} = \frac{(\lambda_1 - 4\lambda_3)(-f_1^2 + 32\kappa_2\lambda_3)}{16\lambda_3(\beta_1 - 2\lambda_1 + 8\lambda_3)}\langle\phi\rangle^2 \quad = \frac{-f_1^2 + 32\kappa_2\lambda_3}{16\lambda_3}v_R^2 \qquad (2.71d)$$

In addition, there are six would-be-NGBs $\pi_1$, $\pi_2$, $\pi_3$, $\pi_4$, $\pi_5$ and $\chi^0_{Ri}$. The superposed fields are given by:

$$\begin{pmatrix} \pi_1 \\ h \end{pmatrix} = \frac{1}{\sqrt{n_3^2 + n_4^2}}\begin{pmatrix} n_3 & n_4 \\ -n_4 & n_3 \end{pmatrix}\begin{pmatrix} \phi^0_{1i} \\ \phi^0_{2r} \end{pmatrix}, \qquad (2.72a)$$

$$\begin{pmatrix} \pi_2 \\ \pi_3 \\ \sigma_3 \end{pmatrix} = \mathcal{N}\begin{pmatrix} 16\lambda_3 n_4 & 0 & f_1 n_2 \\ -16\lambda_3 f_1 n_2 n_3 & (16\lambda_3)^2 n_3 n_4 & \\ -f_1 n_2 & 16\lambda_3 n_3 & 16\lambda_3 n_4 \end{pmatrix}\begin{pmatrix} \chi^-_{Rr} \\ \phi^+_{1r} \\ \phi^-_{2i} \end{pmatrix} \qquad (2.72b)$$

and

$$\begin{pmatrix} \pi_4 \\ \pi_5 \\ \sigma_4 \end{pmatrix} = \mathcal{N}\begin{pmatrix} -16\lambda_3 n_4 & 0 & f_1 n_2 \\ -16\lambda_3 f_1 n_2 n_3 & f_1^2 n_2^2 + (16\lambda_3)^2 n_4^2 & -(16\lambda_3)^2 n_3 n_4 \\ f_1 n_2 & 16\lambda_3 n_3 & 16\lambda_3 n_4 \end{pmatrix}\begin{pmatrix} \chi^-_{Ri} \\ \phi^+_{1i} \\ \phi^-_{2r} \end{pmatrix} 7nonumber \qquad (2.72c)$$

with the normalizing matrix $\mathcal{N} = \text{diag}(\mathcal{N}_1, \mathcal{N}_2, \mathcal{N}_3)$, where

$$\mathcal{N}_1 = \frac{1}{\sqrt{256\lambda_3^2 n_4^2 + f_1^2 n_2^2}} \qquad (2.72d)$$

$$\mathcal{N}_2\frac{1}{\sqrt{256\lambda_3^2 f_1^2 n_2^2 n_3^2 + (f_1^2 n_2 + 256\lambda_3^2 n_4^2)^2 + (16\lambda_3)^4 n_3^2 n_4^2}} \qquad (2.72e)$$

$$\mathcal{N}_3 = \frac{1}{\sqrt{f_1^2 n_2^2 + 256\lambda_3^2(n_3^2 + n_4^2)}}. \qquad (2.72f)$$

Finally, the one-loop scalon mass is given by

$$
m_s^{\text{1-loop}} = \left[ \frac{3g_1^4 + 6g_2^2 g_2^2 + 9g_2^4 + 2f_1^2(-\kappa_2 + \lambda_1 - 4\lambda_3)}{64\pi^2} + \mathcal{O}\left( \frac{\kappa^2 + \kappa'^2}{v_R^2} \right) \right] v_R^2 - \tag{2.73}
$$

One can see that in the particle spectrum there is one light state $h$ with a mass proportional to the bidoublet VEV whereas all the other masses are mainly given by the right-handed VEV. Having the same transformation properties under Standard Model gauge group, $h$ can be interpreted as the Standard Model Higgs boson. Thus, just as in the case IIa, a small little hierarchy corresponds to one light Standard Model-like Higgs boson in the mass spectrum while the remaining physical scalar particles have masses of order $v_R$.

## 2.2.4 Little Hierarchy

In Ref. [6] it has been shown that in the classically conformal invariant LR symmetric model the GW method can be applied and that in a large fraction of parameter space solutions to parity breaking GW conditions can be found, thereby generating a large hierarchy between the Planck scale and the parity breaking scale, which is given by the VEV right-handed doublet, $v_R$. It has remained, however, unsatisfactory that, in order to generate the hierarchy between the $v_R$ scale and the electroweak scale, which is referred to as the *small hierarchy*, the parameters apparently have to be fine-tuned. The little hierarchy is expressed here in terms of the ratio of the squared bidoublet VEVs, $\kappa$ and $\kappa'$ to $v_R$. For the various flat directions, this ratio is given in the last column of table 2.1 in terms of the scalar couplings. In Ref. [6], the discussion was concentrated on type IIa flat directions as type Ia solutions were considered to be disfavored since consistency requires the scalar couplings to be fine-tuned to a high degree of precision. From a natural perspective it had been assumed that all parameters are of the same order of magnitude. An admittedly mild fine-tuning was however encountered also for flat directions of type IIa. For this type of directions the little hierarchy is given by the expression[5]

$$
\frac{\kappa^2}{v_R^2} = \frac{f_1 - 2\beta_1}{4\lambda_1}. \tag{2.74}
$$

---

[5]Note that by expressing the little hierarchy in this way, a small value corresponds to a large little hierarchy. Hence, the ratio of $\frac{\kappa^2}{v_R^2} = 0$ corresponds to an infinitely large little hierarchy.

As $\lambda_1$ is fixed by the Higgs mass (e.g. (2.55)), $f_1$ and $\beta_1$, assumed to be of order one, have to cancel each other to give a value of order $\mathcal{O}\left(10^{-4}\right)$ in order to gain $v_R = \mathcal{O}\left(10\,\mathrm{TeV}\right)$ for the bidoublet VEV given by $\kappa = \mathcal{O}\left(174\,\mathrm{GeV}\right)$. According to the classical fine-tuning measure $\Delta_{BC}$ due to Giudice and Barbieri [26], which is defined as

$$\Delta_{BC}(\mathcal{O}) = \max_i \left[ \frac{\partial \log(\mathcal{O})}{\partial \log p_i} \right], \tag{2.75}$$

where $\mathcal{O}$ is an observable and the $p_i$ the model parameters, the fine-tuning of the little hierarchy is $\Delta_{BC} = \mathcal{O}\left(10^4\right)$.

Note, however, that in this diploma-thesis the fine-tuning will not be adressed in terms of such quantifying measures such as the fine-tuning definition of Giudice and Barbieri. Rather, the reduction of free parameters is already considered as a reduction in fine-tuning.

# Chapter 3

# A Shift Symmetry at the Planck Scale

## 3.1 Definition

In this diploma thesis it is assumed that at the Planck scale the scalar potential is invariant under the transformation

$$\underline{\Phi} \to \underline{\Phi} + \alpha \qquad (3.1)$$

which shifts the bidoublet field by a constant 2-dimensional square matrix $\alpha$. In the following, this symmetry will be referred to just as *shift symmetry*. Imposing this symmetry effectively constrains all scalar couplings, except for the doublet self-couplings $\kappa_1$ and $\kappa_2$, to vanish at the Planck scale, such that at that scale the Higgs potential is given by

$$\frac{\kappa_1}{2}\bar{\underline{\Psi}}\underline{\Psi} + \frac{\kappa_2}{2}\bar{\underline{\Psi}}\Gamma\underline{\Psi},$$

while the remaining scalar interactions being not apparent at tree-level are purely generated by quantum corrections. This situation, as already mentioned in the introduction, is similar to a Standard Model which, with respect to LHC data, exhibits a vanishing quartic coupling near the Planck scale under the assumption that it is valid up to such high scales with no new physics[1] in between.

In this chapter it will be investigated if, within the restricted 2-dimensional parameter space spanned by $\kappa_1$ and $\kappa_2$, parity breaking flat directions emerge and if a phenomenologically acceptable little hierarchy can be obtained.

---

[1]The presumable introduction of three heavy right-handed neutrinos might modify the running of $\lambda$ and change this picture [22, 23].

## 3.2 Stability of the Higgs Potential

In order to embed the theory successfully at the Planck scale the scalar potential should be stable over the whole range, from the Planck scale down to the symmetry breaking scale. Furthermore, the model should be perturbative, *i.e.* no Landau poles should show up, as was already emphasized by the authors of [6].

For this purpose, in this section the stability conditions of the model are considered with regard to the shift symmetry.

### 3.2.1 Stability Conditions and their Connection to Flat Directions

The stability conditions, given in [6], read

$$\kappa_1 > 0, \tag{3.2a}$$

$$\kappa_+ = \kappa_1 + \kappa_2 > 0, \tag{3.2b}$$

$$\lambda_1 > 0, \tag{3.2c}$$

$$\lambda_1 + 4\lambda_2 > 0, \tag{3.2d}$$

$$\lambda_1 - 4\lambda_3 > 0, \tag{3.2e}$$

and

$$\min\left[\kappa_1, \kappa_1 + \frac{f_1^2}{32\lambda_2}, \kappa_1 - \frac{f_1^2}{32\lambda_3}\right] > 0, \tag{3.2f}$$

$$\min\left[\kappa_+, \kappa_+ + \frac{f_1^2}{32\lambda_2}, \kappa_+ - \frac{f_1^2}{32\lambda_3}\right] > 0, \tag{3.2g}$$

from which the last two do not entail new constraints, as shift symmetry implies $f_1 \equiv 0$.

Note that these conditions can be read off from the Gildener-Weinberg conditions. This connection may need further explanation: In (2.41), a general Gildener-Weinberg condition was expressed as a function $f^n$ of the scalar couplings, which here are given by $\kappa_1, \kappa_2, \ldots$, that equals zero

$$f^n(\kappa_1, \kappa_2, \ldots) = 0. \tag{3.3}$$

This function $f^n$ corresponds to a certain direction $n$ in the field space defined by

$$n = (n_1, n_2, \ldots, n_m) \tag{3.4}$$

which lies on the unit sphere, meaning

$$n_1^2 + n_2^2 + \ldots n_m^2 = 1, \tag{3.5}$$

and $m$ represents the number of real-valued scalar fields.

If for a certain renormalization point $\mu_{GW}$ the condition (2.41) is fulfilled, the potential vanishes (and becomes stationary) in this direction $n$ in field space, as discussed in the preceding chapter. The direction $n$ is then called *flat*. In general, the function $f^n$ represents the value of the potential along the field direction $n$. For the normal case, or rather the desired case, the functions $f^n$ will have positive values at the Planck scale and run according to the renormalization group functions, until for some energy scale $\mu_{GW}$ one of them vanishes, thereby satisfying the associated Gildener-Weinberg condition and a flat direction emerges. Then, if this flat direction corresponds to a minimum and not just to a stationary point, spontaneous symmetry breaking takes place. The fact that $f^n$ becomes seemingly negative for energies below $\mu_{GW}$ then is meaningless since symmetry is already broken. Apart from that, for energies below the symmetry breaking scale the couplings run according to the beta-functions of the broken theory.

It has, however, to be ensured, that there is no function $f^n$ being negative for energies above the breaking scale. Otherwise, if *e.g.* for a direction $n_0$ the function $f^{n_0}$ is negative for some energy scale $\mu$, the potential is not bounded from below anymore. In principle the potential then can be lowered to arbitrary small values by a large radial field component $\phi$ and therefore becomes unstable in this direction.

Before now discussing the stability conditions (3.2), it has to be pointed out that in Ref. [6] only those flat directions have been considered which do not break the $U(1)$ of electro-magnetism as these are the phenomenologically interesting ones. Concerning the stability of the potential, however, one also has to account for the possibility that the potential becomes unstable in those directions in field space that involve charged field components. For simplicity, in this diploma thesis, this possibility of instabilities originating from flat directions which break electromagnetism is omitted. Generally, it is a highly non-trivial task to determine all stability conditions given a complicated potential such as (2.26). For a recent attempt see *e.g.*

Ref. [27] and references therein. In the following, the stability conditions associated to the bidoublet field direction will be discussed in some detail.

## 3.2.2 Stability in the Bidoublet Field Direction

### Running of the Stability Conditions

The beta-functions of the bidoublet self-couplings $\lambda_1$, $\lambda_2$ and $\lambda_3$ (see appendix A.19), reveal that their running does not depend on the doublet self-couplings $\kappa_1$ and $\kappa_2$ at one-loop level. Hence, their running is essentially fixed by imposing the shift symmetry. Being zero at the Planck scale, as shift symmetry implies, they are essentially generated by gauge and fermion loops[2]. Thus, the sign of the gauge contribution and the sign of the Yukawa contribution in (A.19) dictate if the bidoublet self-couplings become negative or positive valued at lower energies. Demanding shift symmetry, at the Planck scale $\Lambda_{\mathrm{Pl}}$ the beta-functions of the bidoublet self-couplings are given by

$$\beta_{\lambda_1}(\Lambda_{\mathrm{Pl}}) = \frac{1}{128\pi^2}\left[9g_2^4(\Lambda_{\mathrm{Pl}}) - 4T_4(\Lambda_{\mathrm{Pl}})\right], \tag{3.6a}$$

$$\beta_{\lambda_2}(\Lambda_{\mathrm{Pl}}) = \frac{1}{512\pi^2}\left[3g_2^4(\Lambda_{\mathrm{Pl}}) + 2T_4(\Lambda_{\mathrm{Pl}})\right], \tag{3.6b}$$

$$\beta_{\lambda_3}(\Lambda_{\mathrm{Pl}}) = \frac{1}{256\pi^2}\left[-3g_2^4(\Lambda_{\mathrm{Pl}}) - T_4(\Lambda_{\mathrm{Pl}})\right], \tag{3.6c}$$

where the Yukawa contribution $T_4$ is defined according to (A.20b).

By this argument, $\lambda_2$ is expected to develop negative values starting at the Planck scale while $\lambda_1$ and $\lambda_3$ are expected to become positive. In the case of $\lambda_1$ this is due to the fact that the top-Yukawa contribution in (3.6a) dominates the positive-sign gauge contribution. In figure (3.1) the running of the bidoublet self-couplings is plotted. There, the doublet self-couplings were set to $\kappa_1 = -\kappa_2 = 0.2$ at the Planck scale. A survey of different initial conditions for $\kappa_1$ and $\kappa_2$ confirmed that, indeed, these couplings do not affect the running of the bidoublet self-couplings significantly. Using the same initial values of $\kappa_1$ and $\kappa_2$, figure 3.2 shows the running of the stability conditions (3.2d) and (3.2e). As the plots in figure 3.2 shows, the functions $\lambda_1 + 4\lambda_2$ and $\lambda_1 - 4\lambda_3$ are negative for energies above approximately $\mu = 10^{17}\,\mathrm{GeV}$ and $\mu = 10^{11}\,\mathrm{GeV}$ respectively. Hence, for high energies the potential seems to be

---

[2]Note that the main contribution of the latter clearly comes from the top-quark loops due to the strong tree-level top-Yukawa coupling to the bidoublets. For this reason, all numerical results obtained in this diploma thesis are based on the one-flavor limit.
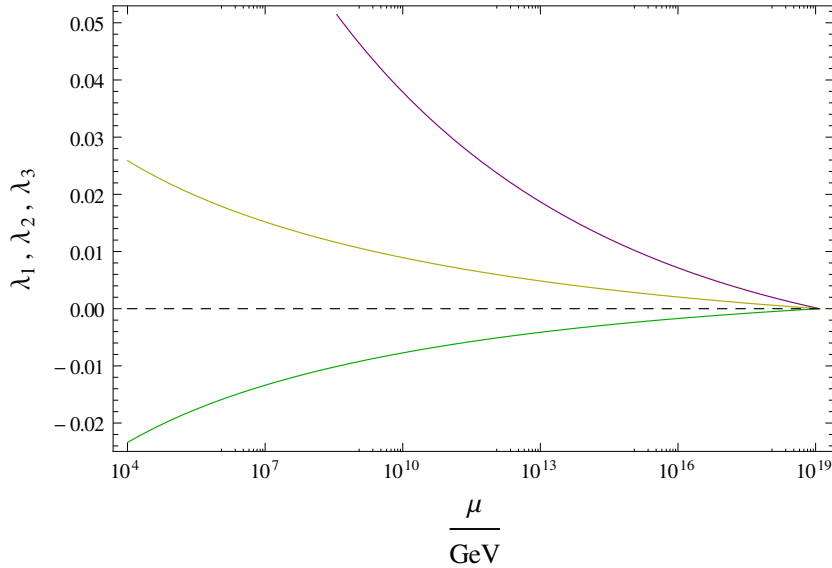
Figure 3.1: The bidoublet self couplings are plotted. The purple, green and yellow lines correspond to $\lambda_1$, $\lambda_2$ and $\lambda_3$ respectively. The doublet self-couplings have been chosen to $\kappa_1 = -\kappa_2 = 0.2$ at $\mu = 10^4$ GeV, while all other couplings are fixed by the shift symmetry to vanish at the Planck scale. As the beta-functions of $\lambda_1$, $\lambda_2$ and $\lambda_3$ their dependence on the choice of the initial conditions of $\kappa_1$ and $\kappa_2$ is marginal.

unbounded from below. For energies below $\mu = 10^{11}$ GeV, however, the stability is restored again. The situation found here is similar to the SM with a relatively light Higgs mass of $125$ GeV. There, assuming that the theory is valid up to high scales, the light Higgs mass results in a potential which is unstable above energy scales around $10^{11}$ GeV. Around that scale, the quartic coupling $\lambda$ becomes negative as its running is dominated by top-loop contributions driving it towards small values. The Standard Model potential does however not fall off completely. It is rescued by gauge contributions at higher energy scales.

**Metastability and the Renormalization Group Improved Potential**

The interpretation of such bumps of negative quartic couplings as in figure 3.2 becomes clear consulting the *renormalization group (RG) improved effective potential*. It is obtained applying the RG equation to the effective potential. A good review to this topic is found in Ref. [7]. The RG equation states that a physical quantity, such as the effective potential, cannot depend on the choice of the arbitrary scale parameter $\mu$ which is just introduced to define the parameters of the theory, *i.e.* its

couplings. Here, as a placeholder for the couplings of the theory it will be used $\lambda$. The RG equation for the effective potential is then given by

$$0 = \frac{\mathrm{d}V_{\mathrm{eff}}}{\mathrm{d}\mu} = \left[\mu\frac{\partial}{\partial\mu} + \beta_\lambda\frac{\partial}{\partial\lambda} - \gamma\phi\frac{\partial}{\partial\phi}\right]V_{\mathrm{eff}}, \tag{3.7}$$

where $\beta_\lambda = \mu\frac{\mathrm{d}\lambda}{\mathrm{d}\mu}$ is the beta-function with respect to $\lambda_i$ and $\gamma := \frac{\mu}{\phi}\frac{\mathrm{d}\phi}{\mathrm{d}\mu}$ is called the *anomalous dimension* which reflects the scale dependence of the wavefunction normalization $Z$ of the field $\phi$. Under the assumption that the contribution due to the anomalous dimension is small and therefore negligible, the equation 3.7 is solved by the ansatz

$$V_{\mathrm{eff}} = \lambda\left(\log[\phi/\mu]\right)\phi^4, \tag{3.8}$$

where due to dimensional reasons the dimensionless coupling $\lambda$ can depend only on the ratio $\phi/\mu$. Furthermore, here, $\lambda$ is given by $\lambda_1 + 4\lambda_2$ and $\lambda_1 - 4\lambda_3$ respectively as the potential V is considered in those field directions in which these combinations of bidoublet self-couplings represent the terms multiplying the radial field $\phi$. These field directions correspond to the flat directions of type Ic and Id respectively. For the two cases one finds the approximate renormalization group improved effective potentials

$$V_{\mathrm{eff}}^{\lambda_1+4\lambda_2} \approx \left(\lambda_1\left[\log(\phi/\mu)\right] + 4\lambda_2\left[\log(\phi/\mu)\right]\right)\phi^4 \tag{3.9}$$

and

$$V_{\mathrm{eff}}^{\lambda_1-4\lambda_3} \approx \left(\lambda_1\left[\log(\phi/\mu)\right] - 4\lambda_3\left[\log(\phi/\mu)\right]\right)\phi^4 \tag{3.10}$$

where the functional dependence of these couplings $\lambda_1[\phi]$ and $(\lambda_1 + \lambda_2)[\phi]$ on the field $\phi$ is just as the dependence of the corresponding couplings on $\mu$. Thus, the quantum corrections to the tree-level potential are expressed in terms of the running coupling $\lambda(\mu)$ with a renormalization point chosen at $\mu = \phi$. In figure 3.3 the effective potentials $V_{\mathrm{eff}}^{\lambda_1+4\lambda_2}$ and $V_{\mathrm{eff}}^{\lambda_1-4\lambda_3}$ according to (3.9) are shown. From this, it can be understood that the violation of the stability conditions (3.2d) and (3.2e) have to be interpreted as the emergence of additional minima of the potential for field values far away from the origin, always with regard to the corresponding field directions. These minima actually have to be considered as the true minima since they clearly exhibit smaller values of the potential in comparison to the minima near the origin.

This is due to the large field values they correspond to. Hence, the (false) minima near the origin are just meta-stable. Such metastable vacua may decay to the true vacuum states by tunneling through the potential barrier which seperates the two minima from each other. This mechanism, limited to the case of zero temperature, is described in Ref. [28] using a semi-classical approach. The author of [28], however, notes that before there was a quantitative description, the qualitative features of vaccum decay were already understood due to the analogy to nucleation processes in statistical physics: If in a certain volume $V$ vacuum decay occurs, a localized bubble of converted vacuum is formed. In this process, energy proportional to $V$ is set free which leads to further conversion at the surface. The bubble then grows until the total universe is in the new (true) vacuum state. For this to happen the bubble has, however, to exceed a critical size in the first place. Otherwise the loss in surface energy compensates the gain of energy due to the conversion and the bubble shrinks to nothing.

The possibility of vacuum decay, however, does not represent a problem to the consistency of the theory as long as the decay time is greater than the age of the universe. In fact, in the past this argument was used in order to set lower bounds on the SM Higgs mass [29] as such bounds are less stringent than demanding absolute stability. Besides zero temperature tunneling, which is a pure quantum effect, barrier penetration can also be thermally induced due to field fluctuations at finite temperature (see *e.g.* [30]). Under the assumption that the universe once was in an extremely hot phase, finite temperature penetration is considered the dominant process. However, as emphasized by the authors of [29], this assumption has not been proved to the present day as it is unclear if the universe has ever been hotter than $T \sim$ MeV. Although they admit that it is a plausible assumption, they argue further that such high temperatures in the early universe would not only exclude low SM Higgs masses but also many other popular models. For this reason, they focus on the metastability bound given by the assumption that vacuum decay occurs only due to zero temperature tunneling. This viewpoint will be shared here.

**Decay Probability due to Pure Quantum Tunneling**

In the analysis of Ref. [29], first the semi-classical approximation of the tunneling rate based on Ref. [28] is given and then a complete one-loop calculation is performed. Here, the discussion is restricted to the translation of their appoximate result to the

case of the LR symmetric model with shift symmetry.

In the semi-classical discussion the probability $p$ that the vacuum has decayed to the true vacuum is given by

$$p \sim \left(\frac{T_U}{R}\right)^4 e^{-S_0}, \tag{3.11}$$

where $T_U \sim 10^{10}$ yr is the age of the universe, $S_0$ is the classical so-called *bounce* action which describes the penetration process and $R$ is a dimensionful quantity that is associated to the *bounce* solutions. According to [29], $S_0$ is given by

$$S_0 = \frac{2\pi^2}{3|\lambda|}, \tag{3.12}$$

where $|\lambda|$ is the absolute value of the minimum of $\lambda$. Note that here it has already been accounted for the normalization factors used in [29] which differ from those used in this work. From this, demanding $p < 1$, a lower bound for $|\lambda|$ is found:

$$|\lambda| < 0.016 \tag{3.13}$$

Recall that $\lambda$ here represents $\lambda_1 + 4\lambda_2$ and $\lambda_1 - 4\lambda_3$ respectively. As can be seen from figure 3.4 these couplings do not fall below the bound expressed by (3.13). It can therefore be concluded that the electroweak minimum for the LR symmetric model including shift symmetry indeed can be at most metastable, but as the decay time of its vacuum exceeds the age of the universe this does not contradict the consistency of the model.

## 3.2.3 Stability in the Doublet Field Direction

The stability conditions corresponding to the field directions in the (electrically neutral) doublet subspace,

$$\kappa_1 > 0$$

$$\kappa_1 + \kappa_2 > 0,$$

require $\kappa_1$ and $\kappa_+ = \kappa_1 + \kappa_2$ to have positve values at the Planck scale.

The beta-functions of $\kappa_1$ and $\kappa_2$ (*cf.* (A.19)),

$$\beta_{\kappa_1} = \frac{1}{512\pi^2}\left[\kappa_1\left(-96g_1^2 - 144g_2^2 + 576\kappa_1 + 384\kappa_2\right) + 192\kappa_2^2 + 256\beta_1^2 + 128f_1^2\right]$$

$$+ 24g_1^4 + 12g_1^2 g_2^2 + 9g_2^4],$$

$$\beta_{\kappa_2} = \frac{1}{512\pi^2}\big[\kappa_2(-96g_1^2 - 144g_2^2 + 512\kappa_1 + 384\kappa_2) + 128f_1^2 + 12g_1^2 g_2^2 + 9g,$$

are dominated by positive-sign gauge contributions. Thus, $\kappa_1$ and $\kappa_2$ are driven to smaller values[3] such that they eventually become zero. This, however, is no problem for stability when sufficiently large initial conditions of both $\kappa_1$ and $\kappa_1 + \kappa_2$ are chosen. In fact, this ensures that, within the frame of shift symmetry, the Gildener-Weinberg conditions corresponding to the phenomenologically interesting parity-breaking flat directions of types Ia, Ib, IIa and IIb can be satisfied. In this context, observe that within shift symmetry the bidoublet-doublet couplings $\beta_1$ and $f_1$ are supposed to be small. In the case of $f_1$, shift symmetry even implies $f_1 \equiv 0$, which is a direct consequence of $\beta_{f_1}$ being proportional to $f_1$ [4]. For this reason, these Gildener-Weinberg conditions are mainly given by $\kappa_+ = \kappa_1 + \kappa_2 = 0$. Analogously the Gildener-Weinberg conditions to the associated parity-conserving flat directions are mainly given by $\kappa_1 = 0$. Hence, at the Planck scale $\kappa_1$ and $\kappa_2$ have to be chosen such that, on the one hand, symmetry breaking takes place at a phenomenologically interesting scale and, on the other hand, the parity-breaking flat directions, *i.e.* $\kappa_1 + \kappa_2 = 0$, emerge in the first place. This implies, $\kappa_1 > \kappa_+$ at the breaking scale and thus $\kappa_2$ being either negative at the Planck scale or evolving to negative values.

The discussion about stability is concluded presenting in Fig 3.5 the renormalization group flow of $\kappa_1$ and $\kappa_+$. An almost identical plot was already given in Ref. [6]. The RG flow shows clearly that for a large fraction of parameter space the parity-breaking Gildener-Weinberg conditions (green bar) can be reached without violating $\kappa_1 > 0$ before, *i.e.* before the emergence of parity-conserving flat directions (red bar). Yet it is not clear from the flow diagram alone, how fast the couplings run into the solutions. Thus, it is not clear, how large the initial values have to be chosen. In the next section, however, this will find further attention. It will turn out that $\kappa_1 + \kappa_2 = 0$ at the Gildener-Weinberg scale, which is approximately the breaking scale does not imply too large values of $\kappa_1$ and $\kappa_2$ at the Planck scale.

---

[3]There are no compensatory contributions from Yukawa couplings as the scalar doublets do not couple to fermions in the minimal model.

[4]The remaining scalar couplings exhibit the enhanced symmetry of separate $SU(2)_L \times SU(2)_R$ transformations of $\underline{\Phi}$ and $\underline{\Psi}$. For this reason, $f_1$ is not generated by quantum corrections at one loop level. Yet the situation should change at the two-loop level, as this symmetry is also explicitly broken by gauge interactions.

## 3.3 Symmetry Breaking

### 3.3.1 Adjusting the Big Hierarchy

Precedingly it was shown that in a large fraction of parameter space the potential is sufficiently (meta-)stable. In order to break the symmetry at a scale $v_R$, many orders of magnitude below the Planck scale $\Lambda_{\mathrm{Pl}}$, one has to choose appropriate values for the doublet self-couplings at $\Lambda_{\mathrm{Pl}}$. The running of the couplings then generates the big hierarchy. In practice however, $\kappa_1$ and $\kappa_2$ are not chosen at the Planck scale, but rather at the Gildener-Weinberg scale $\mu_{\mathrm{GW}}$ to satisfy the GW condition $\kappa_1 + \kappa_2 = 0$ that, as argued before, applies approximately for all maximally parity-breaking flat directions[5]. Then, one lets $\kappa_1$ and $\kappa_2$ evolve to obtain their values at the Planck scale. Finally, one is left with one free parameter. Here, this free parameter is chosen to be $\kappa_1$. In order to decide then in which flat direction the symmetry is actually broken, in the usual case of multiple simultaneously emerging flat directions, one has to consult the corresponding second derivatives of the potential, *i.e.* the scalar mass spectra. This was already mentioned in section 2.2.3 where the scalar masses to the various flat directions were given. One finds that, in the case of the shift symmetry imposed on the bidoublet, only flat direction of type Ib corresponds to a minimum. To be more precise, in the case of flat direction Ia (2.2.3) one has for instance

$$m_h^2 = -16(\lambda_2 + \lambda_3)(\kappa^2 + \kappa'^2) < 0,$$

as $\lambda_2 + \lambda_3 < 0$ (see figure 3.1). Similarly, for flat direction type IIa (2.2.3) one finds

$$m_{\phi_{2r}^0}^2 = f_1 v_R^2 + 8\lambda_2 \kappa^2 < 0 \qquad \text{and} \qquad m_{\phi_{2i}^0}^2 = f_1 v_R^2 - 8\lambda_3 \kappa^2 < 0, \qquad (3.14)$$

as shift symmetry implies $f_1 \equiv 0$ and $\lambda_2 < 0$ and $\lambda_3 > 0$ respectively. Since flat directions of types IIa and IIb are essentially connected via $(f_1 \to -f_1)$, the flat direction of type IIb does not represent a minimum neither.

Finally, for flat direction IIc (2.2.3) it is

$$m_{\{\phi_1^0, \phi_2^-\}}^2 = \frac{2\beta_1 - f_1}{2} v_R^2 < 0 \qquad \text{and} \qquad m_{\{\phi_2^0, \phi_1^+\}}^2 = \frac{2\beta_1 + f_1}{2} v_R^2 < 0. \qquad (3.15)$$

Here, one additionally has to use that $\beta_1$ is negative. This can be seen from its

---

[5]These include the phenomenologically interesting directions Ia, Ib, IIa and IIb plus the direction IIc which only breaks the $SU(2)_R$-subgroup while leaving the SM gauge group unbroken.

beta-function (A.19), which, at the Planck scale $\Lambda_{\text{Pl}}$, is generated by the positive gauge contribution

$$\beta_{\beta_1}(\Lambda_{\text{Pl}}) = \frac{9g_2^4(\Lambda_{\text{Pl}})}{256\pi^2}, \tag{3.16}$$

which remains the dominant contribution for its running. Thus, it is driven to negative values.

In contrast, for solution Ib it turns out that all scalar masses (2.2.3) are positive.Hence the symmetry is broken in this direction. Note that these considerations concerning the scalar masses did not require assumptions about the values of the doublet self couplings. This means that, in the minimal model, shift symmetry implies that symmetry breaking is exclusively possible along flat direction Ib. In Ref. [6] it has been stated that the flat directions of type I are disfavored with respect to directions IIa and IIb as they require additional means of fine-tuning, assuming that all scalar couplings be of the same order. This is however not the case when shift symmetry is imposed. Thus, *a priori* there is no problem of naturalness concerning flat direction Ib.

## 3.3.2 Little Hierarchy

Within shift symmetry, a big hierarchy can be generated by appropriate choice of the free parameters $\kappa_1$ and $\kappa_2$ following the procedure explained above. The only flat direction that corresponds to a minimum is then given by direction Ib. Even though one parameter, let it be $\kappa_1$, remains free it can however not be expected that adjusting this parameter affects the little hierarchy significantly. The little hierarchy in direction Ib, represented by the ratio

$$\frac{\kappa^2 + \kappa'^2}{v_R^2} = \frac{-\beta_1}{2\lambda_1 - 8\lambda_3} \tag{3.17}$$

is given by the doublet-bidoublet coupling $\beta_1$ and the bidoublet self-couplings $\lambda_1$ and $\lambda_3$, whose running is essentially fixed by the shift symmetry: While the combination $\lambda_1 - 4\lambda_3$ does not depend on the $\kappa_1$ and $\kappa_2$ at one loop, the doublet-bidoublet coupling has only little dependence on them, which can be seen from their beta-functions (see (A.19)). Hence, shift symmetry cannot be expected to provide freedom in the choice of parameters in order to adjust the little hierarchy to any desired value. Before presenting the results based on the numerical solution of the full system of the beta-functions, the little hierarchy (3.17) is roughly estimated. For this purpose, it is

used a linear approximation of $\beta_1$ and $\lambda_1 - 4\lambda_3$ from the Planck scale $\Lambda_{\mathrm{Pl}}$ down to the Gildener-Weinberg scale at $\mu_{GW} = 10\,\mathrm{TeV}$:

$$\beta_1(\mu_{\mathrm{GW}}) - \underbrace{\beta_1(\Lambda_{\mathrm{Pl}})}_{=0} \approx \beta_{\beta_1}(10^{11.5}\,\mathrm{GeV}) \log\left(\frac{\mu_{\mathrm{GW}}}{\Lambda_{\mathrm{Pl}}}\right), \tag{3.18}$$

where the the beta-function $\beta_{\beta_1}$ is taken at the center between $\Lambda_{\mathrm{Pl}}$ and $\mu_{\mathrm{GW}}$ on the logarithmic scale. Analogously, the combination $\lambda_1 - 4\lambda_3$ of doublet self-couplings which are generated not only by gauge loops, but dominantly by top-loops, is linearly approximated to

$$(\lambda_1 - 4\lambda_3)(\mu_{\mathrm{GW}}) - \underbrace{(\lambda_1 - 4\lambda_3)(\Lambda_{\mathrm{Pl}})}_{=0} \approx \beta_{\lambda_1 - 4\lambda_3}(\lambda_1 - 4\lambda_3) \log\left(\frac{\mu_{\mathrm{GW}}}{\Lambda_{\mathrm{Pl}}}\right) \tag{3.19}$$

As the gauge- and top-loops give the main contribution to both beta-functions in (3.18) and (3.19), all the other contributions will be neglected for this estimate. While the expression for $\beta_{\beta_1}(10^{11.5}\,\mathrm{GeV})$ is obtained from (3.16) by simply exchanging $\Lambda_{\mathrm{Pl}}$ by $\mu = 10^{11.5}\,\mathrm{GeV}$, the beta-function of $\lambda_1 - 4\lambda_3$ at that scale is given by

$$\beta_{\lambda_1 - 4\lambda_3}(10^{11.5}\,\mathrm{GeV}) \approx \frac{1}{128\pi^2}\left(15g_2^4(10^{11.5}\,\mathrm{GeV})) - 2T_4(10^{11.5}\,\mathrm{GeV})\right). \tag{3.20}$$

Thus, the little hierarchy can be estimated to

$$\frac{\kappa^2 + \kappa'^2}{v_R^2} \approx \frac{-9g_2^4(\Lambda_{\mathrm{Pl}})}{4(15g_2^4(\mu_{\mathrm{GW}}) - 2T_4(\mu_{\mathrm{GW}})}) \approx 0.35. \tag{3.21}$$

This value is of the same order of magnitude as those values obtained by solving the full differential equation system given by the beta-functions of the model. In figure 3.7 these results are shown, including the dependence on $\kappa_1$ which is chosen to be the only free parameter of the model. Note that doublet-self couplings above $\kappa_1(\Lambda_{\mathrm{Pl}}) \approx 2.5$ lead to the emergence of Landau poles and thus have not been considered any further.

The little hierarchy (3.17) obtained is not sufficiently large in order to fit present bounds on the right-handed scale [17–20]. With the (left-handed) electroweak scale fixed at

$$\kappa^2 + \kappa'^2 = (174\,\mathrm{GeV})^2. \tag{3.22}$$

a value of 0.15 (*cf.* figure 3.7) fore instance corresponds to a right-handed scale at

$$v_R = \sqrt{\frac{\kappa^2 + \kappa'^2}{0.15}} = 450 \, \text{GeV}, \tag{3.23}$$

which is already excluded. It can be concluded that with shift symmetry alone, the electroweak scale cannot be stabilized against the breaking scale of left-right symmetry. Instead of setting other boundary conditions at the Planck scale to generate this hierarchy the problem is approached by introducing additional particle representations to the model and thereby modifiing the RG running of the scalar couplings. In particular, the most simple extension, a complete singlet under the gauge group, is introduced.
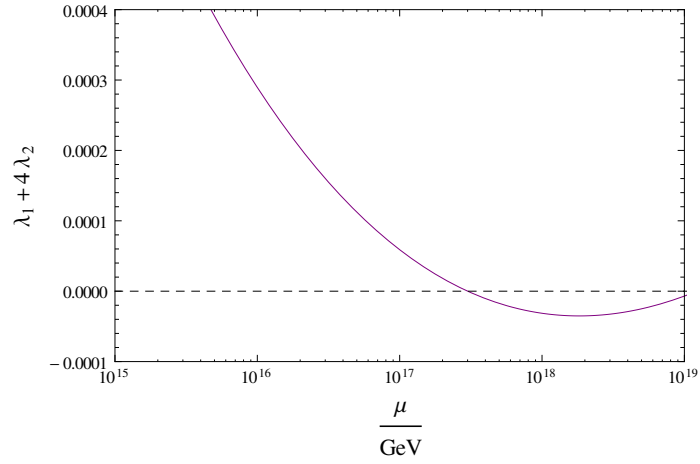
(a) Running of $\lambda_1 + 4\lambda_2$
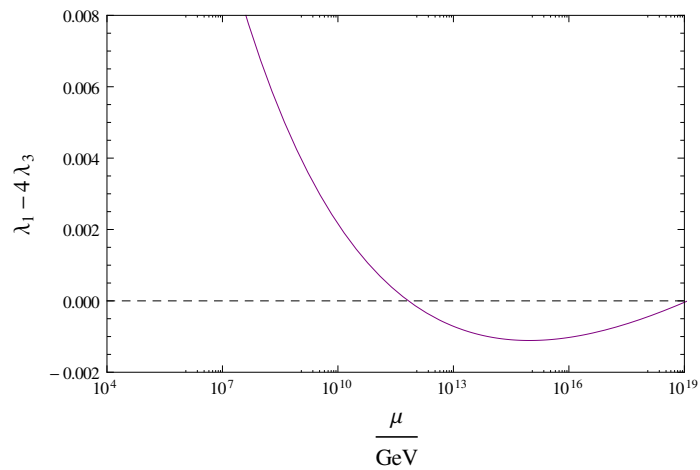


(b) Running of $\lambda_1 - 4\lambda_3$

Figure 3.2: The running of the stability conditions $\lambda_1 + 4\lambda_2$ and $\lambda_1 - 4\lambda_3$ is plotted. At energy scales around $\mu = 10^{17}\,\text{GeV}$ and $\mu = 10^{11}\,\text{GeV}$ the scalar potential is destabilized in the field directions corresponding to the flat directions Ic and Id respectively, as in these directions the potential is given by the expressions $V = (\lambda_1 + 4\lambda_2)\phi$ and $V = (\lambda_1 - 4\lambda_3)\phi$ respectively.
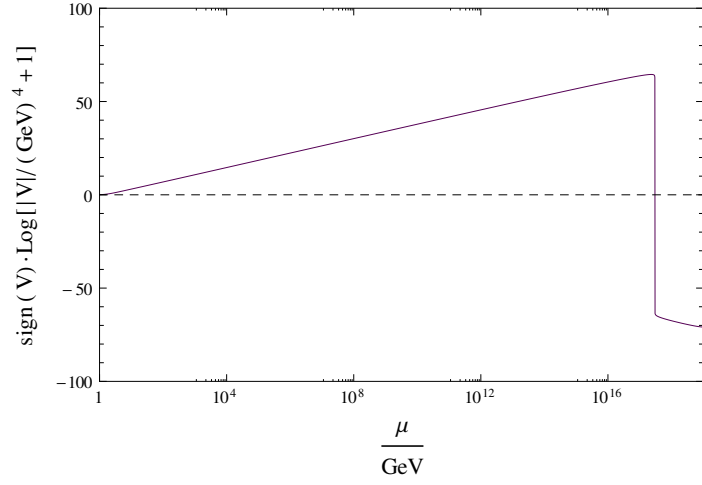
(a) $\left(\lambda_1[\phi] + 4\lambda_2[\phi]\right)\phi^4$
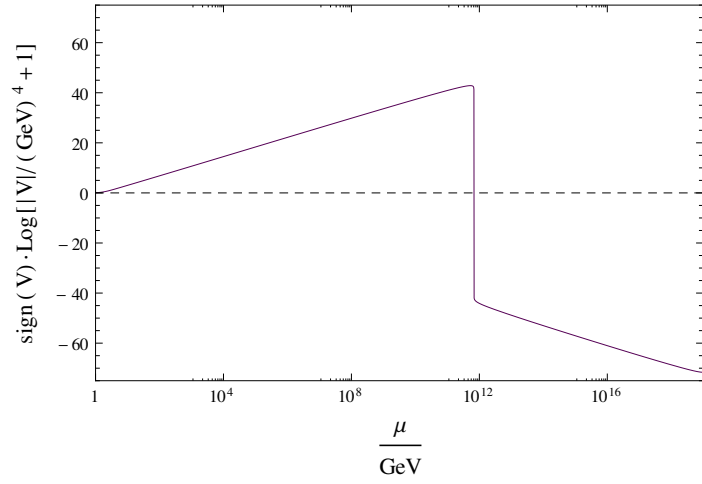


(b) $\left(\lambda_1[\phi] - 4\lambda_3[\phi]\right)\phi^4$

Figure 3.3: The RG improved potentials in the field directions corresponding to the flat directions Ic (fig. 3.3(a)) and Id (fig. 3.3(b)) are plotted. Besides the minima that are supposed to emerge near the origin in field space due to quantum corrections which are treated by the Gildener-Weinberg method, the violation of the stability conditions (3.2d) and (3.2e) lead to additional minima at high field values. These minima have to be viewed as the absolute (true) minima of the theory.
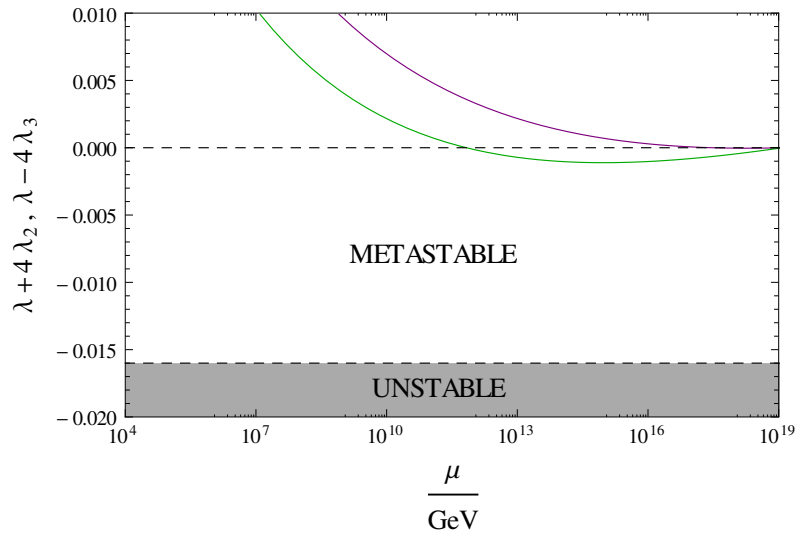
Figure 3.4: The running of the quantities $\lambda_1 + 4\lambda_2$ (purple line) and $\lambda_1 - 4\lambda_3$ (green line), which give the potential in field directions Ic and Id respectively, is replotted in presence of the metastability bound at $\lambda = -0.015$, where $\lambda$ represents $\lambda_1 + 4\lambda_2$ and $\lambda_1 - 4\lambda_2$ respectively. Being above this bound, the low-energy vacuum is metastable in the sense that its decay time exceeds the age of the universe.
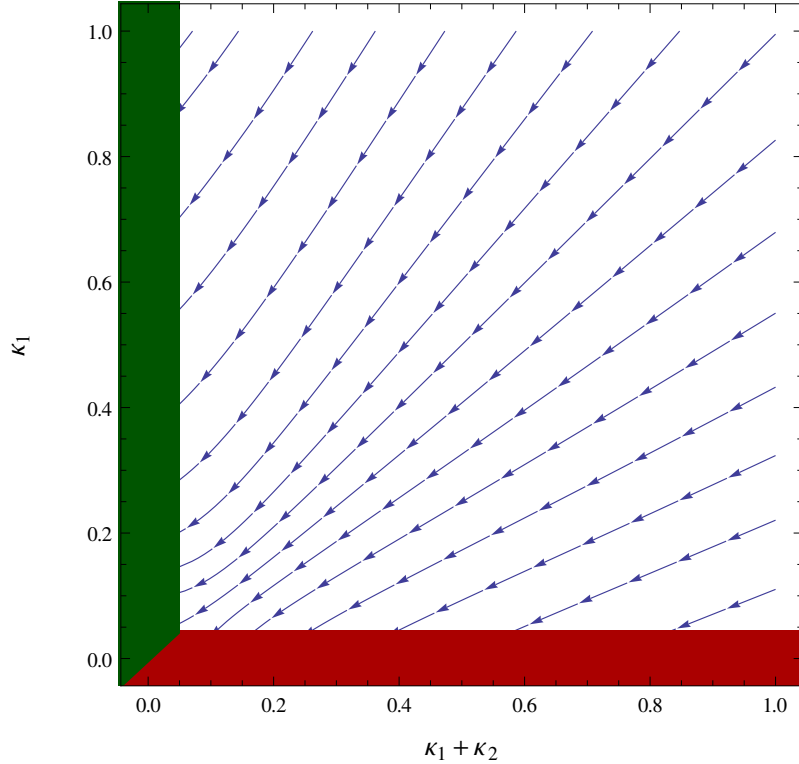
Figure 3.5: The RG group flow, toward lower energies, is shown in the $(\kappa_1, \kappa_+)$-plane (*cf.* Fig. 1 in Ref. [6]). It is assumed that the doublet-bidoublet couplings do not contribute, which is a good approximation as they are small due to shift symmetry. Additionally, the gauge couplings are fixed to their values at $M_Z$ for simplicity. The flow reveals that the potential is (meta-)stable for a large parameter space region in field directions of the doublet subspace. Furthermore there is a large fraction that corresponds to maximally parity-breaking solutions which require (approximately) $\kappa_1 + \kappa_2$ (green bar). Even for small positive starting values of $\kappa_2$ the couplings run into these solutions as gauge contributions let the combination $\kappa_1 + \kappa_2$ run down faster than $\kappa_1$.
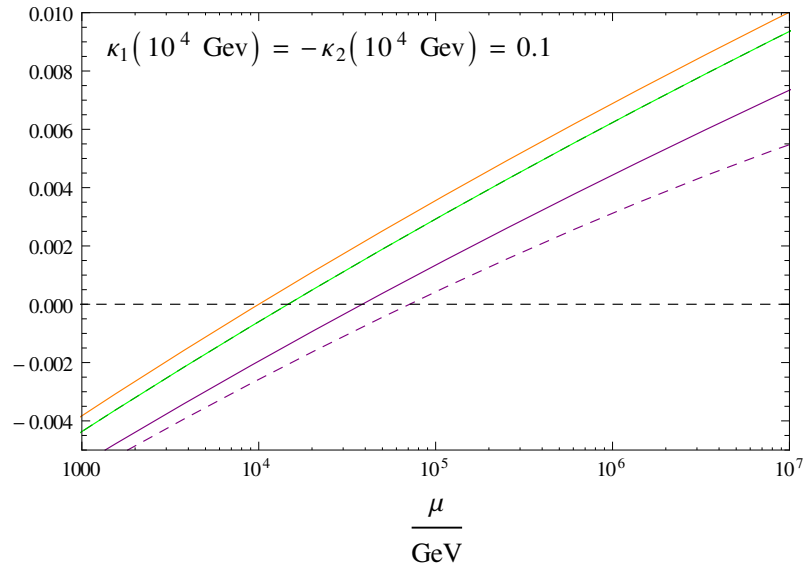
Figure 3.6: The running of the GW conditions is depicted. Every line corresponds to a maximally parity-breaking GW condition: Ia (purple line), Ib (dashed purple line), IIa and IIb (degenerate green line) and IIc (orange line). Once a line hits the zero line the associated GW condition is fulfilled. Symmetry breaking, however, occurs only when the flat direction corresponds to a minimum of the potential, *i.e.* if all second derivatives are greater than zero. The plot is obtained by setting $\kappa_1 = -\kappa_2 = 0.1$ at $\mu_{\mathrm{GW}} = 10^4\,\mathrm{GeV}$.
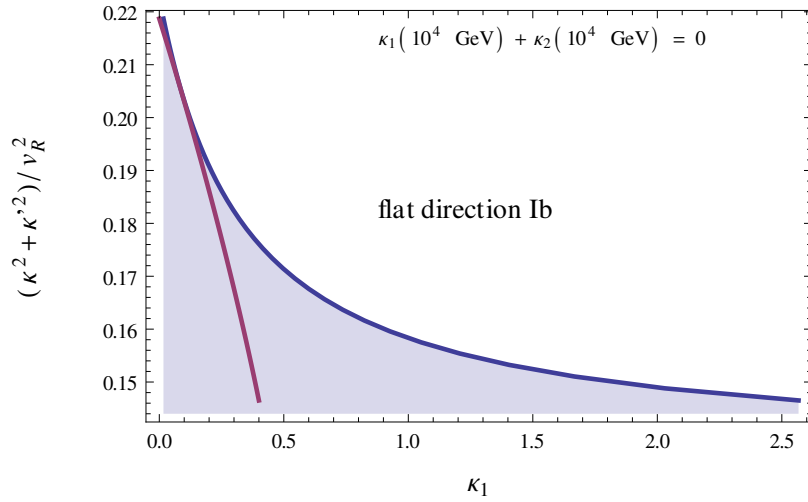
Figure 3.7: Within shift symmetry radiative symmetry breaking occurs exclusively in flat directions of type Ib. Here, the little hierarchy between the breaking scale of the left-right symmetry and the electroweak scale is plotted in dependence of the doublet self coupling $\kappa_1$ at the Planck scale (blue curve) and at the GW scale $\mu_{GW} = 10^4$ GeV (red curve). The value of the little hierarchy is essentially fixed by the gauge- and top-loops generating the intermiediate doublet-bidoublet couplings and bidoublet self-couplings.

# Chapter 4

# Extension I: Fermionic Singlet

## 4.1 Introduction

### 4.1.1 Definition

A Majorana-type fermionic singlet, called $f$ in the following, is added to the minimal LR symmetric model. It is a singlet under the whole gauge group. It transforms trivially under parity and the $\mathbb{Z}_4$-symmetry. In the notation introduced in 2.5 the quantum numbers of $f$ are given by

$$f \sim [(\tfrac{\mathbf{1}}{\mathbf{2}}, \mathbf{0}) \oplus (\mathbf{0}, \tfrac{\mathbf{1}}{\mathbf{2}})](\mathbf{1}, \mathbf{1}, \mathbf{1}, 0) \tag{4.1}$$

Furthermore, being a Majorana representation it is constrained by the condition

$$f^c \equiv f. \tag{4.2}$$

Though an explicit mass term $m\bar{f}f$ does not violate any of these symmetries it is forbidden by scale invariance. In addition to the kinetic term, introducing $f$ leads to a Yukawa interaction to leptons and scalar doublets

$$\mathcal{L}_{\text{Yuk},\,f} = -g_f^i \underline{\bar{L}}^i \underline{\Psi} f + h.c. \tag{4.3a}$$

In terms of the right- and left-handed fields this becomes:

$$\mathcal{L}_{\text{Yuk},\,f} = -g_f^i \bar{L}^i \chi_L f - g_f^i \bar{R}^i \chi_R f + H.c.. \tag{4.3b}$$

Here, the index $i$ denotes the flavor of the lepton. Thus, $f$ is coupled to each flavor by an individual coupling $g_f^i$. It is easy to convince oneself that this term respects

the symmetries of the theory[1]. Note that there does not emerge an interaction that couples the *quarks* to the scalar doublets since such would not be invariant under $SO(3)$-color and $U(1)_{B-L}$. Beside the Yukawa interaction (4.3) no further terms with dimension smaller or equal than four emerge. Thus, the original Lagrangian is modified by

$$\mathcal{L}_f = \bar{f} i \slashed{\partial} f - g_f^i \underline{\bar{L}}^i \underline{\Psi} f + h.c.. \tag{4.4}$$

Clearly, a fermionic singlet represents the most simple extension to the model in terms of additional particle representations. Coupling to doublets and leptons, $f$ contributes via fermion loops to the scalar doublet self-couplings $\kappa_1$ and $\kappa_2$ and to the intermediate couplings $\beta_1$ and $f_1$. In the following, these contributions to the renormalization group running of the scalar (and lepton Yukawa) couplings will be calculated and its effect on the symmetry breaking mechanism discussed. In particular, it will be analysed if the desired little hierarchy can be obtained by appropriate adjustment of $g_f^i$.

## 4.1.2 Phenomenological Implications

Before turning to the renormalization group analysis it will be discussed briefly which phenomenological implications arise by introduction of a fermionic singlet. As it is not observed it must be ensured that it is hidden. The interaction term (**??**) technically represents a mass term, as $\chi_R^0$ is supposed to acquire a vacuum expectation value, and thus leads to a mixing between standard neutrinos $\nu^i$ and the singlet fermion $f$. For the uncharged fermions one then finds the general mass matrix

$$\mathcal{L} \subset \left( \bar{\nu}_L^i, \bar{\nu}_R^i, \bar{f} \right) \cdot \begin{pmatrix} 0 & \frac{\kappa Y_{\underline{L}}^{+ij} + \kappa' Y_{\underline{L}}^{-ij}}{\sqrt{2}} & g_f^i v_L \\ \frac{\kappa Y_{\underline{L}}^{+ij} + \kappa' Y_{\underline{L}}^{-ij}}{\sqrt{2}} & 0 & g_f^i v_R \\ g_f^j v_L & g_f^j v_R & m \end{pmatrix} \cdot \begin{pmatrix} \nu_L^j \\ \nu_R^j \\ f \end{pmatrix}. \tag{4.5}$$

For a vanishing vacuum expectation value of the left scalar doublet which corresponds to the parity breaking flat directions, and without explicit mass term $m$ as

---

[1] In this chapter the $\mathbb{Z}_4$-transformation property of the scalar doublet is redefined to be: $\chi_R \to i\chi_R$. This, however, does not affect any other doublet interaction term.

required by scale invariance this becomes

$$
\mathcal{L} \subset \left( \bar{\nu}_L^i, \bar{\nu}_R^i, \bar{f} \right) \cdot \begin{pmatrix} 0 & \frac{\kappa Y_L^{+ij} + \kappa' Y_L^{-ij}}{\sqrt{2}} & 0 \\ \frac{\kappa Y_L^{+ij} + \kappa' Y_L^{-ij}}{\sqrt{2}} & 0 & g_f^i v_R \\ 0 & g_f^j v_R & 0 \end{pmatrix} \cdot \begin{pmatrix} \nu_L^j \\ \nu_R^j \\ f \end{pmatrix}. \tag{4.6}
$$

In the limit of a single generation and for $v_R \gg \kappa, \kappa'$ one finds one massless eigenstate $\nu$ with

$$
m_\nu = 0 \tag{4.7}
$$

and two degenerate heavy states $N_1$ and $N_2$ with

$$
m_{N_{1,2}} = \pm g_f v_R \left( 1 + \frac{(\kappa Y_L^+ + \kappa' Y_L^-)^2}{4(g_f v_R)^2} \right). \tag{4.8}
$$

Under the assumption of $g_f$ and the lepton Yukawa couplings being of comparable magnitude the mixing matrix is approximated by

$$
\begin{pmatrix} \nu \\ N_1 \\ N_2 \end{pmatrix} = \begin{pmatrix} 1 + \mathcal{O}\left(\frac{\kappa + \kappa'}{v_R}\right) & 0 & \mathcal{O}\left(\frac{\kappa + \kappa'}{v_R}\right) \\ \mathcal{O}\left(\frac{\kappa + \kappa'}{v_R}\right) & \frac{-1}{\sqrt{2}} + \mathcal{O}\left(\frac{\kappa^2 + \kappa'^2}{v_R^2}\right) & \frac{1}{\sqrt{2}} \\ \mathcal{O}\left(\frac{\kappa + \kappa'}{v_R}\right) & \frac{1}{\sqrt{2}} + \mathcal{O}\left(\frac{\kappa^2 + \kappa'^2}{v_R^2}\right) & \frac{1}{\sqrt{2}} \end{pmatrix} \cdot \begin{pmatrix} \nu_L \\ \nu_R \\ f \end{pmatrix}. \tag{4.9}
$$

One finds that for a sufficiently large little hierarchy the massless state is mainly given by the left-handed active neutrino $\nu_L$ while the heavy states are given by the right-handed active neutrino $\nu_R$ and $f$. Thus, though there was no explicit massterm introduced for the fermionic singlet it is hidden as it acquires a mass proportional to the right handed VEV via the Yukawa interaction (4.3). Simultaneously it lowers the mass of the left-handed neutrinos via a seesaw-type mechanism (see Ref. [4] and references therein).

## 4.2 Contributions to Renormalization Group Functions

The introduction of the fermionic singlet $f$ leads to contributions to the doublet self-couplings, $\kappa_1$ and $\kappa_2$, and doublet-bidoublet couplings, $\beta_1$ and $f_1$, via one-loop

box diagrams of the following kinds:

- doublet self-coupling:



$$\text{and} \tag{4.10}$$

and

- doublet-bidoublet coupling:



$$\text{and} \tag{4.11}$$

In the following section 4.2.1, the resulting corrections to the beta-functions of $\kappa_1$ and $\kappa_2$ will be calculated. For this purpose, the counterterms to these diagrams have to be calculated. Likewise, in section 4.2.2 the contributions to $\beta_{\beta_1}$ and $\beta_{f_1}$ are determined. In fact, the latter contributions are the more interesting ones, as they, together with the bidoublet self-couplings, determine the little hierarchy.

## 4.2.1 Doublet Self-Couplings

### Vertex Corrections

In order to calculate the contributions to $\kappa_1$ and $\kappa_2$ the standard notation of left- and right-handed fields is used. Furthermore, it is convenient to rearrange the doublet self-couplings: In terms of $\kappa_1$ and $\kappa_2$ the doublet self-couplings are given by

$$V \subset \kappa_1(\chi_L^\dagger \chi_L + \chi_R^\dagger \chi_R)^2 + \kappa_2(\chi_L^\dagger \chi_L - \chi_R^\dagger \chi_R)^2. \tag{4.12}$$

Thus, the $\kappa_1$- and $\kappa_2$-terms represent the *symmetric* and the *antisymmetric* parts of the doublet self-coupling respectively. These will be combined to a chirality

conserving coupling, which will be called $\bar{\kappa}_1$ and one that mixes the left- and right-handed fields, called $\bar{\kappa}_2$:

$$
\begin{aligned}
&\frac{\kappa_1}{2}(\chi_L^\dagger \chi_L + \chi_R^\dagger \chi_R)^2 + \frac{\kappa_2}{2}(\chi_L^\dagger \chi_L - \chi_R^\dagger \chi_R)^2 \\
&= \frac{\kappa_1}{2}\left[(\chi_L^\dagger \chi_L)^2 + 2\chi_L^\dagger \chi_L \chi_R^\dagger \chi_R + (\chi_R^\dagger \chi_R)^2\right] + \frac{\kappa_2}{2}\left[(\chi_L^\dagger \chi_L)^2 - 2\chi_L^\dagger \chi_L \chi_R^\dagger \chi_R + (\chi_R^\dagger \chi_R)^2\right] \\
&= \underbrace{(\frac{\kappa_1 + \kappa_2}{2})}_{\equiv \bar{\kappa}_1}\left[(\chi_L^\dagger \chi_L)^2 + (\chi_R^\dagger \chi_R)^2\right] + \underbrace{(\kappa_1 - \kappa_2)}_{\equiv \bar{\kappa}_2}\left[\chi_L^\dagger \chi_L \chi_R^\dagger \chi_R\right]
\end{aligned}
\tag{4.13}
$$

Thus, $\kappa_1$ and $\kappa_2$ in terms of $\bar{\kappa}_1$ and $\bar{\kappa}_2$ are given by

$$
\kappa_1 = \bar{\kappa}_1 + \frac{\bar{\kappa}_2}{2} \qquad \text{and} \qquad \kappa_2 = \bar{\kappa}_1 - \frac{\bar{\kappa}_2}{2}. \tag{4.14}
$$

Using this basis, the diagrams contributing to $\bar{\kappa}_1$ then are



$$\tag{4.15}$$

And there is one diagram contributing to $\beta_{\bar{\kappa}_2}$. It is given by



$$\tag{4.16}$$

In order to extract the divergent parts of these diagrams the following momentum assignments will be used:



$$
\text{where} \quad
\begin{cases}
k' = k + p_3 \\[2mm]
k'' = k + p_2 + p_3 \\[2mm]
k''' = k + p_2 + p_3 + p_4 \\[2mm]
0 = p_1 + p_2 + p_3 + p_4
\end{cases}
\tag{4.17}
$$

The external momenta are denoted by $p_1$, $p_2$, $p_3$ and $p_4$ while $k$ denotes the loop-momentum which it is integrated over.

The first diagram in (4.15) then gives:[2]

$$
\begin{aligned}
&\underbrace{(-1)}_{\text{fermion loop}}(-i)^4 \sum_{i,j}(g_f^i g_f^j)^2 \mu^{2\epsilon} \int \frac{\mathrm{d}^d k}{(2\pi)^d} \mathrm{Tr}\left[ \frac{i\slashed{k}}{k^2 + i\epsilon} \cdot \frac{i\slashed{k}'}{k'^2 + i\epsilon} \cdot \frac{i\slashed{k}''}{k''^2 + i\epsilon} \cdot \frac{i\slashed{k}'''}{k'''^2 + i\epsilon} \right] \\[3mm]
&= -\sum_{i,j}(g_f^i g_f^j)^2 \mu^{2\epsilon} \int \frac{\mathrm{d}^d k}{(2\pi)^d} \mathrm{Tr}\left[ \frac{(\slashed{k})(\slashed{k}+\slashed{p}_3)(\slashed{k}+\slashed{p}_2+\slashed{p}_3)(\slashed{k}-\slashed{p}_1)}{k^2(k+p_3)^2(k+p_2+p_3)^2(k-p_1)^2} \right] \\[3mm]
&= -\sum_{i,j}(g_f^i g_f^j)^2 \mu^{2\epsilon} \mathrm{Tr}\left[ \gamma_\mu \gamma_\nu \gamma_\rho \gamma_\sigma \right] \int \frac{\mathrm{d}^d k}{(2\pi)^d} \frac{(k^\mu)(k^\nu + p_3^\nu)(k^\rho + p_2^\rho + p_3^\rho)(k^\sigma - p_1^\sigma)}{k^2(k+p_3)^2(k+p_2+p_3)^2(k-p_1)^2}
\end{aligned}
$$

Here only the term proportional to $k^4$ gives a divergent contribution. Thus, one obtains:



---

[2]The feynman rules of the minimal model are take from Ref. [25] and the loop integrals occuring here, which are the well known Passarino-Veltman functions [31] (for a review see Ref. [32]).

$$= \text{UV finite} - \sum_{i,j}(g_f^i g_f^j)^2 \mu^{2\epsilon} \underbrace{\text{Tr}\left[\gamma_\mu \gamma_\nu \gamma_\rho \gamma_\sigma\right]}_{=4(\eta_{\mu\nu}\eta_{\rho\sigma}-\eta_{\mu\rho}\eta_{\nu\sigma}+\eta_{\mu\sigma}\eta_{\nu\rho})} \cdot \underbrace{\int \frac{\mathrm{d}^d k}{(2\pi)^d} \frac{k^\mu k^\nu k^\rho k^\sigma}{k^2(k+p_3)^2(k+p_2+p_3)^2(k-p_1)^2}}_{=\text{UV finite}+\frac{i\pi^2}{(2\pi)^d\mu^\epsilon}\frac{1}{12\epsilon}(\eta^{\mu\nu}\eta^{\rho\sigma}+\eta^{\mu\rho}\eta^{\nu\sigma}+\eta^{\mu\sigma}\eta^{\nu\rho})}$$

$$= \text{UV finite} - \sum_{i,j}(g_f^i g_f^j)^2 \mu^\epsilon \frac{i\pi^2}{(2\pi)^d}\frac{4(d^2+2d)}{12\epsilon}$$

$$= \text{UV finite} - i\mu^\epsilon \frac{8\vec{g}_f^4}{16\pi^2\epsilon} \tag{4.18}$$

where in the last step $d$ has been set to 4 since the expression multiplying $1/\epsilon$ is analytical at $4-d = \epsilon = 0$. Note that in the following this will be done without mentioning explicitly. Furthermore in the last line the notation $\vec{g}_f^T = (g_f^1, g_f^2, g_f^3)$ has been introduced.

As the divergent part of the just calculated diagram does not depend on the external momenta, the divergent parts of the remaining diagrams must be the identical to (4.18). Adding up the diagrams then results in:



$$= \text{UV finite} - (S_1 + S_2 + S_3 + S_4)\left(\vec{g}_f^4 \mu^\epsilon \frac{i\pi^2}{(2\pi)^4}\frac{8}{\epsilon}\right) \tag{4.19}$$

and



$$= \text{UV finite} - S_6\left(\vec{g}_f^4 \mu^\epsilon \frac{i\pi^2}{(2\pi)^4}\frac{8}{\epsilon}\right) \tag{4.20}$$

To obtain the correct symmetry factors $S_i$, recall that these diagrams are of order $\mathcal{O}\left(g_f^4\right)$ in the perturbation series. Hence, naturally there emerges a factor of 1/4! coming from the expansion of the exponential function. In addition, there is a

factor of 4 due to Pascal's law and a factor of 2 coming from choosing the vertex for one of the daggered fields. Thus, one finds $S_i = (1/4!) \cdot 4 \cdot 2 = 1/3$. In the following, upcoming symmetry factors are obtained by analogous considerations and will not be discussed in detail. In order to calculate the contribution to the $\beta$-functions $\beta_{\bar{\kappa}_1}$ and $\beta_{\bar{\kappa}_2}$ the counterterms corresponding to the above diagrams are needed. As already mentioned, in the MS-scheme the counterterms exactly subtract the divergent parts. This is equivalent to requesting:

UV finite = $S_1$  $+ S_2$  $+ S_3$  $S_4$  $+$ 

and

UV finite = $S_5$  $+$  ,

where the diagrams  represent the counterterms of $\bar{\kappa}_1$ and $\bar{\kappa}_2$ respectively.

Finally one finds, the contribution due to $f$ to the counterterms corresponding to $\bar{\kappa}_1$ and $\bar{\kappa}_2$ is

$$\Delta_f \delta\bar{\kappa}_1 = -\frac{16}{3}\vec{g}_f^4 \frac{1}{16\pi^2}\frac{1}{\epsilon} \qquad \text{and} \qquad \Delta_f \delta\bar{\kappa}_2 = -\frac{4}{3}\vec{g}_f^4 \frac{1}{16\pi^2}\frac{1}{\epsilon}. \tag{4.21}$$

In terms of $\kappa_1$ and $\kappa_2$ this becomes using equation (4.14)

$$\Delta_f \delta\kappa_1 = -\frac{18}{3}\vec{g}_f^4 \frac{1}{16\pi^2}\frac{1}{\epsilon} \qquad \text{and} \qquad \Delta_f \delta\kappa_2 = -\frac{14}{3}\vec{g}_f^4 \frac{1}{16\pi^2}\frac{1}{\epsilon}. \tag{4.22}$$

One further ingredient for the corrections to the beta-functions of $\kappa_1$ and $\kappa_2$ is needed, namely the contribution to the doublet wavefunction renormalization.

**Scalar Doublet Wavefunction Correction**

The contribution to the wavefunction renormalization of $\underline{\Psi}$ due to $f$ is given by a loop diagram which contains virtual leptons and $f$. Its divergent part is calculated to be

$$
S_6 \cdot \underline{\Psi} \to \bigcirc\!\!\!\!\overset{\underline{L}}{\underset{f}{}}\!\!\! \to \underline{\Psi} \;=\; S_6 \underbrace{(-1)}_{\text{fermion loop}} (-i)^2 \sum_i g_f^i g_f^i \mu^\epsilon \int \frac{\mathrm{d}^d k}{(2\pi)^d} \mathrm{Tr}\left[ \frac{i \slashed{k}}{k^2 + i\epsilon} \cdot \frac{i(\slashed{p} - \slashed{k})}{(p-k)^2 + i\epsilon} \right]
$$

$$
= -S_6 \vec{g}_f^2 \mu^\epsilon \mathrm{Tr}\left[\gamma_\mu \gamma_\nu\right] \int \frac{\mathrm{d}^d k}{(2\pi)^d} \frac{k^\mu (p^\nu - k^\nu)}{k^2(p-k)^2}
$$

$$
= \text{UV finite} - S_6 \vec{g}_f^2 \mu^\epsilon \underbrace{\mathrm{Tr}\left[\gamma_\mu \gamma_\nu\right]}_{=4\eta_{\mu\nu}} \frac{i\pi^2}{(2\pi)^d \mu^\epsilon} \left[ -\frac{1}{\epsilon} p^\mu p^\nu + \frac{1}{6\epsilon} p^2 \eta^{\mu\nu} - \frac{2}{3\epsilon} p^\mu p^\nu \right]
$$

$$
= \text{UV finite} - S_6 \vec{g}_f^2 \frac{i4\pi^2}{(2\pi)^d} \frac{1}{\epsilon} \left[ -p^2 + \frac{d}{6} p^2 - \frac{2}{3} p^2 \right]
$$

$$
= \text{UV finite} \; + S_6 \vec{g}_f^2 \frac{i4\pi^2}{(2\pi)^4} \frac{1}{\epsilon} p^2. \tag{4.23}
$$

Here, the symmetry factor is given by $S_6 = 1/2! \cdot 2 = 1$. From this the contribution to the wavefunction renormalization of $\underline{\Psi}$ can be obtained

$$
ip^2 \Delta_f \delta Z_{\underline{\Psi}} = -ip^2 \vec{g}_f^2 \frac{4}{16\pi^2 \epsilon}. \tag{4.24}
$$

**Contribution to beta-functions**

Using now the defining expression for one-loop $\beta$-functions in the MS-scheme (A.18), one finally obtains for $\kappa_1$ and $\kappa_2$

$$
\Delta_f \beta_{\kappa_1} = \underbrace{D_g}_{=1/2} \frac{\partial \Delta_f \delta \kappa_1^{(1)}}{\partial g_f^i} g_f^i - 2\kappa_1 \underbrace{D_g}_{=1/2} \frac{\partial Z_{\underline{\Psi}}^{(1)}}{\partial g_f^i} g_f^i - D_g \Delta_f \delta \kappa_1
$$

$$
= \frac{3}{2} \Delta_f \delta \kappa_1 - 2\kappa_1 \Delta_f \delta Z_{\underline{\Psi}}
$$

$$
= \frac{1}{16\pi^2} [ -9 \vec{g}_f^4 + 8\kappa_1 \vec{g}_f^2 ] \tag{4.25}
$$

and

$$\Delta_f \beta_{\kappa_2} = \underbrace{D_g}_{=1/2} \frac{\partial \Delta_f \delta \kappa_2^{(1)}}{\partial g_f^i} g_f^i - 2\kappa_2 \underbrace{D_g}_{=1/2} \frac{\partial Z_{\underline{\Psi}}^{(1)}}{\partial g_f^i} g_f^i - D_g \Delta_f \delta_{\kappa_2}$$

$$= \frac{3}{2} \Delta_f \delta \kappa_2 - 2\kappa_2 \Delta_f \delta Z_{\underline{\Psi}}$$

$$= \frac{1}{16\pi^2} [-7\vec{g}_f^4 + 8\kappa_2 \vec{g}_f^2]. \tag{4.26}$$

## 4.2.2 Doublet-Bidoublet Couplings

### Vertex Corrections

The diagrams in (4.11) contribute to the doublet-bidoublet couplings $\beta_1$ and $f_1$. Note that their contribution to $f_1$ is due to the fact that the Yukawa coupling (4.3) explicitly violates the symmetry of separate $SU(2)_L \times SU(2)_R$ transformations of $\underline{\Phi}$ and $\underline{\Psi}$ as it couples leptons to scalar doublets. In order to extract the divergent part of the first diagram in (4.11) the following momentum assignments will be used:



$$\text{where} \quad \begin{cases} k' = k + p_2 + p_3 + p_4 \\ \\ k'' = k + p_2 + p_4 \\ \\ k''' = k + p_2 \\ \\ 0 = p_1 + p_2 + p_3 + p_4 \end{cases} \tag{4.27}$$

The diagram then gives[3]



$$\tag{4.28}$$

---

[3]Here, for the moment the $\mathbb{Z}_4$ symmetry is omitted to obtain also the contributions to the $\mathbb{Z}_4$ breaking couplings $\beta_2$, $\beta_3$.

$$
= \underbrace{(-1)}_{\text{fermion loop}} (-i\mu^{\frac{\epsilon}{2}})^2 (-\tfrac{1}{2}\mu^{\frac{\epsilon}{2}})^2 \Big[ g_f{}^g \Big( \delta_{j,1}(\bar{Y}_{\underline{L}}^{+gh} - \bar{Y}_{\underline{L}}^{-gh})(\Gamma\Gamma^D)_{BE} + i\delta_{j,2}(\bar{Y}_{\underline{L}}^{+gh} + \bar{Y}_{\underline{L}}^{-gh})\Gamma^D_{BE} \Big) \cdot
$$

$$
\cdot \Big( \delta_{i,1}(\bar{Y}_{\underline{L}}^{+hf} - \bar{Y}_{\underline{L}}^{-hf})(\Gamma\Gamma^C)_{EA} + i\delta_{i,2}(\bar{Y}_{\underline{L}}^{+hf} + \bar{Y}_{\underline{L}}^{-hf})\Gamma^C_{EA} \Big) g_f{}^f \Big] \underbrace{\int \frac{\mathrm{d}^d k}{(2\pi)^d} \frac{\mathrm{Tr}\left[k'''k''k'k\right]}{k'''^2 k''^2 k'^2 k^2}}_{=\text{UV finite}+\frac{i\pi^2}{(2\pi)^4 \mu^\epsilon}\frac{8}{\epsilon}}
$$

$$
= \frac{i\mu^\epsilon}{16\pi^2\epsilon} 4 \Big[ g_f{}^g \Big( \delta_{j,1}(\bar{Y}_{\underline{L}}^{+gh} - \bar{Y}_{\underline{L}}^{-gh})(\Gamma\Gamma^D)_{BE} + i\delta_{j,2}(\bar{Y}_{\underline{L}}^{+gh} + \bar{Y}_{\underline{L}}^{-gh})\Gamma^D_{BE} \Big) \cdot
$$

$$
\cdot \Big( \delta_{i,1}(\bar{Y}_{\underline{L}}^{+hf} - \bar{Y}_{\underline{L}}^{-hf})(\Gamma\Gamma^C)_{EA} + i\delta_{i,2}(\bar{Y}_{\underline{L}}^{+hf} + \bar{Y}_{\underline{L}}^{-hf})\Gamma^C_{EA} \Big) g_f{}^f \Big] \quad (4.29)
$$

$$(4.30)$$

The value of the second diagram can be obtained from the first one by the transformation $(p_3, C, i) \leftrightarrow (p_4, D, j)$. One then gets for the second diagram



$$(4.31)$$

$$
= \frac{i\mu^\epsilon}{16\pi^2\epsilon} 4 \Big[ g_f{}^g \Big( \delta_{i,1}(\bar{Y}_{\underline{Q}}^{+gh} - \bar{Y}_{\underline{Q}}^{-gh})(\Gamma\Gamma^C)_{BE} + i\delta_{i,2}(\bar{Y}_{\underline{Q}}^{+gh} + \bar{Y}_{\underline{Q}}^{-gh})\Gamma^C_{BE} \Big) \cdot
$$

$$
\cdot \Big( \delta_{j,1}(\bar{Y}_{\underline{Q}}^{+hf} - \bar{Y}_{\underline{Q}}^{-hf})(\Gamma\Gamma^D)_{EA} + i\delta_{j,2}(\bar{Y}_{\underline{Q}}^{+hf} + \bar{Y}_{\underline{Q}}^{-hf})\Gamma^D_{EA} \Big) g_f{}^f \Big] \quad (4.32)
$$

Adding up the two diagrams yields



$$
= \frac{i\mu^\epsilon}{16\pi^2\epsilon} 4\vec{g}_f{}^T \Big[ -\delta_{i,1}\delta_{j,1}(\bar{Y}_{\underline{L}}^+ - \bar{Y}_{\underline{L}}^-)^2 \{\Gamma^C, \Gamma^D\} - \delta_{i,2}\delta_{j,2}(\bar{Y}_{\underline{L}}^+ + \bar{Y}_{\underline{L}}^-)^2 \{\Gamma^C, \Gamma^D\}
$$

$$
- i\delta_{i,2}\delta_{j,1}(\bar{Y}_{\underline{L}}^+ + \bar{Y}_{\underline{L}}^-)(\bar{Y}_{\underline{L}}^+ - \bar{Y}_{\underline{L}}^-)\Gamma\Gamma^C\Gamma^D + i\delta_{i,2}\delta_{j,1}(\bar{Y}_{\underline{L}}^+ - \bar{Y}_{\underline{L}}^-)(\bar{Y}_{\underline{L}}^+ + \bar{Y}_{\underline{L}}^-)\Gamma\Gamma^D\Gamma^C
$$

$$
- i\delta_{i,1}\delta_{j,2}(\bar{Y}_{\underline{L}}^+ + \bar{Y}_{\underline{L}}^-)(\bar{Y}_{\underline{L}}^+ - \bar{Y}_{\underline{L}}^-)\Gamma\Gamma^D\Gamma^C + i\delta_{i,1}\delta_{j,2}(\bar{Y}_{\underline{L}}^+ - \bar{Y}_{\underline{L}}^-)(\bar{Y}_{\underline{L}}^+ + \bar{Y}_{\underline{L}}^-)\Gamma\Gamma^C\Gamma^D \Big]_{BA} \vec{g}_f
$$

$$
= \frac{i\mu^\epsilon}{16\pi^2\epsilon} 4 \cdot \vec{g}_f{}^T \Big[ -2(\bar{Y}_{\underline{L}}^{+2} + \bar{Y}_{\underline{L}}^{-2})\delta_{ij}\delta_{CD}\delta_{BA} + 2\{\bar{Y}_{\underline{L}}^+, \bar{Y}_{\underline{L}}^-\}(\delta_{i,1}\delta_{j,1} - \delta_{i,2}\delta_{j,2})\delta_{CD}\delta_{BA}
$$

$$
+ 4i(\bar{Y}_{\underline{L}}^{+2} - \bar{Y}_{\underline{L}}^{-2})\epsilon_{ij}(\Gamma\Sigma^{CD})_{BA} + i2[\bar{Y}_{\underline{L}}^+, \bar{Y}_{\underline{L}}^-](1 - \delta_{ij})\Gamma_{BA}\delta_{CD} \Big] \vec{g}_f
$$

$$= \frac{i\mu^\epsilon}{16\pi^2\epsilon} 4 \left[ -2T_f^+ \delta_{ij}\delta_{CD}\delta_{BA} + 2T_f^{\{\}}(\delta_{i,1}\delta_{j,1} - \delta_{i,2}\delta_{j,2})\delta_{CD}\delta_{BA} \right.$$

$$\left. + i4T_f^- \epsilon_{ij}(\Gamma\Sigma^{CD})_{BA} - 2T_f^{[]}(1-\delta_{ij})\Gamma_{BA}\delta_{CD} \right]\vec{g}_f \tag{4.33}$$

where it has been used that the symmetry factors are given by $S_{12} = S_{13} = 1$. In the last line it has been defined

$$\vec{g}_f{}^T(\bar{Y}_{\underline{L}}^{+2} + \bar{Y}_{\underline{L}}^{-2})\vec{g}_f \equiv T_f^+, \tag{4.34a}$$

$$\vec{g}_f{}^T(\bar{Y}_{\underline{L}}^{+2} - \bar{Y}_{\underline{L}}^{-2})\vec{g}_f \equiv T_f^-, \tag{4.34b}$$

$$\vec{g}_f{}^T\{\bar{Y}_{\underline{L}}^+, \bar{Y}_{\underline{L}}^-\}\vec{g}_f \equiv T_f^{\{\}} \tag{4.34c}$$

$$\vec{g}_f{}^T[\bar{Y}_{\underline{L}}^{+2}, \bar{Y}_{\underline{L}}^{-2}]\vec{g}_f \equiv iT_f^{[]}. \tag{4.34d}$$

Note that the commutator $[\bar{Y}_{\underline{L}}^{+2}, \bar{Y}_{\underline{L}}^{+2}]$ is anti-hermitian. Thus, the expression (4.34d) is imaginary with $g_f$ being real. Given the feynman rule (**??**), the doublet-bidoublet interaction counterterms read according to (4.33):

$$\Delta_f\delta\beta_1 = \frac{-4T_f^+}{16\pi^2\epsilon} \tag{4.35a}$$

$$\Delta_f\delta f_1 = \frac{-4T_f^-}{16\pi^2\epsilon} \tag{4.35b}$$

$$\Delta_f\delta\beta_2 = \frac{2T_f^{\{\}}}{16\pi^2\epsilon} \tag{4.35c}$$

$$\Delta_f\delta\beta_3 = \frac{T_f^{[]}}{16\pi^2\epsilon} \tag{4.35d}$$

**Beta-Functions**

Together with the contribution to the doublet wavefunction renormalization (4.24), the vertex correction (4.35a) can be inserted into (A.18) to obtain $f$'s contribution to the $\beta$-function of $\beta_1$:

$$\Delta_f\beta_{\beta_1} = D_{g_f}\frac{\partial\Delta_f\delta\beta_1^{(1)}}{\partial g_f{}^i}g_f{}^i + D_Y\frac{\partial\Delta_f\delta\beta_1^{(1)}}{\partial Y_{\underline{L}}^{\pm kl}}Y_{\underline{L}}^{\pm kl} - D_{\beta_1}\Delta_f\delta\beta_1^{(1)} - \beta_1 D_{g_f}\frac{\partial\Delta_f\delta Z_{\underline{\Psi}}^{(1)}}{\partial g_f{}^i}g_f{}^i$$

$$= \Delta_f\delta\beta_1^{(1)} - 2\beta_1\Delta_f\delta Z_{\underline{\Psi}}^{(1)}$$

$$= \frac{1}{16\pi^2}\left(-4T_f^+ + 4\beta_1\vec{g}_f^2\right) \tag{4.36}$$

In the same way inserting (4.35b) into (4.24) one finds:

$$
\begin{aligned}
\Delta_f \beta_{f_1} &= D_{g_f} \frac{\partial \Delta_f \delta f_1^{(1)}}{\partial g_f{}^i} g_f{}^i + D_Y \frac{\partial \Delta_f \delta f_1^{(1)}}{\partial Y_{\underline{L}}^{\pm kl}} Y_{\underline{L}}^{\pm kl} - D_{f_1} \Delta_f \delta f_1^{(1)} - f_1 D_{g_f} \frac{\partial \Delta_f \delta Z_{\underline{\Psi}}^{(1)}}{\partial g_f{}^i} g_f{}^i \\
&= \Delta_f \delta f_1^{(1)} - 2 f_1 \Delta_f \delta Z_{\underline{\Psi}}^{(1)} \\
&= \frac{1}{16\pi^2} \left( -4 T_f^- + 4 f_1 \vec{g}_f^2 \right)
\end{aligned}
\tag{4.37}
$$

And for the $\mathbb{Z}_4$-breaking terms one finds, using (4.35c) and (4.35d)

$$
\begin{aligned}
\Delta_f \beta_{\beta_2} &= \Delta_f \delta \beta_2^{(1)} - 2 \beta_2 \Delta_f \delta Z_{\underline{\Psi}}^{(1)} \\
&= \frac{1}{16\pi^2} \left( 2 T_f^{\{\}} + 4 \beta_2 \vec{g}_f^2 \right)
\end{aligned}
\tag{4.38}
$$

and

$$
\begin{aligned}
\Delta_f \beta_{\beta_3} &= \Delta_f \delta \beta_3^{(1)} - 2 \beta_3 \Delta_f \delta Z_{\underline{\Psi}}^{(1)} \\
&= \frac{1}{16\pi^2} \left( T_f^{[]} + 4 \beta_3 \vec{g}_f^2 \right).
\end{aligned}
\tag{4.39}
$$

### 4.2.3 Standard Lepton Yukawa Couplings

Beside the contributions to the $\beta$-functions discussed so far, it is clear that there are further contributions of order $\mathcal{O}\left(g_f{}^2\right)$ to couplings involving leptons due to its contribution to their wavefunction renormalization. Thus, in addition, $g_f$ will contribute to the lepton Yukawa couplings.

The contribution to the wavefunction counterterm of the leptons is given by

$$
\underline{L}_{\alpha a}^i \;\blacktriangleright\!\!\bigcirc\!\!\blacktriangleright\; \underline{L}_{\beta b}^j \;=\; (-i)^2 (\mu^{\frac{\epsilon}{2}})^2 \delta_{ba} g_f{}^j g_f{}^i \int \frac{\mathrm{d}^d k}{(2\pi)^d} \frac{i \slashed{k}_{\beta\alpha}}{k^2 + i\epsilon} \frac{i}{(k-p)^2 + i\epsilon}
$$

$$
= \mu^\epsilon \delta_{ba} \gamma_{\beta\alpha}^\mu g_f{}^j g_f{}^i \underbrace{\int \frac{\mathrm{d}^d k}{(2\pi)^d} \frac{k_\mu}{k^2 (k-p)^2}}_{=\text{UV finite} - \frac{i\pi^2}{(2\pi)^4 \mu^\epsilon} \frac{1}{\epsilon} p_\mu}
$$

$$
= \text{UV finite} - i \delta_{ba} \gamma_{\beta\alpha}^\mu g_f{}^j g_f{}^i p_\mu \frac{1}{16\pi^2 \epsilon}
\tag{4.40}
$$

Thus, $g_f$ contributes to the lepton wavefunction renormalization by

$$i\slashed{p}\Delta_f \delta Z_{\underline{L}}^{ji} = i\slashed{p}\frac{g_f{}^j g_f{}^i}{16\pi^2 \epsilon}. \tag{4.41}$$

Inserting this into the defining expression of the Yukawa coupling $\beta$-function one obtains the contribution

$$\Delta_f \beta_{Y_{\underline{L}}^{\pm ij}} = -\frac{1}{2}(Y_{\underline{L}}^{\pm}\Delta_f \delta Z_{\underline{Q}}^{(1)})^{ij} = \frac{-1}{16\pi^2}\frac{1}{2}Y_{\underline{L}}^{\pm ik} g_f{}^k g_f{}^j. \tag{4.42}$$

## 4.3 Renormalization

### 4.3.1 Counterterm Lagrangian

In the previous sections various contributions to $\beta$-functons of both scalar and lepton Yukawa couplings at one-loop order have been calculated. They arose introducing a fermionic singlet to the model. In a next step, $g_f$ itself and the wavefunction of $f$ will be renormalized. The wavefunction renormalization $Z_f$ is defined according to

$$f_B = Z_f^{\frac{1}{2}} f, \tag{4.43}$$

where $f_B$ and $f$ are the bare and renormalized fields. The renormalized coupling $g_f$ is then given by

$$g_{fB}^i = Z_{\underline{L}_{ij}}^{-\frac{1}{2}}\left[g_f^j + \delta g_f^j\right]\mu^{\frac{\epsilon}{2}} Z_{\underline{\Psi}}^{-\frac{1}{2}} Z_f^{-\frac{1}{2}}, \tag{4.44}$$

where $g_{fB}^i$ and $\delta g_f^i$ denote the bare coupling and the counterterm respectively. The counterterm lagrangian corresponding to $f$ then is

$$\delta\mathcal{L}_f = \bar{f}i\slashed{D}(\delta Z_f)f + \mu^{\frac{\epsilon}{2}}\underline{\bar{L}}_i \delta g_f^i \underline{\Psi} f + h.c.. \tag{4.45}$$

In the following, first the vertex counterterm $\delta g_f$ will be determined. In a second step the wavefunction counterterm $\delta Z_f$ will be calculated and finally the $\beta$-function corresponding to $g_f$ will be derived.
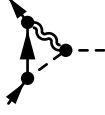
### 4.3.2 Vertex Renormalization

There are two diagrams contributing to the $g_f$ renormalization. They are given by the exchange of $U(1)$- and $SU(2)$-gauge bosons between the lepton and doublet

scalar. The coupling $g_f$ is then renormalized by demanding

$$
\text{UV finite} = \quad \text{[diagram]} \quad + S_9 \quad \text{[diagram]} \quad + S_{10} \quad \text{[diagram]} \quad + \quad \text{[diagram]} \quad , \qquad (4.46)
$$

where the symmetry factors are given by $S_9 = S_{10} = 1/3! \cdot 6 = 1$. In order to calculate the diagrams external and internal momenta are assigned to the graphs in the following way, where the wiggly line represents $U(1)$- and $SU(2)$-propagators respectively:



$$
\text{where} \quad \begin{cases} k' = k + p_2 \\[2mm] k'' = k + p_2 + p_3 \\[2mm] 0 = p_1 + p_2 + p_3 \end{cases} \qquad (4.47)
$$

Given these momentum assignments, the diagrams in (4.47) give:



$$
(4.48a)
$$

$$
= \mu^{\frac{3\epsilon}{2}} \left( \frac{g_1}{2} \right)^2 g_f^i (\gamma^\nu \gamma_\rho)_{ba} \cdot \delta_{BA} \int \frac{\mathrm{d}^d k}{(2\pi)^d} \left[ \frac{k''^\rho (p_1^\mu - k'^\mu) \left( \eta_{\mu\nu} - (1 - \xi_1) \frac{k_\mu k_\nu}{k^2} \right)}{(k''^2 + i\epsilon)(k'^2 + i\epsilon)(k^2 + i\epsilon)} \right]
$$

$$
= \mu^{\frac{3\epsilon}{2}} \left( \frac{g_1}{2} \right)^2 g_f^i (\gamma^\nu \gamma_\rho)_{ba} \cdot \delta_{BA} \underbrace{\int \frac{\mathrm{d}^d k}{(2\pi)^d} \left[ \frac{(k^\rho + p_3^\rho)(2p_2^\mu - k^\mu)\left( \eta_{\mu\nu} - (1 - \xi_1) \frac{k_\mu k_\nu}{k^2} \right)}{(k + p_3)^2 (k - p_2)^2 k^2} \right]}_{=\text{UV finite}+\frac{i\pi^2}{(2\pi)^4 \mu^\epsilon} \frac{1}{2\epsilon} (-\xi_1) \eta^\rho{}_\nu}
$$

$$
= \text{UV finite} + \mu^{\frac{\epsilon}{2}} \left( \frac{g_1}{2} \right)^2 g_f^i (\underbrace{\gamma^\nu \gamma_\nu}_{4 \cdot \mathbb{1}})_{ba} \delta_{BA} \frac{i\pi^2}{(2\pi)^4} \frac{1}{2\epsilon} (-\xi_1)
$$

$$= \text{UV finite} + i\mu^{\frac{\epsilon}{2}} \frac{g_1^2}{4} g_f^i \delta_{ba} \delta_{BA} \frac{1}{16\pi^2} \frac{4}{2\epsilon} (-\xi_1)$$

and



(4.48b)

$$= -\mu^{\frac{3\epsilon}{2}} \left( \frac{g_2}{\sqrt{8}} \right)^2 g_f^i \left( \gamma^\nu \gamma_\rho \right)_{ba} \left( \Sigma^{EF} \Sigma^{GH} \right)_{BA} \left( \delta^{EG} \delta^{FH} - \delta^{EH} \delta^{FG} \right) \cdot$$

$$\cdot \int \frac{d^d k}{(2\pi)^d} \left[ \frac{k''^\rho (p_2^\mu - k'^\mu) \left( \eta_{\mu\nu} - (1 - \xi_2) \frac{k_\mu k_\nu}{k^2} \right)}{(k''^2 + i\epsilon)(k'^2 + i\epsilon)(k^2 + i\epsilon)} \right]$$

$$= -\mu^{\frac{3\epsilon}{2}} \left( \frac{g_2}{\sqrt{8}} \right)^2 g_f^i \left( \gamma^\nu \gamma_\rho \right)_{ba} \underbrace{\left( \Sigma^{EF} \Sigma^{GH} \right)_{BA} \left( \delta^{EG} \delta^{FH} - \delta^{EH} \delta^{FG} \right)}_{=-3 \cdot \mathbb{1}_{BA}} \cdot$$

$$\cdot \underbrace{\int \frac{d^d k}{(2\pi)^d} \left[ \frac{(k^\rho + p_3^\rho)(2p_2^\mu - k^\mu) \left( \eta_{\mu\nu} - (1 - \xi_2) \frac{k_\mu k_\nu}{k^2} \right)}{(k + p_3)^2 (k - p_2)^2 k^2} \right]}_{=\text{UV finite} + \frac{i\pi^2}{(2\pi)^4 \mu^\epsilon} \frac{1}{2\epsilon} (-\xi_2) \eta^\rho{}_\nu}$$

$$= \text{UV finite} + i\mu^{\frac{\epsilon}{2}} \frac{3g_2^2}{8} g_f^i \delta_{ba} \delta_{BA} \frac{1}{16\pi^2} \frac{4}{2\epsilon} (-\xi_2)$$

Note that the gauge parameters $\xi_1$ and $\xi_2$ are not physical and therefore do not contribute to any observable. In particular, they do not enter the $\beta$-function of $g_f^i$. However, they have been kept here as they provide a consistency check for the calculation. Summing up all the terms contributing to the $\beta$-function they must cancel out.

According to (4.45), the vertex counterterm $\delta g_f^i$ is defined as
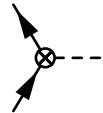


$$= -i\mu^{\frac{\epsilon}{2}} \delta_{BA} \delta_{ba} \delta g_f^i.$$

(4.49)

Using (4.48) one then obtains

$$\delta g_f^i = -\frac{1}{16\pi^2\epsilon}g_f^i\left[\frac{1}{2}g_1^2\xi_1 + \frac{3}{4}g_2^2\xi_2\right]. \tag{4.50}$$

### 4.3.3 Wavefunction Renormalization

The wavefunction renormalization of $f$ is given by

UV finite = ──────▶   $+ S_{11}$  ▶⟲▶   +   ▶⊗▶   , $\tag{4.51}$

where the symmetry factor is given by $S_{11} = 1/2! \cdot 2 = 1$. The diagram $S_{11}$ yields

$$▶⟲▶ \quad = (-i)^2(\mu^{\frac{\epsilon}{2}})^2\delta_{BA}\delta_{AB}\sum_i(g_f^i)^2\int\frac{\mathrm{d}^dk}{(2\pi)^d}\frac{i\slashed{k}_{ba}}{k^2+i\epsilon}\frac{i}{(k-p)^2+i\epsilon}$$

$$= \mu^{\epsilon}4\gamma_{ba}^{\mu}\sum_i(g_f^i)^2\underbrace{\int\frac{\mathrm{d}^dk}{(2\pi)^d}\frac{k_\mu}{k^2(k-p)^2}}_{=\text{UV finite}-\frac{i\pi^2}{(2\pi)^4\mu^\epsilon}\frac{1}{\epsilon}p_\mu}$$

$$= \text{UV finite} + i\vec{g}^2\gamma_{ba}^\mu p_\mu\frac{4}{16\pi^2\epsilon}. \tag{4.52}$$

Thus, the wavefunction counterterm $\delta Z_f$, which according to the counterterm Lagrangian (4.45) is defined as

$$▶⊗▶ \quad = i\slashed{p}\mu^{\frac{\epsilon}{2}}\delta Z_f \tag{4.53}$$

is given by

$$\delta Z_f =: \frac{\delta Z_f^{(1)}}{\epsilon} = \frac{-4\vec{g}^2}{16\pi^2\epsilon}.$$

(4.54)

### 4.3.4 Beta-Function

**Derivation**

In the preceding subsections the wavefunction renormalization of $f$ and the vertex renormalization have been performed. Thereby, having found the counterterms, all the ingredients needed to derive the $\beta$-function of $g_f$ have been collected. According to the defining expression (A.18), one finds for $\beta_{g_f}$[4]

$$
\begin{aligned}
\beta_{g_f^i} &= \frac{1}{2}\left(\sum_{V_A}\left[\frac{\partial\delta g_f^{i(1)}}{\partial V_A} - \frac{1}{2}\frac{\partial\delta Z_f^{(1)}}{\partial V_A} - \frac{1}{2}g_f^j\frac{\partial(\delta Z_{\underline{L}}^{(1)})_{ji}}{\partial V_A} - \frac{1}{2}g_f^i\frac{\partial\delta Z_{\underline{\Psi}}^{(1)}}{\partial V_A}\right]V_A - \delta g_f^{i(1)}\right) \\
&= \frac{1}{2}\left[\delta g_f^{i(1)} + 2\delta g_f^{i(1)} - \delta g_f^{i(1)}\right] - \frac{1}{4}g_f^i\left[2\delta Z_f^{(1)} + 2\delta Z_{\underline{\Psi}}^{(1)}\right] - \frac{1}{4}\left[2(\delta Z_{\underline{L}}^{(1)})_{ij}\right]g_f^j \\
&= \frac{1}{16\pi^2}\left(-\frac{7}{2}\vec{g}_f^2 g_f^i - \frac{3}{4}g_1^2 g_f^i - \frac{9}{8}g_2^2 g_f^i\right) + \left((Y_{\underline{L}}^{+2} + Y_{\underline{L}}^{-2})\vec{g}_f\right)^i.
\end{aligned}
$$

(4.55)

As required by gauge invariance the parameters $\xi_1$ and $\xi_2$ cancel out in (4.55). This provides a non-trivial consistency check for the calculation.

**Running**

As $\beta_{g_f}$ is proportional $g_f$ (*cf.* (4.55)), the coupling exhibits a rather mild running. Under the assumption that $f$ couples exclusively to the third lepton generation, *i.e.* $g_f^e = g_f^\mu = 0$, this is illustrated in figure 4.1, where the running of $g_f^\tau$ is plotted for various initial conditions at the Planck scale.

## 4.4 Symmetry Breaking in the Extended Model I

### 4.4.1 Effect on Doublet Self-Coupling

In the preceding sections the contributions to the beta-functions of the scalar couplings due to the coupling $g_f$ have been calculated. Note that all results found there are collected in the appendix A.2.2. The coupling $g_f$ was introduced for the main

---

[4]For the counterterms of $\underline{L}$ and $\underline{\Psi}$ see Ref. [25].
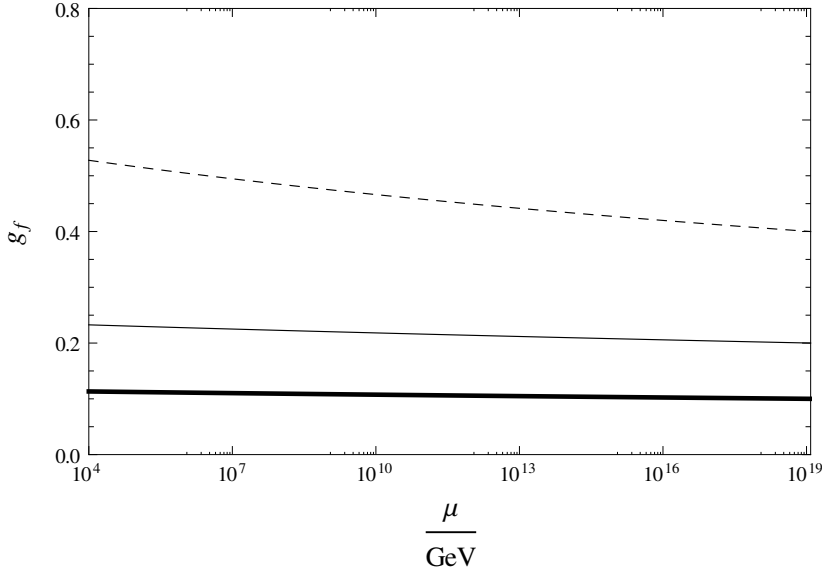
Figure 4.1: The Running of $g_f$ is plotted for the initial conditions $g_f(\Lambda_{\mathrm{Pl}}) = 0.1$ (thick line), $g_f(\Lambda_{\mathrm{Pl}}) = 0.2$ (thin line) and $g_f(\Lambda_{\mathrm{Pl}}) = 0.4$ (dashed line). As $\beta_{g_f} \sim g_f$ the coupling remains small for small initial values over many scales.

purpose to modify the running of the doublet-bidoublet couplings $\beta_1$ and $f_1$ as these determine the little hierarchy.. As shown in section 4.2.1, $g_f$ also contributes to the doublet self-couplings $\kappa_1$ and $\kappa_2$ by

$$\Delta_f \beta_{\kappa_1} = \frac{1}{16\pi^2} \big[ -9\vec{g}_f^4 + 8\kappa_1 \vec{g}_f^2 \big]$$

and

$$\Delta_f \beta_{\kappa_2} = \frac{1}{16\pi^2} \big[ -7\vec{g}_f^4 + 8\kappa_2 \vec{g}_f^2 \big].$$

Here, the order $\mathcal{O}\big(g_f^4\big)$-terms have a negative sign. Thus, for $g_f$ being large these contributions become comparable to the (positive-sign) gauge contributions in $\beta_{\kappa_1}$ and $\beta_{\kappa_2}$ and may eventually dominate them such that $\beta_{\kappa_1}(\Lambda_{\mathrm{Pl}}) < 0$ and $\beta_{\kappa_2}(\Lambda_{\mathrm{Pl}}) < 0$. As argued in section 3.3.1 it was the fact that these beta-functions were positive at the Planck scale, that allowed for fulfilling the parity-breaking GW conditions. Hence, the requirement of generating the big hierarchy sets an upper bound on the possible values $g_f$ that are allowed in order to adjust the little hierarchy. In figure 4.2, the RG flow in the $(\kappa_+, \kappa_1)$-plain is presented with $g_f$ switched on. It reveals that

increasing the value of $g_f$ leads firstly to deflecting the stream lines away from the parity breaking solutions into the parity conserving solutions for small initial values of $\kappa_1$. For higher values, when $g_f$ becomes comparable to the gauge contributions, the parameter space allowed by parity-breaking shrinks drastically and the doublet self-couplings run into a fixpoint, which depends on the value of $g_f$. Note that the position of such a fixpoint can be accessed anlytically by demanding

$$\beta_{\kappa_1} = 0, \quad \beta_{\kappa_2} = 0. \tag{4.56}$$

Under the assumption that the beta-functions are approximated by neglecting the contributions due to the intermediate doublet-bidoublet couplings and by fixing the gauge couplings at $M_Z$ (as these become relevant at lower energies) and $g_f$ at the Planck scale (recall its mild running), the exemplary fixpoint for $g_f(\Lambda_{\text{Pl}}) = 0.5$ is calculated to be at

$$\kappa_1 \approx 0.10, \quad \kappa_2 \approx 0.09. \tag{4.57}$$

It is concluded that, in order to allow for the emergence of parity breaking flat directions and to make the procedure explained in section 3.3.1 be still applicable to the model extended by $f$, $g_f$ must not be comparable to the strength of gauge interactions. In the following analysis, it is set the upper bound $g_f(\Lambda_{\text{Pl}}) < 0.4$. This upper bound is found by demanding $\beta_{\kappa_1} = \beta_{\kappa_2} = 0$.

## 4.4.2 Effect on Doublet-Bidoublet Couplings: Little Hierarchy

In the previous section it was shown that, under the assumption $g_f(\Lambda_{\text{Pl}}) < 0.4$, a big hierarchy between the Planck scale and the left-right breaking scale can be obtained, just as in the minimal model. Here, it is questioned if within the allowed parameter space given by

$$0 < g_f < 0.4$$

a little hierarchy, larger than in the case of shift symmetry alone, can be obtained using the effect of $g_f$ on the doublet-bidoublet couplings. In section 3.3.2 it had been that these couplings are responsable for the little hierarchy[5].

In the minimal model, including shift symmetry, parity breaking was exclusively possible in flat direction Ib as considering the scalar masses revealed that only

---

[5]The running of the bidoublet self- couplings is not significantly altered in this modified model, as $f$ does not couple to the bidoublet at tree-level.

this flat direction corresponded to a minimum of the potential. This was mainly provoked by $f_1 \equiv 0$. Here, the situation might change as $f_1$ is generated by loop corrections involving $f$ and leptons. The correction generating $f_1$ at the Planck scale was calculated to be

$$\Delta_f \beta_{f_1}(\Lambda_{\text{Pl}}) = \frac{-4T_f^-}{16\pi^2} \tag{4.58}$$

with $T_f^- = -\vec{g}_f^{\,T} \bar{Y}_L^{-2} \vec{g}_f$ (cf. (4.37)). Thus, $f_1$ is supposed to develop (negative) non-zero values. This potentially allows for the possibility of symmetry breaking in direction IIb (cf. section 3.3.1). For this purpose, $f_1$ must satisfy the inequality (cf. (3.14))

$$|f_1| > 8 \max\left[|\lambda_2|, |\lambda_3|\right] \cdot \frac{\kappa^2}{v_R^2}. \tag{4.59}$$

Note that the right-hand side of (4.59) is effectively fixed by imposing the shift symmetry. It is of order $\mathcal{O}\left(10^{-5}\right)$, it seems hardly possible to satisfy this inequality. Since $\Delta_f \beta_{f_1}(\Lambda_{\text{Pl}})$, given in (4.58), is highly suppressed by the smallness of the $(\tau-)$lepton Yukawa coupling, being of order $\mathcal{O}\left(10^{-2}\right)$, $f_1$ is expected to be very small. Making the same linear approximation as in section 3.3.1, one finds

$$f_1(\mu_{\text{GW}} = 10^4 \,\text{GeV}) \approx \beta_{f_1}(\Lambda_{\text{Pl}}) \log\left(\frac{\mu_{\text{GW}}}{\Lambda_{\text{Pl}}}\right) \tag{4.60}$$

$$\approx g_f^2 \cdot \mathcal{O}\left(10^{-5}\right).$$

Thus, it seems unlikely for flat directions of type IIb to emerge. In fact, by using the running couplings, based on the full numerical solutions of the RG group equations, it is verified that in this modified model parity breaking occurs solely in directions of type Ib as it was the case in the minimal model. The little hierarchy in direction Ib given by

$$\frac{\kappa^2 + \kappa'^2}{v_R^2} = \frac{-\beta_1}{2\lambda_1 - 8\lambda_3} \tag{4.61}$$

is, as in section 3.3.1, fixed due to shift symmetry except for the value of $\beta_1$.

Again a linear approximation is used to estimate the value of $\beta_1$ at the GW scale. For this purpose, at the Planck scale $\beta_{\beta_1}$ is given by

$$\beta_{\beta_1}(\Lambda_{\text{Pl}}) = \frac{-4T_f^+ + 9g_2^4}{16\pi^2} \tag{4.62}$$

with $T_f^+ = \vec{g}_f^T \bar{Y}_{\underline{L}}^{-2} \vec{g}_f$ (*cf.* (4.36)). One then finds that the correction due to $g_f$ to the value of $\beta_1$ at the GW scale should be of order

$$\frac{\beta_1(\mu_{\mathrm{GW}})|_{g_f \neq 0} - \beta(\mu_{\mathrm{GW}})|_{g_f = 0}}{\beta(\mu_{\mathrm{GW}})|_{g_f = 0}} = \mathcal{O}\left(\frac{-4 T_f^+(\Lambda_{\mathrm{Pl}})}{9 g_2^4(\Lambda_{\mathrm{Pl}})}\right). \tag{4.63}$$

The negative sign in front of $T_f^+$ already indicates that the correction lowers the value of (4.61), thereby enlarging the little hierarchy. Using $g_2(\Lambda_{\mathrm{Pl}}) \approx 0.52$ and for $Y_{\underline{L}}^-(\Lambda_{\mathrm{Pl}}) \approx 0.01$, this yields

$$\frac{\beta_1(\mu_{\mathrm{GW}})|_{g_f \neq 0} - \beta(\mu_{\mathrm{GW}})|_{g_f = 0}}{\beta(\mu_{\mathrm{GW}})|_{g_f = 0}} \approx g_f^2 \cdot \mathcal{O}\left(10^{-2}\right). \tag{4.64}$$

Thus, it is expected to lower (4.61) by less than one per mill for $g_f \approx 0.1$. In figure 4.3 the results using the full running of the couplings are presented, where $g_f$ is varied at the Planck scale in the allowed region of parameters and the doublet self-couplings are fixed to $\kappa_1(\mu_{\mathrm{GW}}) = -\kappa_2(\mu_{\mathrm{GW}}) = 0.2$ with the usual $\mu_{\mathrm{GW}} = 10^4\,\mathrm{GW}$. It reveals that the ratio (4.61) is lowered more than was naively expected. However, the obtained little hierarchy is still not sufficiently large. The obtained value for the right-handed scale is enlarged by about 10% compared to the value found in the minimal model. Thus, this modified model fails to stabalize the electroweak scale. Note however that, in principal, the contributions to the beta-functions of the bidoublet self-couplings, $\beta_1$ and $f_1$, have the correct signs to enlarge the little hierarchy.

(a) $g_f(\Lambda_{\mathrm{Pl}}) = 0.3$

(b) $g_f(\Lambda_{\mathrm{Pl}}) = 0.4$

(c) $g_f(\Lambda_{\mathrm{Pl}}) = 0.5$
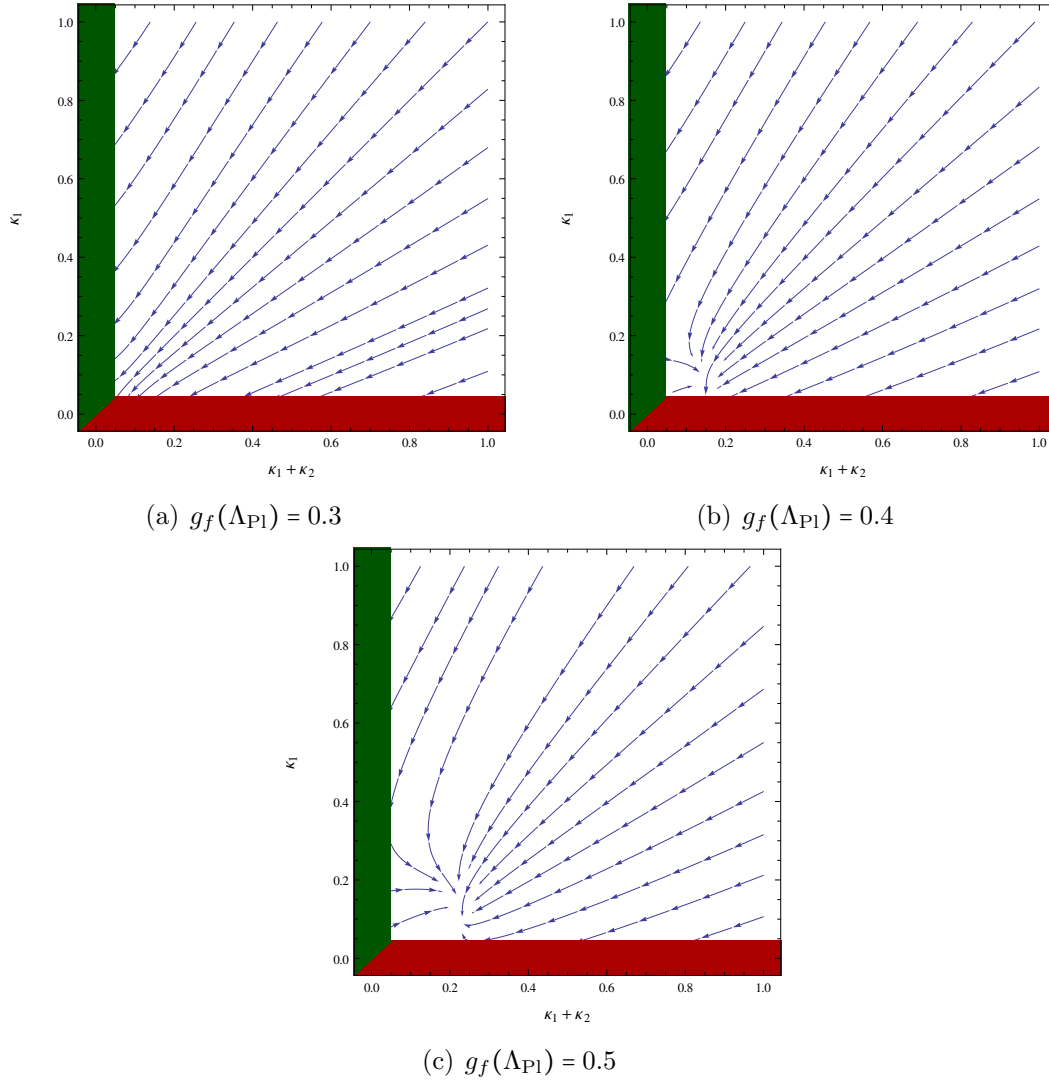
Figure 4.2: The renormalization group flow in the $(\kappa_+, \kappa_1)$-plain is plotted for various values of $g_f$ at the Planck scale. At a value of $g_f(\Lambda_{\mathrm{Pl}}) = 0.3$ (figure 4.2(a)) the gauge couplings remain the dominant contributions and the picture is similar to that given by vanishing $g_f$. For increasing $g_f$ the group flow is more and more deflected into the regime of parity conserving solutions (*cf.* $g_f(\Lambda_{\mathrm{Pl}}) = 0.4$ in figure 4.2(b)). For high initial values of $\kappa_1$ parity breaking can however still be obtained. At $g_f$ comparable to the gauge couplings (*cf.* $g_f(\Lambda_{\mathrm{Pl}}) = 0.5$ in figure 4.2(c)), $\kappa_1$ and $\kappa_2$ run into fixpoints depending on the value of $g_f$.
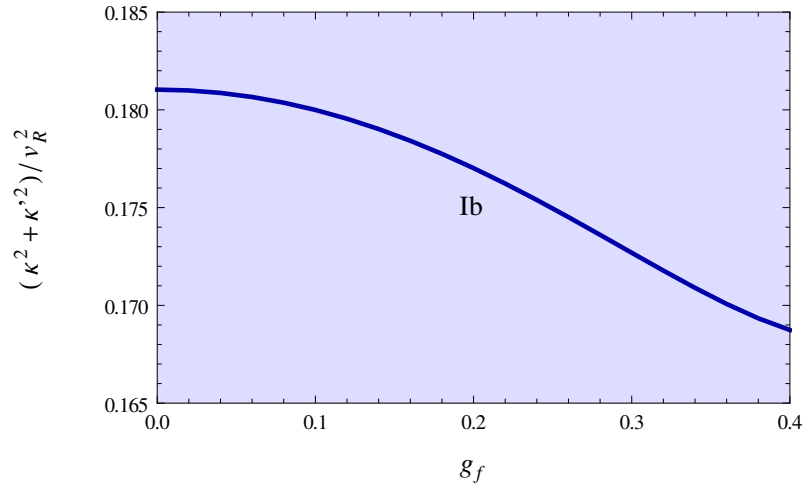
Figure 4.3: The little hierarchy, expressed by the ratio of the squared bidoublet VEVs to the squared right-handed VEV, is plotted as function of $g_f$. As in the minimal model, type Ib flat directions remain the only solutions to the GW conditions. The value of the Yukawa coupling $g_f$, which couples $f$ to doublets to leptons, is varied in the allowed region $0 < g_f < 0.4$. In this allowed parameter space it is not possible to obtain a sufficiently large little hierarchy. The highest value of $g_f$ corresponds to $v_R = 410\,\text{GeV}$ which is by about 10% higher than the value of $v_R$ obtained in the minimal model for the same $\kappa_1$. Here, it was chosen $\kappa_1(\mu_{\text{GW}}) = -\kappa_2(\mu_{\text{GW}}) = 0.2$ with $\mu_{\text{GW}} = 10^4\,\text{GW}$.

# Chapter 5

# Extension II: Fermionic Isosinglet Color Triplet

## 5.1 Introduction

In the preceding chapter a fermionic singlet was added to the model and its effect on the renormalization group functions of the scalar couplings was studied. It was shown that it had just little impact on the running of the doublet-bidoublet couplings such that a desirable little hierarchy could not be obtained. This was due to the fact that the contribution to the doublet-bidoublet couplings (4.35) was suppressed by the small lepton Yukawa couplings. This motivates, in place of a full singlet, the introduction of a fermionic isosinglet color triplet to the model. Such a particle representation, associating the correct $B - L$ charge to it, would allow for an interaction similar to (4.3), replacing leptons by quarks. As the top-quark Yukawa coupling is much stronger than the lepton Yukawa couplings, it is expected that introducing such a colored represention has a significantly larger effect on the doublet-bidoublet couplings than it was the case for the singlet $f$. Thus, in this chapter it will be investigated if a phenomenologically acceptable a little hierarchy can be generated introducing a fermionic isosinglet color triplet. Note that, in the literature, adding such colored isosinglet representations to the standard left-right symmetric model is already discussed. By such extensions some of its naturalness problems concerning fermion masses are addressed [33–35].

### 5.1.1 Definition

Given the preceding motivation a vector-like fermionic isosinglet color triplet, called $P = (P_L, P_R)$, is introduced to the minimal model. Note that this is done alternatively to the singlet which was introduced in chapter 4, shift symmetry will however

still be assumed. It is colored under the $SU(3)$ and carries $U(1)_{B-L}$-charge, while it is a singlet under the $SU(2)_L \times SU(2)_R$ gauge subgroup. Under parity it transforms as

$$P_L \leftrightarrow P_R. \tag{5.1}$$

Furthermore, it transforms trivially under the discrete $\mathbb{Z}_4$-symmetry. In the notation introduced in (2.5) its quantum numbers are given by

$$P = (P_L, P_R) \sim [(\frac{\mathbf{1}}{\mathbf{2}}, \mathbf{0}) + (\mathbf{0}, \frac{\mathbf{1}}{\mathbf{2}})](\mathbf{3}, \mathbf{1}, \mathbf{1}, \frac{4}{3}), \tag{5.2}$$

where the $B - L$ charge is chosen such that $P$ couples to the quarks and scalar doublets via the following Yukawa interaction

$$\mathcal{L}_{Yuk,P} = -g_P{}^i \bar{Q}_L^i \chi_L P_R - g_P{}^i \bar{Q}_R^i \chi_R P_L + H.c., \tag{5.3}$$

which is in complete analogy to (4.3). The original lagrangian is then modified by

$$\mathcal{L}_f = \bar{P} i \slashed{D} P + \mathcal{L}_{Yuk,P}, \tag{5.4}$$

where the covariant derivative $D_\mu$, according to the charge assignments (5.2), is given by

$$D_\mu = D_\mu^P \equiv \partial_\mu + i\frac{2}{3} g_1 B_\mu + i\frac{1}{2} g_3 G_\mu \lambda^m. \tag{5.5}$$

Having introduced $P$, in the following it will be studied how it effects the RG running of the scalar and Yukawa couplings of the model just as it was done for the fermionic singlet in chapter 4. Before doing so, its phenomenological requirements are briefly discussed.

## 5.1.2 Phenomenological Implications

The introduction of $P$, which represents a charged particle, is not as straightforward as it was the case for the the singlet representation $f$. Clearly, the isosinglet $P$ has to be hidden. For this purpose, however, $P$ has to be sufficiently heavy. Hence, a mass term is required. As $P$ is an isosinglet, an explicit mass term

$$-\bar{P}_L M \bar{P}_R - \bar{P}_R M^\dagger \bar{P}_L \tag{5.6}$$

is clearly allowed by gauge symmetry. It does however break classical conformal symmetry, as it introduces a scale to the model. In order to circumvent loosing scale-invariance, alternatively to an *explicit* mass term one could introduce an additional scalar singlet $\varphi$, which acquires a VEV above the right-handed scale. Obviously, such VEV would not lead to symmetry breaking of the LR symmetry. However, the introduction of such scalar singlet $\varphi$ would lead to an enlarged potential. Besides a $|\varphi|^4$ self-coupling, any (gauge and Lorentz) invariant bilinear would form a dimension four operator together with $|\varphi|^2$. Furthermore, also trilinear operators such as $\underline{\bar{\Psi}}\,\underline{\Phi}\,\underline{\Psi}$, which did not enter the potential before due to conformal invariance, would lead to conformal singlets together with $\varphi$,

$$\varphi\underline{\bar{\Psi}}\,\underline{\Phi}\,\underline{\Psi} + h.c.. \tag{5.7}$$

It is clear that such a extension of the scalar sector would complicate the minimization of the model. As introducing $\varphi$ would require to recalculate the flat directions of the model, this possibility is not further considered here. A third ansatz would be to introduce the effective higher-dimensional operator,

$$\frac{1}{\Lambda}\left(\chi_L^\dagger\chi_L\bar{P}_LP_R + \chi_R^\dagger\chi_R\bar{P}_RP_L\right) \quad \text{etc.,} \tag{5.8}$$

which would represent a mass term for $\chi_L$ acquiring a VEV. This possibility is somewhat unsatisfactory as it leaves its origin completely unknown.

Thus, it is assumed here that $P$ acquires mass via the explicit mass term (5.6. Note that the mass term $M$ does not contribute to the beta-functions of the scalar couplings and thus is for the rest of the chapter not considered. It does, however, contribute to the mass renormalization of the quarks and doublet fields. These contributions will not be considered here.

The discussion is concluded by estimating the value of $M$ in order to hide it from observation. As the Yukawa coupling (5.3) mixes the isosinglet $P$ with the up-type quarks, assuming that $\chi_R$ acquires a non-vanishing VEV, one has to consider the mass matrix in the basis of these fields,

$$-\mathcal{L} \supset (\bar{u}_L^i, \bar{P}_L)\cdot\begin{pmatrix} \frac{\kappa Y_Q^{+ij}+\kappa'Y_Q^{-ij}}{\sqrt{2}} & 0 \\ v_R g_P^j & M \end{pmatrix}\cdot\begin{pmatrix} u_R^j \\ P_R \end{pmatrix} + h.c.. \tag{5.9}$$

Assuming that $P$ couples exclusively to top quarks this becomes

$$(\bar{t}_L, \bar{P}_L) \cdot \begin{pmatrix} m_t & 0 \\ v_R g_P^t & M \end{pmatrix} \cdot \begin{pmatrix} t_R \\ P_R \end{pmatrix} + h.c., \tag{5.10}$$

which can be diagonalized to give the eigenstates $P$ with corresponding mass $M$ and the eigenstate

$$\frac{M - m_t}{\sqrt{v_R^2 + (M - m)^2}} t + \frac{v_R g_P^t}{\sqrt{v_R^2 g_P^{t2} + (M - m)^2}} P \tag{5.11}$$

$$\tag{5.12}$$

which corresponds to the top mass. Thus, if one demands for instance to limit the contribution of $P$ to the top quark (the state with mass $m_t$) to 1% it has to be

$$\frac{v_R g_P^t}{\sqrt{v_R^2 g_P^{t2} + (M - m)^2}} \lesssim 1\%. \tag{5.13}$$

This is satisfied for $M \gtrsim 100 \cdot v_R g_P^t$.

# 5.2 Contributions to Renormalization Group Functions

The diagrams emerging due to the introduction of the isosinglet representation $P$ are completely analogous to those which have been ecountered in chapter 4. Most of them are obtained by simple substitution of lepton-propagators by quark-propagators, lepton Yukawa couplings by quark Yukawa couplings *etc.*. There are, however, some subtleties which will be mentioned here briefly. First of all, note that fermion loops will come here with an extra color factor of 3. Secondly, there will be no contribution to $\bar{\kappa}_2$ due to the vector-nature of P. Furthermore, the wavefunction renormalization of $P$ and the vertex renormalization of $g_P$ will involve additional corrections due to gauge interactions as $P$ is charged. For this reason, $P$ will also contribute to the running of $g_3$ and $g_1$.

## 5.2.1 Doublet Self-Couplings

**Vertex Corrections**

In close analogy to section 4.2.1, the isosinglet $P$ contributes to the doublet self-coupling $\bar{\kappa}_1$, which was defined in (4.14), by diagrams of the types



$$ \text{(5.14)} $$

where the crossing fermion lines correspond to $Q_{L/R}$ and $P_{R/L}$ in the first and second diagram respectively. As its right- and left-handed field components represent distint degrees of freedom, in contrast to the fermionic singlet which satisfied the Majorana condition (4.2), $P$ does however not contribute to the coupling $\bar{\kappa}_2$. Accounting for the color factor, from (4.21) one can read off

$$ \Delta_P \delta\bar{\kappa}_1 = \frac{-16\vec{g}_P^4}{16\pi^2}\frac{1}{\epsilon} \qquad \text{and} \qquad \Delta_P \delta\bar{\kappa}_2 = 0. \qquad \text{(5.15)} $$

This, using equation (4.14), in terms of $\kappa_1$ and $\kappa_2$ becomes

$$ \Delta_P \delta\kappa_1 = \frac{-16\vec{g}_P^4}{16\pi^2}\frac{1}{\epsilon} \qquad \text{and} \qquad \Delta_P \delta\kappa_2 = \frac{-16\vec{g}_P^4}{16\pi^2}\frac{1}{\epsilon}. \qquad \text{(5.16)} $$

**Scalar Doublet Wavefunction Correction**

In the same way, including the color factor, with regard to section 4.2.1 one finds the scalar doublet wavefunction correction



$$ \Psi \blacktriangleright \!\!\!\!\! \Psi = \underbrace{3}_{\text{color factor}} \underbrace{(-1)}_{\text{fermion loop}} (-i)^2 \sum_i g_P^i g_P^i \mu^\epsilon \int \frac{\mathrm{d}^d k}{(2\pi)^d} \mathrm{Tr}\left[ \frac{i\slashed{k}}{k^2 + i\epsilon} \cdot \frac{i(\slashed{p} - \slashed{k})}{(p-k)^2 + i\epsilon} \right] $$

$$ = \text{UV finite} \; + \vec{g}_P^2 \frac{i12\pi^2}{(2\pi)^4}\frac{1}{\epsilon}p^2. \qquad \text{(5.17)} $$

And thus the contribution to the wavefunction counterterm $\delta Z_{\underline{\Psi}}$ is

$$-ip^2 \Delta_P \delta Z_{\underline{\Psi}} = -ip^2 \vec{g}_P^2 \frac{12}{16\pi^2\epsilon}. \tag{5.18}$$
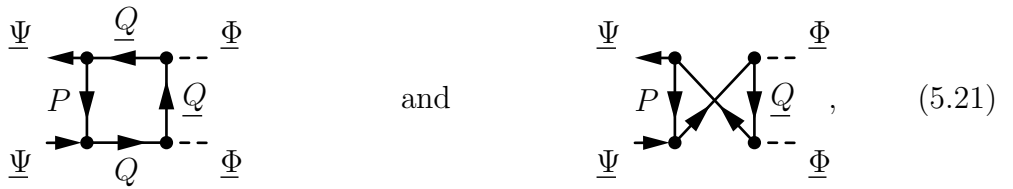
**Contribution to Beta-functions**

Given the results (5.15) and (5.18) the contribution to the beta-function of the doublet self-couplings yields

$$\Delta_P \beta_{\kappa_1} = \underbrace{D_{g_P}}_{=1/2} \frac{\partial \Delta_P \delta \kappa_1^{(1)}}{\partial g_P^i} g_P^i - 2\kappa_1 \underbrace{D_{g_P}}_{=1/2} \frac{\partial Z_{\underline{\Psi}}^{(1)}}{\partial g_P^i} g_P^i - \underbrace{D_{g_P}}_{=1/2} \Delta_P \delta \kappa_1^{(1)}$$

$$= \frac{3}{2} \Delta_P \delta \kappa_1^{(1)} - 2\kappa_1 \Delta_P \delta Z_{\underline{\Psi}}$$

$$= \frac{1}{16\pi^2} [-24\vec{g}_P^4 + 24\kappa_1 \vec{g}_P^2] \tag{5.19}$$

$$\Delta_P \beta_{\kappa_2} = \underbrace{D_{g_P}}_{=1/2} \frac{\partial \Delta_P \delta \kappa_2^{(1)}}{\partial g_P^i} g_P^i - 2\kappa_2 \underbrace{D_{g_P}}_{=1/2} \frac{\partial Z_{\underline{\Psi}}^{(1)}}{\partial g_P^i} g_P^i - \underbrace{D_{g_P}}_{=1/2} \Delta_P \delta \kappa_2^{(1)}$$

$$= \frac{3}{2} \Delta_P \delta \kappa_2^{(1)} - 2\kappa_2 \Delta_P \delta Z_{\underline{\Psi}}^{(1)}$$

$$= \frac{1}{16\pi^2} [-24\vec{g}_P^4 + 24\kappa_2 \vec{g}_P^2]. \tag{5.20}$$

## 5.2.2 Doublet-Bidoublet Couplings

Also here, the contributions to the doublet-bidoublet couplings are obtained in complete analogy to section 4.2.2. The contributing diagrams are

 and  , (5.21)

where in the second diagram the crossing lines are given by quarks. Again accounting for the color factor, from (4.35), one obtains for the counterterms[1]

$$\Delta_P \delta\beta_1 = \frac{-12 T_P^+}{16\pi^2 \epsilon} \tag{5.22a}$$

$$\Delta_P \delta f_1 = \frac{-12 T_P^-}{16\pi^2 \epsilon} \tag{5.22b}$$

$$\Delta_P \delta\beta_2 = \frac{6 T_P^{\{\}}}{16\pi^2 \epsilon} \tag{5.22c}$$

$$\Delta_P \delta\beta_3 = \frac{3 T_P^{[]}}{16\pi^2 \epsilon} \tag{5.22d}$$

$$\tag{5.22e}$$

with

$$T_P^+ \equiv \vec{g}_P^T (\bar{Y}_{\underline{Q}}^{+2} + \bar{Y}_{\underline{Q}}^{-2}) \vec{g}_P \tag{5.23a}$$

$$T_P^- \equiv \vec{g}_P^T (\bar{Y}_{\underline{Q}}^{+2} - \bar{Y}_{\underline{Q}}^{-2}) \vec{g}_P, \tag{5.23b}$$

$$T_P^{\{\}} \equiv \vec{g}_P^T \{\bar{Y}_{\underline{Q}}^{+}, \bar{Y}_{\underline{Q}}^{-}\} \vec{g}_P, \tag{5.23c}$$

$$T_P^{[]} \equiv \vec{g}_P^T [\bar{Y}_{\underline{Q}}^{+2}, \bar{Y}_{\underline{Q}}^{-2}] \vec{g}_P. \tag{5.23d}$$

Together with the contribution to the doublet wavefunction renormalization (5.18) one obtains $P$'s contribution to the beta-function of $\beta_1$

$$\Delta_P \beta_{\beta_1} = \frac{1}{16\pi^2} \left( -12 T_P^+ + 12\beta_1 \vec{g}_P^2 \right) \tag{5.24}$$

In the same way one finds for $f_1$:

$$\Delta_P \beta_{f_1} = \frac{1}{16\pi^2} \left( -12 T_P^- + 12 f_1 \vec{g}_P^2 \right) \tag{5.25}$$

And for the $\mathbb{Z}_4$-breaking terms one finds

$$\Delta_P \beta_{\beta_2} = \frac{1}{16\pi^2} \left( 6 T_P^{\{\}} + 12\beta_2 \vec{g}_P^2 \right) \tag{5.26}$$

---

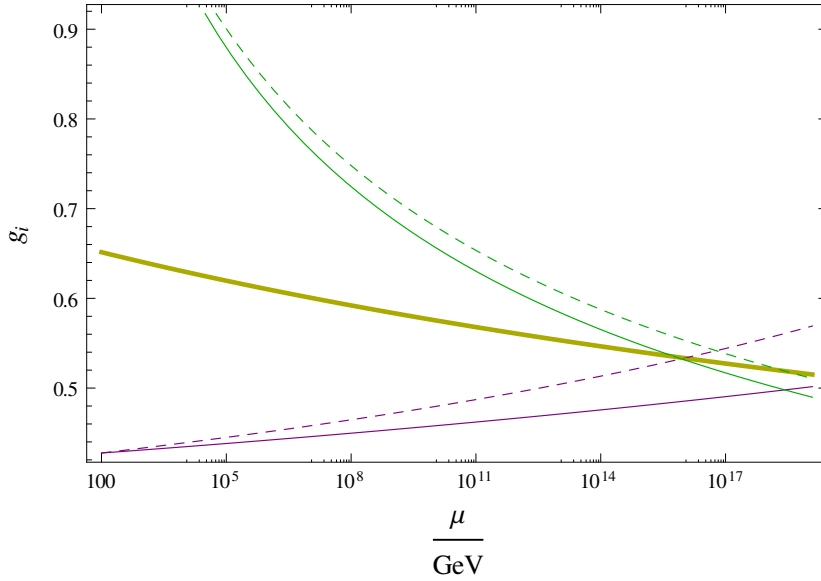[1]For completeness, also the $\mathbb{Z}_4$ breaking terms are given.

and

$$\Delta_P \beta_{\beta_3} = \frac{1}{16\pi^2} \left( 3T_P^{[]} + 12\beta_3 \vec{g}_P^2 \right).$$ (5.27)

## 5.2.3 Standard Quark Yukawa Couplings

The contribution to the wavefunction counterterm of the quarks is given by



$$\underline{Q}_{aA}^i \quad \text{---} \quad \underline{Q}_{bB}^j \; = \text{UV finite} - i\delta_{BA} \gamma_{ba}^\mu g_P^j g_P^i p_\mu \frac{1}{16\pi^2 \epsilon}$$ (5.28)

Thus, $g_P$ contributes to the quark wavefunction renormalization by

$$i\not{p}\Delta_P \delta Z_{\underline{Q}}^{ji} = i\not{p}\frac{g_P^j g_P^i}{16\pi^2 \epsilon}.$$ (5.29)

Inserting this into the defining expression of the Yukawa coupling $\beta$-function (**??**) one obtains the contribution

$$\Delta_P \beta_{Y_{\underline{Q}}^{\pm ij}} = -\frac{1}{2}(Y_{\underline{Q}}^{\pm} \Delta_P \delta Z_{\underline{Q}}^{(1)})^{ij} = \frac{-1}{16\pi^2}\frac{1}{2}Y_{\underline{Q}}^{\pm ik}g_P^k g_P^j.$$ (5.30)

## 5.2.4 Gauge Couplings

In contrast to the fermionic singlet discussed in chapter 4, the isosinglet $P$ is charged under the $SU(3)$-color and the $U(1)_{B-L}$. Hence, it affects the running of the gauge couplings $g_3$ and $g_1$. At one-loop order the gauge coupling $\beta$-functions are given by

$$\beta_g = -\frac{g^3}{(4\pi)^2}\left[ \frac{11}{3}C_{\text{adj}} - \frac{2}{3}\sum_f C_f - \frac{1}{6}\sum_h C_h \right],$$ (5.31)

where $C_{adj}$, $C_f$ and $C_h$ denote the Dynkin indices of the adjoint representation, the representation of the left-handed Weyl fermions and the representation of the (real) Higgs field respectively (see *e.g.* [36]). Since $P$ is just like the quarks in the

Figure 5.1: The running of the gauge couplings at one-loop is shown. The green, yellow and purple lines correspond to the $SU(3)$, $SU(2)$ and $U(1)$ gauge couplings respectively. While the continous lines represent the running in the minimal model, the dashed lines give the couplings which are modified by the introduction of the isosinglet color triplet representation $P$. As $P$ is a singlet under the $SU(2)$, the running of $g_2$ is not altered.

fundamental representation regarding the $SU(3)$-color it contributes

$$\Delta_P \beta_{g_3} = -\frac{g_3^3}{(4\pi)^2}\left[-\frac{2}{3}2C_P\right] = \frac{2}{3}\frac{g_3^3}{(4\pi)^2} \tag{5.32}$$

to the $\beta$-function of $g_3$.

With regard to the $U(1)$ it carries a charge of $B - L = \frac{4}{3}$ and therefore modifies the $\beta$-function of $g_1$ by

$$\Delta_P \beta_{g_1} = -\frac{g_1^3}{(4\pi)^2}\left[-\frac{2}{3}2C_P\right] = \frac{16}{9}\frac{g_1^3}{(4\pi)^2}. \tag{5.33}$$

Note the factor of 3 stemming from the color degrees of freedom. In figure 5.1, the running of the gauge couplings in the minimal and extended model, respectively, is shown.

## 5.3 Renormalization

### 5.3.1 Counterterm Lagrangian

Finally, the coupling $g_P$ will be renormalized. The wavefunction renormalization $Z_P$ is given by

$$P_B = Z_P^{\frac{1}{2}} P. \tag{5.34}$$

The renormalized coupling $g_P$ is then given by

$$g_{PB}^i = (Z_{\underline{Q}}^{-\frac{1}{2}})_{ij} \left[ g_P^j + \delta g_P^j \right] \mu^{\frac{\epsilon}{2}} Z_{\underline{\Psi}}^{-\frac{1}{2}} Z_P^{-\frac{1}{2}}, \tag{5.35}$$

where $g_{PB}{}^i$ and $\delta g_P^i$ denote the bare coupling and the counterterm respectively. The counterterm lagrangian corresponding to $P$ then is

$$\delta \mathcal{L}_P = \bar{P} i \not{D} (\delta Z_P) P - \mu^{\frac{\epsilon}{2}} \bar{Q}_L^i \delta g_P^i \chi_L P_R - \mu^{\frac{\epsilon}{2}} \bar{Q}_R^i \delta g_P^i \chi_R P_L + h.c.. \tag{5.36}$$

In the following, first the vertex counterterm $\delta g_P$ will be determined. In a second step the wavefunction counterterm $\delta Z_P$ will be calculated and finally the $\beta$-function corresponding to $g_P$ will be derived.

### 5.3.2 Vertex Renormalization

There are five diagrams contributing to the $g_P$ renormalization:



$$\tag{5.37}$$

Thus, the vertex renormalization is given by



$$\tag{5.38}$$

where the symmetry factors are given by $S_i = 1/3! \cdot 6 = 1$.

The divergent parts of the diagrams $S_{12}$, $S_{13}$ and $S_{15}$ can be obtained from the analogous diagrams (4.48) in the case of the fermionic singlet accounting for the correct $U(1)_{B-L}$ charge of the quarks and $P$ repectively. They yield



$$= \text{UV finite} + i\mu^{\frac{\epsilon}{2}} g_P^i \delta_{ba} \delta_{BA} \frac{1}{16\pi^2 \epsilon} \left( \frac{-g_1^2}{2} \xi_1 - \frac{3g_2^2}{4} \xi_2 \right).$$

$$(5.39)$$

To calculate the diagrams $S_{14}$ and $S_{15}$ the same momentum assignments as in (4.47) will be used. For the diagram $S_{14}$ is then given by



$$(5.40)$$

$$= -\mu^{\frac{3\epsilon}{2}} \frac{g_1^2}{9} g_P^i \delta_{BA} \int \frac{\mathrm{d}^d k}{(2\pi)^d} \frac{(\gamma^\mu \slashed{k}'' \slashed{k}' \gamma^\sigma)_{ba} \left( \eta_{\mu\nu} - (1-\xi) \frac{k_\mu k_\nu}{k^2} \right)}{(k''^2 + i\epsilon)(k'^2 + i\epsilon)(k^2 + i\epsilon)}$$

$$= -\mu^{\frac{3\epsilon}{2}} \frac{g_1^2}{9} g_P^i \delta_{BA} (\gamma^\mu \gamma^\nu \gamma^\rho \gamma^\sigma)_{ba} \int \frac{\mathrm{d}^d k}{(2\pi)^d} \frac{k_\nu'' k_\rho' \left( \eta_{\mu\sigma} - (1-\xi_1) \frac{k_\mu k_\sigma}{k^2} \right)}{(k''^2 + i\epsilon)(k'^2 + i\epsilon)(k^2 + i\epsilon)}$$

$$= -\mu^{\frac{3\epsilon}{2}} \frac{g_1^2}{9} g_P^i \delta_{BA} (\gamma^\mu \gamma^\nu \gamma^\rho \gamma^\sigma)_{ba} \underbrace{\int \frac{\mathrm{d}^d k}{(2\pi)^d} \frac{(k_\nu + p_{2\nu} + p_{3\nu})(k_\rho + p_{2\rho}) \left( \eta_{\mu\sigma} - (1-\xi_1) \frac{k_\mu k_\sigma}{k^2} \right)}{(k + p_2 + p_3)^2 (k + p_2)^2 k^2}}_{= \text{UV finite} + \frac{i\pi^2}{(2\pi)^4 \mu^\epsilon} \left( \frac{1}{2\epsilon} \eta_{\nu\rho} \eta_{\mu\sigma} - (1-\xi_1) \frac{1}{12\epsilon} (\eta_{\mu\nu} \eta_{\rho\sigma} + \eta_{\mu\rho} \eta_{\nu\sigma} + \eta_{\mu\sigma} \eta_{\nu\rho}) \right)}$$

$$= \text{UV finite} - i\mu^{\frac{\epsilon}{2}} \frac{g_1^2}{9} g_P^i \delta_{BA} \delta_{ba} \frac{1}{16\pi^2 \epsilon} (6 + 2\xi_1) \qquad (5.41)$$

And for the diagram $S_{16}$ one finds



$$(5.42)$$

$$
\begin{aligned}
&= -\mu^{\frac{3\epsilon}{2}} g_3^2 g_P^i \delta_{BA} \frac{1}{4} (\lambda^c \lambda^c)_{lk} (\gamma^\mu \gamma^\nu \gamma^\rho \gamma^\sigma)_{ba} \int \frac{\mathrm{d}^d k}{(2\pi)^d} \frac{k_\nu'' k_\rho' \left( \eta_{\mu\sigma} - (1 - \xi_1) \frac{k_\mu k\sigma}{k^2} \right)}{(k''^2 + i\epsilon)(k'^2 + i\epsilon)(k^2 + i\epsilon)} \\
&= -i\mu^{\frac{\epsilon}{2}} g_3^2 g_P^i \delta_{BA} \delta_{ba} \frac{1}{4} \underbrace{(\lambda^c \lambda^c)_{lk}}_{= \frac{16}{3}} \frac{1}{16\pi^2 \epsilon} (6 + 2\xi_3) \\
&= -i\mu^{\frac{\epsilon}{2}} g_3^2 g_P^i \delta_{BA} \delta_{ba} \delta_{lk} \frac{1}{16\pi^2 \epsilon} \left( 8 + \frac{8}{3}\xi_3 \right)
\end{aligned}
\tag{5.43}
$$

As it was already noted in chapter 4, the gauge parameters $\xi_1$, $\xi_2$ and $\xi_3$ are not physical, but are kept here as a consistency check.

According to (5.36), the vertex counterterm $\delta g_P^i$ is defined as



$$
= -i\mu^{\frac{\epsilon}{2}} \delta_{BA} \delta_{ba} \delta_{lk} \delta g_P^i
\tag{5.44}
$$

and therefore yields

$$
\delta g_P^i = -\frac{1}{16\pi^2 \epsilon} g_P^i \left[ \left( -\frac{2}{3} - \frac{13}{18}\xi_1 \right) g_1^2 - \frac{3}{4}\xi_2 g_2^2 + \left( -8 - \frac{8}{3}\xi_3 \right) g_3^2 \right].
\tag{5.45}
$$

### 5.3.3 Wavefunction Renormalization

The wavefunction renormalization of $P$ is given by



$$
\tag{5.46}
$$

where the symmetry factors are given by $S_i = 1/2! \cdot 2 = 1$. The $U(1)$ contribution yields



$$= (-i\mu^{\frac{\epsilon}{2}})^2 (\gamma^\mu \gamma^\nu \gamma^\rho)_{ba} \left(\frac{2g_1}{3}\right)^2 \int \frac{\mathrm{d}^d k}{(2\pi)^d} \frac{(p_\nu - k_\nu)\left(\eta_{\mu\rho} - (1-\xi_1)\frac{k_\mu k_\rho}{k^2}\right)}{(p-k)^2 k^2}$$

(5.47)

$$= \text{UV finite} + (-i\mu^{\frac{\epsilon}{2}})^2 \left(\frac{2g_1}{3}\right)^2 \frac{i\pi^2}{(2\pi)^4 \mu^\epsilon} \frac{1}{\epsilon} (-2\slashed{p}_{ba}\xi_1)$$

(5.48)

$$= \text{UV finite} + i\mu^{\frac{\epsilon}{2}} \slashed{p} \frac{1}{16\pi^2\epsilon} \frac{8g_1^2}{9} \xi_1$$

(5.49)

And, analogously, the gluon contribution gives



$$= (-i\mu^{\frac{\epsilon}{2}})^2 (\gamma^\mu \gamma^\nu \gamma^\rho)_{ba} \left(\frac{\lambda^c}{2}\frac{\lambda^c}{2}\right)_{lk} g_3^2 \int \frac{\mathrm{d}^d k}{(2\pi)^d} \frac{i(p_\nu - k_\nu)}{(p-k)^2 + i\epsilon} \frac{-i}{k^2 + i\epsilon} \left(\eta_{\mu\rho} - (1-\xi_3)\frac{k_\mu k_\rho}{k^2}\right)$$

$$= \text{UV finite} + i\mu^{\frac{\epsilon}{2}} \slashed{p}_{ba} \frac{1}{16\pi^2\epsilon} \frac{8g_3^2}{3} \xi_3$$

(5.50)

And, finally, the Yukawa coupling $g_P$ contributes



$$= (-i)^2 (\mu^{\frac{\epsilon}{2}})^2 \delta_{BA} \delta_{AB} \sum_i (g_P^i)^2 \int \frac{\mathrm{d}^d k}{(2\pi)^d} \frac{i\slashed{k}_{ba}}{k^2 + i\epsilon} \frac{i}{(k-p)^2 + i\epsilon}$$

$$= \mu^\epsilon 4\gamma_{ba}^\mu \sum_i (g_P^i)^2 \underbrace{\int \frac{\mathrm{d}^d k}{(2\pi)^d} \frac{k_\mu}{k^2 (p-k)^2}}_{=\text{UV finite} + \frac{i\pi^2}{(2\pi)^4 \mu^\epsilon} \frac{1}{\epsilon} p_\mu}$$

$$= \text{UV finite} + i\mu^{\frac{\epsilon}{2}} \vec{g}_P^{\,2} \gamma_{ba}^\mu p_\mu \frac{4}{16\pi^2\epsilon}$$

(5.51)

Thus, the wavefunction counterterm that is defined as

$$\text{—⊗—} \quad = i\not{p}\mu^{\frac{\epsilon}{2}}\delta Z_P \tag{5.52}$$

is given by

$$\delta Z_P =: \frac{\delta Z_P^{(1)}}{\epsilon} = \frac{1}{16\pi^2\epsilon}\left(\frac{-8g_1^2}{9}\xi_1 - \frac{8}{3}g_3^2\xi_3 - 4\vec{g}_P^{\,2}\right). \tag{5.53}$$

## 5.3.4 Beta-Function

In the preceding subsections the wavefunction renormalization of $P$ and the vertex renormalization have been performed. Thereby, having found the counterterms, all the ingredients needed to derive the $\beta$-function of $g_P$ have been collected. The $\beta$-function is given by:

$$\beta_{g_P^i} = \frac{1}{2}\left(\sum_{V_A}\left[\frac{\partial\delta g_P^{i(1)}}{\partial V_A} - \frac{1}{2}\frac{\partial\delta Z_f^{(1)}}{\partial V_A} - \frac{1}{2}g_P^j\frac{\partial(\delta Z_{\underline{Q}}^{(1)})_{ji}}{\partial V_A} - \frac{1}{2}g_P^i\frac{\partial\delta Z_{\underline{\Psi}}^{(1)}}{\partial V_A}\right]V_A - \delta g_P^{i(1)}\right) \tag{5.54}$$

where $V_A$ runs over all couplings including $g_P^i$ and the upper index (1) represents the coefficient multiplying $1/\epsilon$ in the Laurent expansion. Inserting the counterterms then gives:

$$\begin{aligned}
\beta_{g_P^i} &= \delta g_P^{i(1)} - \frac{1}{2}g_P^i\left(\delta Z_P^{(1)} + \delta Z_{\underline{\Psi}}^{(1)}\right) - \frac{1}{2}\delta Z_{\underline{Q}}^{(1)ij}g_P^j \\
&= \frac{1}{16\pi^2}\left[g_P^i\left(8\vec{g}_P^{\,2} - \frac{17}{12}g_1^2 - \frac{9}{8}g_2^2 - 8g_3^2\right) + \left((\bar{Y}_{\underline{Q}}^{+2} + \bar{Y}_{\underline{Q}}^{-2})\vec{g}_P\right)^i - \frac{1}{2}\vec{g}_P^{\,2}g_P^i\right]
\end{aligned} \tag{5.55}$$

This result concludes the renormalization due to $g_P$. As for the last chapter, all results obtained here are collected in the appendix A.2.3.
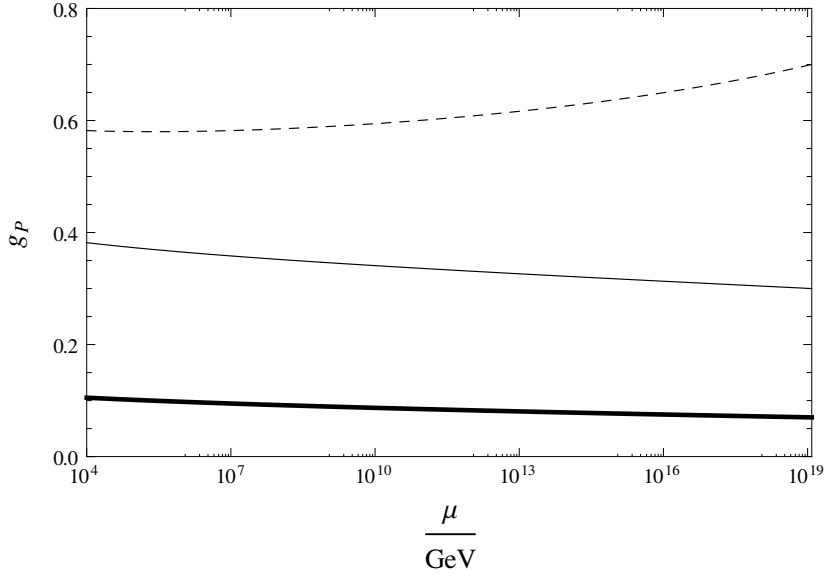
Figure 5.2: The running of the $g_P$ is plotted for the initial values $g_P(\Lambda_{\mathrm{Pl}}) = 0.07$ (thick line) , $g_P(\Lambda_{\mathrm{Pl}}) = 0.3$ (thin line) and $g_P(\Lambda_{\mathrm{Pl}}) = 0.7$(*dashedline*). Just as the coupling $g_f$ in the case of the fermionic singlet, $g_P$ exhibits a mild running, as its beta-function is proportional to $g_P$.

## 5.4 Symmetry Breaking in the Extended Model II

### 5.4.1 Metastability Revisited

As the introduction of the isosinglet representation affects the running of the gauge couplings $g_3$ and $g_1$ (see section 5.2.4), the discussion of metastability (see section 3.2) has to be revisited. Qualitatively the effect is not easily seen since the beta-functions of the bidoublet self-couplings $\lambda_1$, $\lambda_2$ and $\lambda_3$ do not depend directly on $g_3$ and $g_1$ at one-loop[2]. It is a two-loop effect. The discussion, here, is thus based on the numerical solution of the beta-functions. In figure 5.3 the modified running of the bidoublet self-couplings is shown and in figure 5.4 the stability conditions in question are depicted in presence of the lower bound given by the requirement of metastability. It reveals that the situation worsened but not drastically. The potential still resides in the metastable regime.

---

[2]The bidoublet is not colored and does not carry $U(1)$ charge.
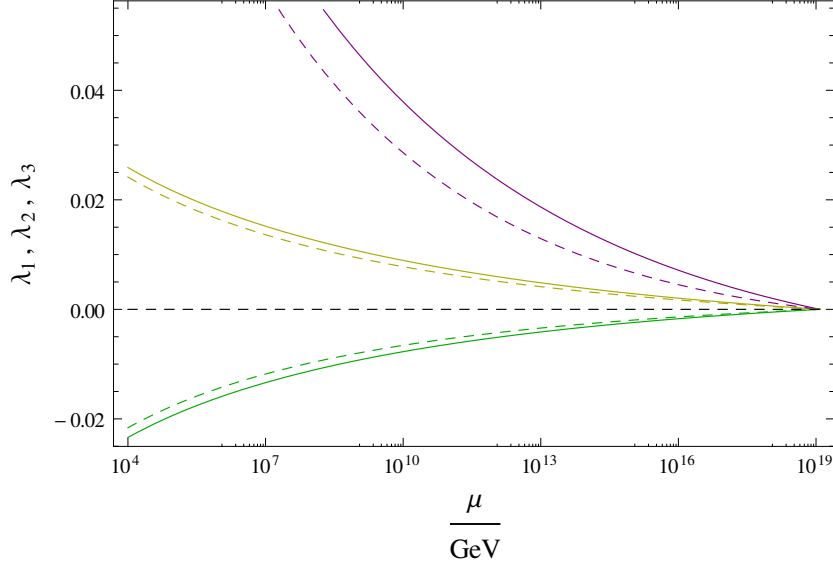
Figure 5.3: The running of the bidoublet self-couplings, $\lambda_1$ (purple line), $\lambda_2$ (green line) and $\lambda_3$ (yellow line). The continous lines correspond to the minimal model while the dashed lines represent the running in presence of the isosinglet $P$. These corrections are two-loop effects as the bidoublet is solely charged under the $SU(2)_L \times SU(2)_R$, under which $P$ is a singlet.

## 5.4.2 Effect on Doublet Self-Coupling

The effect on the doublet self-couplings $\kappa_1$ and $\kappa_2$ is discussed in complete analogy to the case of the fermionic singlet (see section 4.4.1). The contribution of $g_P$ to the doublet self-couplings is essentially the same as in the case of the singlet $f$,

$$\Delta_P \beta_{\kappa_1} = \frac{1}{16\pi^2} [-24\vec{g}_P^4 + 24\kappa_1 \vec{g}_P^2] \tag{5.56}$$

$$\Delta_P \beta_{\kappa_2} = \frac{1}{16\pi^2} [-24\vec{g}_P^4 + 24\kappa_2 \vec{g}_P^2]. \tag{5.57}$$

It differs slightly due to color factors and the vector-nature of $P$. The signs and orders of magnitude are however identical. Thus, as in section 4.4.1, there is an upper bound for $g_P$ which, if crossed, leads to $\kappa_1$ and $\kappa_2$ run into parity conserving solutions first and finally leads to the emergence of fixpoints that correspond to vanishing doublet VEVs. Above this upper bound the $g_P$-contributions in (5.56) dominate the gauge contributions, it can roughly be estimated by demanding

$$\beta_{\kappa_1}(\max[g_P])|_{\kappa_1 = \kappa_2 = 0} = 0, \quad \beta_{\kappa_2}(\max[g_P])|_{\kappa_1 = \kappa_2 = 0} = 0. \tag{5.58}$$
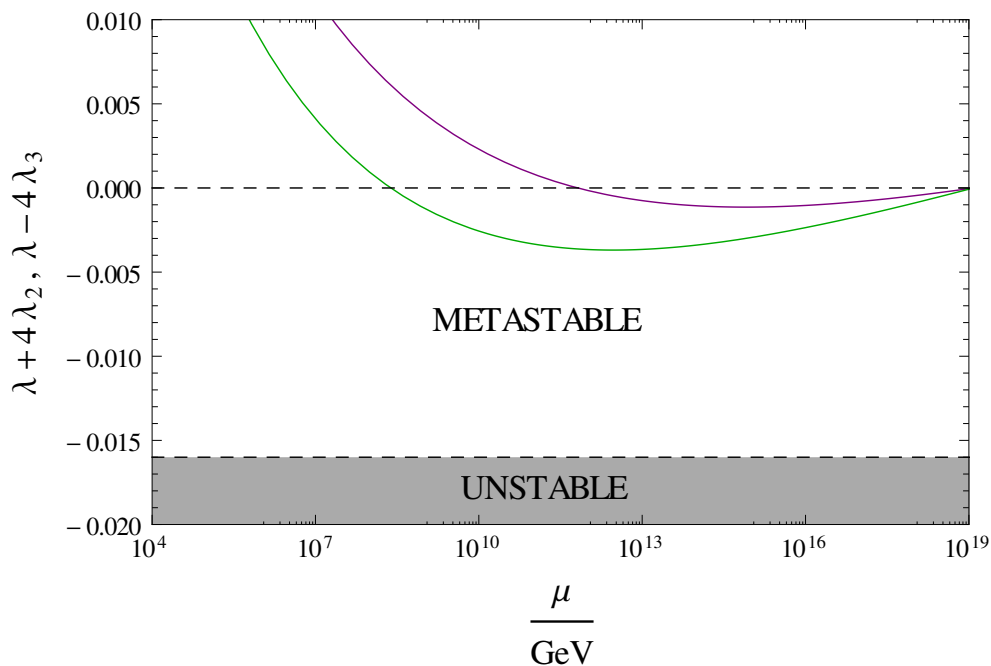
Figure 5.4: The quantities $\lambda_1 + 4\lambda_2$ (purple line) and $\lambda_1 - 4\lambda_3$ (green line) are plotted in the model including the isosinglet $P$. Being above the lower bound given by $\lambda_1 \pm 4\lambda_{2,3} = -0.015$ it is ensured that the low-energy vacuum of the model is metastable in the sense that its decay time is greater than the age of the universe (*cf.* figure 3.4).

This leads to $\max[g_P] \approx 0.25$. Below this upper bound, however, a big hierarchy can be generated. This is illustrated in figure 5.5. As the $\mathcal{O}(g_P^4)$ contributions enter the beta-functions with coefficients greater than in the case $f$, the allowed parameter region for $g_P$ is smaller. Therefore, $g_P$ is constraint to be within the region

$$0 < g_P < 0.25, \tag{5.59}$$

which, as will turn out subsequently, is sufficiently large to generate the little hierarchy.

## 5.4.3 Effect on Doublet-Bidoublet Couplings: Little Hierarchy

As in section 4.4.2, here it is studied which flat directions emerge under variation of $g_P(\Lambda_{\mathrm{Pl}})$ within the allowed region $0 < g_P < 0.25$. This region has been obtained previously by the requirement that only parity-breaking solutions are accepted. Fur-

thermore, it is studied which little hierarchies they correspond to.

The coupling $g_P$ has a much greater impact on the doublet-bidoublet couplings $\beta_1$ and $f_1$ than $g_f$ had in the previous chapter. This is due to the corresponding loop diagrams involving quarks instead of leptons, which was the motivation for introducing this represention. For convenience the contributions to $\beta_{\beta_1}$ and $\beta_{f_1}$ are reproduced here,

$$\Delta_P \beta_{\beta_1} = \frac{1}{16\pi^2}\left(-12T_P^+ + 12\beta_1 \vec{g}_P^2\right)$$
$$\Delta_P \beta_{f_1} = \frac{1}{16\pi^2}\left(-12T_P^- + 12f_1 \vec{g}_P^2\right)$$

with

$$T_P^+ = \vec{g}_P^T(\bar{Y}_{\underline{Q}}^{+2} + \bar{Y}_{\underline{Q}}^{-2})\vec{g}_P \qquad \text{and} \qquad T_P^- = \vec{g}_P^T(\bar{Y}_{\underline{Q}}^{+2} - \bar{Y}_{\underline{Q}}^{-2})\vec{g}_P.$$

In contrast to the case of the singlet $f$, it is expected that for sufficiently large $g_P(\Lambda_{\mathrm{Pl}})$ a flat direction of type IIa emerges[3], while in the preceding chapter the only flat direction was of type Ib. In section 4.4.2 it has been argued that, for this to happen, $f_1$ has to satisfy the inequality,

$$|f_1| > 8\max\left[|\lambda_2|, |\lambda_3|\right] \cdot \frac{\kappa^2}{v_R^2}. \tag{5.60}$$

Note that, although this inequality has been considered with regard to type IIb flat directions, it is applicable here as types IIa and IIb are essentially connected by $f_1 \leftrightarrow -f_1$, which does not alter this condition. It can be shown, using a linear approximation as in (4.4.2), that (5.60) is indeed satisfied within the allowed values for $g_P$. Note that once the flat direction of type IIa emerges, the type Ib flat direction does not correspond to a minimum anymore. Hence, the situation is as follows. For small values of $g_P(\Lambda_{\mathrm{Pl}})$ symmetry breaking takes place in flat directions of type Ib until $g_P$ crosses a threshold after which the breaking is along type IIa flat direction. The *little hierarchies* for these directions are expressed by

$$\frac{\kappa^2 + \kappa'^2}{v_R^2} = \begin{cases} \frac{-\beta_1}{2\lambda_1 - 8\lambda_3} & \text{for flat direction Ib} \\ \\ \frac{f_1 - 2\beta_1}{4\lambda_1} & \text{for flat direction IIa} \end{cases}.$$

---

[3]As in the case of quarks $\bar{Y}_{\underline{Q}}^{+2} \neq 0$ and $\bar{Y}_{\underline{Q}}^{-2} = 0$, one has $\beta_{f_1}(\Lambda_{\mathrm{Pl}}) < 0$, which leads to $f_1 > 0$. Thus, here the emergence of flat directions of type IIa are discussed, rather than type IIb directions.

As in the case of the singlet $f$, for direction Ib the little hierarchy is expected to increase, which corresponds to a decreasing expression above, when $g_P$ becomes larger. Since the contribution $\Delta_P \beta_{\beta_1}(\Lambda_{\mathrm{Pl}})$ compensates the positive gauge contributions in $\beta_{\beta_1}$, the generation of $\beta_1$, which is not present at $\Lambda_{\mathrm{Pl}}$, is retarded. In contrast, for type IIa flat directions the little hierarchy is essentially given by the difference $f_1 - 2\beta_1$. One can use the linear approximation approach to estimate at which value of $g_P$ this difference becomes small. As this difference is zero at the Planck scale, it remains small if its beta-function vanishes at $\Lambda_{\mathrm{Pl}}$, too. It is made the ansatz

$$\left(\beta_{f_1} - 2\beta_{\beta_1}\right)\big|_{\mu=\Lambda_{\mathrm{Pl}}} = 0. \tag{5.61}$$

This leads to

$$\left(-12T_P^- - 2\left(-12T_P^+ + \frac{9g_2^4}{16}\right)\right)\Bigg|_{\mu=\Lambda_{\mathrm{Pl}}} = 0, \tag{5.62}$$

which is satisfied for

$$g_P^2(\Lambda_{\mathrm{Pl}}) = \frac{3}{128} \frac{g_2^4(\Lambda_{\mathrm{Pl}})}{Y_{\underline{Q}}^{+2}(\Lambda_{\mathrm{Pl}})} \tag{5.63}$$

and one finds

$$g_P(\Lambda_{\mathrm{Pl}}) \approx 0.077. \tag{5.64}$$

This value clearly is in the allowed region of $g_P$. Thus, it can be expected that by adjusting $g_P$ one can generate a little hierarchy as large as desired. The results obtained by solving the full system of beta-functions, are depicted in figure 5.6. It reveals that the estimated value of $g_P$ leading to large little hierarchies is in good agreement with the result taking into account the full running of the couplings. Note that $f_1 - 2\beta_1 < 0$ corresponds to the symmetry being broken in direction IIc. In this direction the only right-handed doublet acquires a VEV such that only the $SU(2)_R$ is broken, while the SM gauge group remains unbroken.

(a) $g_P(\Lambda_{\mathrm{Pl}}) = 0.1$

(b) $g_P(\Lambda_{\mathrm{Pl}}) = 0.3$
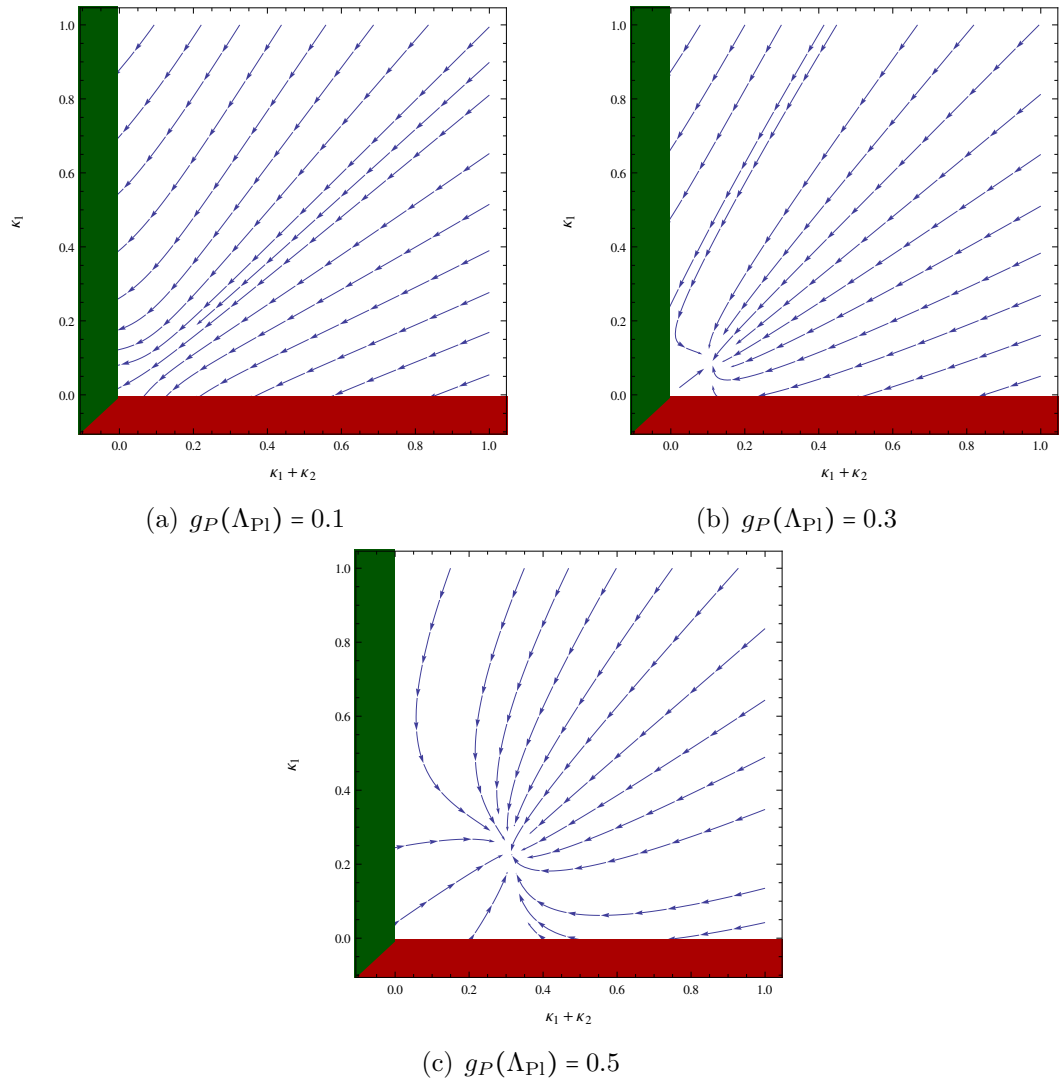
(c) $g_P(\Lambda_{\mathrm{Pl}}) = 0.5$

Figure 5.5: In analogy to fig. 4.2, the renormalization group flow of the doublet self-couplings $\kappa_1$ and $\kappa_+ = \kappa_1 + \kappa_2$ is shown in presence of the Yukawa coupling $g_P$, which couples $P$ to quarks and leptons. For values of $g_P$ below $g_P(\Lambda_{\mathrm{Pl}}) = 0.25$ (*cf.* fig. 5.5(a)) the running of $\kappa_1$ and $\kappa_2$ is dominated by gauge contributions, allowing for the emergence of parity breaking GW-solutions in a large fraction of parameter space. For $g_P \gtrsim 0.25$, contributions due to quark-$P$ loops dominate, driving the couplings into fixpoint away from the emergence of neither parity breaking nor parity conserving flat directions.
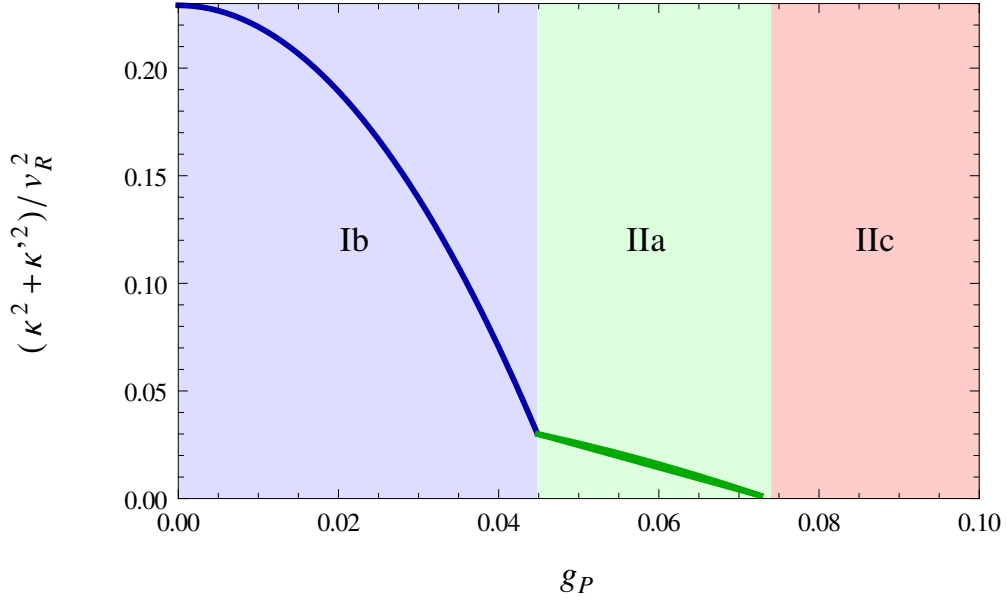
Figure 5.6: The little hierarchy is plotted as a function of the Yukawa coupling $g_P$ at $\Lambda_{\mathrm{Pl}}$. The plot is split into 3 regions corresponding to flat directions of types Ib, IIa and IIc. For $0 < g_P \lesssim 0.044$, symmetry breaking occurs exclusively in type Ib flat directions. The decreasing ratio $(\kappa^2 + \kappa'^2)/v_R$ corresponds to an increasing little hierarchy, *i.e.* an increasing $v_R$ when the bidoublet VEVs are fixed. For $0.044 \lesssim g_P \lesssim 0.073$ the symmetry is broken along flat directions of type IIa. In this region the little hierarchy can be adjusted to arbitrarily high values by appropriate choice of $g_P$. For $0.073 \lesssim g_P \lesssim 0.10$ the bidoublet VEVs vanish, the LR symmetry is broken to the SM which remains unbroken.

# Chapter 6

# Conclusions and Outlook

In this diploma-thesis, the radiative symmetry breaking of the LR symmetric model with a minimal Higgs sector has been considered in the presence of a shift symmetry at the Planck scale $\Lambda_{\text{Pl}}$. It has been shown that in the reduced parameter space, given by the doublet self-couplings $\kappa_1$ and $\kappa_2$, a large hierarchy between the breaking scale of LR symmetry, given by $v_R$, and $\Lambda_{\text{Pl}}$ can be obtained, as the breaking of the LR symmetry is triggered by the running of these couplings.

At the same time, however, the running of the bidoublet self-couplings as well as the running of the doublet-bidoublet couplings, is essentially fixed by imposing the shift symmetry in the minimal model. This is due to the fact that $\kappa_1$ and $\kappa_2$ do not contribute to their beta-functions at the one-loop level. As the little hierarchy between the electroweak scale and $v_R$ is set by the relative strength of these couplings, it is nearly fixed by the shift symmetry. With the electroweak scale being given, one obtains a right-handed scale of order $v_R = 500\,\text{GeV}$, which is clearly excluded by experiment. Furthermore, similar to the SM, the vanishing bidoublet self-couplings at $\Lambda_{\text{Pl}}$ leads to the potential minimum being metastable. Under consideration of the tunneling decay probability of the vacuum, it could be shown, however, that the model is still consistent as the decay time exceeds the age of the universe.

In order to find a way to extend the little hierarchy to phenomenologically acceptable values, two extensions of the minimal model have been considered.

In chapter 4, a fermionic singlet, called $f$, has been added to the model. Via its Yukawa coupling to scalar doublets and leptons, such a representation contributes, on the one hand, to the running of the doublet self-couplings and, on the other hand, to the running of the intermediate doublet-bidoublet couplings. As the contributions to $\kappa_1$ and $\kappa_2$ have the effect of deflecting these couplings away from parity breaking solutions, an upper bound for suitable couplings of this additional representation is found. Although its contribtions to the doublet-bidoublet couplings have the correct

signs to lower the little hierarchy, the obtained effect is marginal, as the contributing loop-diagrams are suppressed by the smallness of the lepton Yukawa couplings.

This motivates the introduction of a colored isosinglet $P$ in section 5. It contributes essentially by the same diagrams under the replacement of leptons by quarks. It can be shown that by an appropriate choice of its Yukawa coupling, a arbitrarily large little hierarchy can be generated.

To introdruce this representation consistently an explicit massterm is added to the lagrangian. Thus, conformal symmetry is explicitly broken at the classical level. It remains however a symmetry of the scalar potential. To circumvent this unsatisfactory aspect, one could alternatively introduce a scalar singlet to the model, which acquires a non-vanishing expectation value. As this would lead to an enlarged scalar potential, this possibility is not appreciated. An interesting task for future work could, however, be to consider the radiative symmetry breaking in the minimal classically conformally invariant model with triplet Higgs fields instead of doublets. Here, it has been the fact that the additional fermionic representations coupled standard fermions to doublets, which led to the possibility of affecting the doublet-bidoublet couplings. In the triplet model, where the role of the doublets $\chi_{L/R}$ is taken by the triplets $\Delta_{L/R}$, these couplings are naturally present. They are given by the Majorana couplings

$$\mathcal{L} \supset i \left( L^{iT} C \tau_2 \Delta_L L^j + R^{iT} C \tau_2 \Delta_R R^j \right) + h.c.. \tag{6.1}$$

The beta-functions of the minimal model with triplets are known [37], thus the only part missing for the analysis of radiative symmetry breaking in this model are the Gildener-Weinberg conditions. As the potential of the triplet model includes more couplings than the doublet model, it is not clear if the GW conditions can be obtained analytically, even under consideration of a simplifying $\mathbb{Z}_4$ symmetry.

# Appendix A

# Renormalization Group Functions

## A.1 Derivation of General Formula

Here, a derivation of the $\beta$-function for a coupling $Q$ in the MS-Scheme is given. The treatment, which is presented here, is found in [38]. For simplicity, however, here it is assumed that the couplings of the model including $Q$ be scalar quantities. For the complete treatment, involving couplings of general tensorial structure, consult [38].

Let $Q$ be a quantity that represents the strength of the coupling between the fields $\phi_i$ with $i \in \{1, \ldots, N\}$:

$$\mathcal{L} \supset Q \prod_i \phi_i^{n_i} \tag{A.1}$$

Then, the bare coupling $Q_B$ and the renormalized coupling Q are related by

$$Q_B = (Q + \delta Q)\mu^{D_Q \epsilon} \prod_i Z_{\phi_i}^{\frac{n_i}{2}} \tag{A.2}$$

where the $Z_{\phi_i}$ represent the wavefunction renormalization of the $\phi_i$ according to the usual definition

$$\phi_{iB} = Z_{\phi_i}^{-\frac{1}{2}} \phi_i \tag{A.3}$$

and $\mu^{D_Q \epsilon}$ occurs due to dimensional regularization with $D_Q$ related to the dimension of the operator in (A.1) such that $Q_B$ is a dimensionless quantity.

The $\beta$-function of a coupling Q is defined as its logarithmic derivative with respect to $\mu$,

$$\beta_Q = \mu \frac{\mathrm{d}Q}{\mathrm{d}\mu}. \tag{A.4}$$

As the bare coupling $Q_B$ is energy independent and the counterterm $\delta Q$ and the wavefunction renormalization terms do only depend on $\mu$ implicitly via the dependence on $Q$ and, in general, on the other couplings of the model, denoted by $\{V_A\}$,

*Appendix A Renormalization Group Functions*

the logarithmic derivative with respect to $\mu$ acting on equation (A.2) yields

$$0 = \left(\beta_Q + \frac{\partial \delta Q}{\partial V_A}\beta_{V_A}\right)\prod_i Z_{\phi_i}^{\frac{n_i}{2}} + (Q + \delta Q)\left(D_Q \epsilon \prod_i Z_{\phi_i}^{\frac{n_i}{2}} + \prod_i \frac{n_i}{2} Z_{\phi_i}^{\frac{n_i}{2}-1}\frac{\partial Z_{\phi_i}}{\partial V_A}\beta_{V_A}\right) \quad (A.5)$$

where the sum over the couplings $V_A$ includes $Q$. In order to obtain an expression for $\beta_Q$ which only depends on the counterterms $\delta Q$ and $\delta V_A$, recall that in the MS-scheme the counterterms subtract pure poles in $\epsilon$, using dimensional regularization. This means that the counterterms can be expanded as

$$\delta Q = \frac{\delta Q^{(1)}}{\epsilon} + \mathcal{O}\left(\epsilon^{-2}\right) \quad (A.6)$$

$$\delta V_A = \frac{\delta V_A^{(1)}}{\epsilon} + \mathcal{O}\left(\epsilon^{-2}\right). \quad (A.7)$$

The same holds for the field renormalization $\delta Z_{\phi_i}$:

$$Z_{\phi_i} = 1 + \delta Z_{\phi_i} = 1 + \frac{\delta Z_{\phi_i}^{(1)}}{\epsilon} + \mathcal{O}\left(\epsilon^{-2}\right) \quad (A.8)$$

The $\beta$-function, however, must be finite for $\epsilon \to 0$. Thus, one can make the ansatz

$$\beta_Q = \beta_Q^{(0)} + \beta_Q^{(1)}\epsilon + \ldots + \beta_Q^{(n)}\epsilon^n \quad (A.9)$$

$$\beta_{V_A} = \beta_{V_A}^{(0)} + \beta_{V_A}^{(1)}\epsilon + \ldots + \beta_{V_A}^{(n)}\epsilon^n. \quad (A.10)$$

Inserting these expansions into equation (A.5) one can determine the $\beta$-function by equating the coefficients for every order in $\epsilon$. For this purpose, note that from (A.8) it follows

$$\frac{\partial Z_{\phi_i}}{\partial V_A} = \frac{\partial \delta Z_{\phi_i}^{(1)}}{\partial V_A}\epsilon^{-1} + \mathcal{O}\left(\epsilon^{-2}\right). \quad (A.11)$$

Beginning with $\epsilon^n$, one therefore finds that the only term of order $\epsilon^n$ on the right-hand side of (A.5) is $\beta_Q^{(n)}$. Thus, it is

$$\beta_Q^{(n)} = 0. \quad (A.12)$$

As for every coupling $V_A$ there is an equation similar to (A.5), it holds generally

$$\beta_{V_A}^{(n)} = 0. \quad (A.13)$$

Using this argument successively leads to

$$\beta_Q^{(k)} = \beta_{V_A}^{(k)} = 0 \qquad \text{for} \qquad k \geqslant 2. \tag{A.14}$$

As there is an extra factor of $\epsilon$ multiplying $D_Q$ on the right-hand side of (A.5) for $k = 1$ one finds instead

$$\beta_Q^{(1)} = -D_Q Q \tag{A.15}$$

and, again, by analogy

$$\beta_{V_A}^{(1)} = -D_{V_A} V_A \tag{A.16}$$

Using these results one obtains for zeroth order in $\epsilon$

$$0 = \beta_Q^{(0)} + \beta_Q^{(1)} \sum_i \frac{n_i}{2} \delta Z_{\phi_i}^{(1)} + \frac{\partial \delta Q^{(1)}}{\partial V_A} \beta_{V_A}^{(1)} + Q D_Q \sum_i \frac{n_i}{2} \delta Z_{\phi_i}^{(1)} + Q \sum_i \frac{n_i}{2} \frac{\partial \delta Z_{\phi_i}^{(1)}}{\partial V_A} \beta_{V_A}^{(1)} + \delta Q^{(1)} D_Q \tag{A.17}$$

By inserting the previous results one finally arrives at

$$\beta_Q^{(0)} = D_V \frac{\partial \delta Q^{(1)}}{\partial V_A} V_A - D_Q \delta Q^{(1)} - D_Q \sum_i \frac{n_i}{2} Q \delta Z_{\phi_i}^{(1)} - Q \sum_i \frac{n_i}{2} \frac{\partial \delta Z_{\phi_i}^{(1)}}{\partial V_A} V_A \tag{A.18}$$

As $\beta_Q \xrightarrow{\epsilon \to 0} \beta_Q^{(0)}$, equation (A.18) represents the beta-function of $Q$ in $d = 4$ dimensions. It should be emphasized that in (A.18) the summation over the couplings $V_A$ includes $Q$.

# A.2  Collection of β-Functions

Here, the beta-functions of the model are listed. Furthermore, their modifications due to the introduction of a fermionic singlet and a fermionic isosinglet color triplet are collected.

*Appendix A Renormalization Group Functions*

## A.2.1 Minimal LR-symmetric Model

The one-loop beta-functions of the minimal model have been calculated by [6]. The scalar and Yukawa coupling beta-functions are

$$\beta_{\beta_1} = \frac{1}{256\pi^2}\left[-4\beta_1\left(-8\beta_1 + 6g_1^2 + 27g_2^2 - 2(20\kappa_1 + 4\kappa_2 + 40\lambda_1 + 32\lambda_2 - 32\lambda_3 + T_2)\right)\right.$$
$$\left. + 24f_1^2 + 9g_2^4\right] \tag{A.19a}$$

$$\beta_{f_1} = \frac{f_1}{64\pi^2}\left[16\beta_1 - 6g_1^2 - 27g_2^2 + 8\kappa_1 + 8\kappa_2 + 16(\lambda_1 - 4\lambda_2) + 64\lambda_3 + 2T_2\right] \tag{A.19b}$$

$$\beta_{\kappa_1} = \frac{1}{512\pi^2}\left[\kappa_1(-96g_1^2 - 144g_2^2 + 576\kappa_1 + 384\kappa_2) + 192\kappa_2^2 + 256\beta_1^2 + 128f_1^2\right.$$
$$\left. + 24g_1^4 + 12g_1^2g_2^2 + 9g_2^4\right] \tag{A.19c}$$

$$\beta_{\kappa_2} = \frac{1}{512\pi^2}\left[\kappa_2(-96g_1^2 - 144g_2^2 + 512\kappa_1 + 384\kappa_2) + 128f_1^2 + 12g_1^2g_2^2 + 9g_2^4\right] \tag{A.19d}$$

$$\beta_{\lambda_1} = \frac{1}{128\pi^2}\left[\lambda_1(-72g_2^2 + 256(\lambda_1 + \lambda_2 - \lambda_3) + 8T_2) + 1024(\lambda_2^2 + \lambda_3^2) + 32\beta_1^2 + \right.$$
$$\left. + 8f_1^2 + 9g_2^4 - 2T_4\right] \tag{A.19e}$$

$$\beta_{\lambda_2} = \frac{1}{512\pi^2}\left[\lambda_2(-288g_2^2 + 768\lambda_1 + 3072\lambda_2 + 1024\lambda_3 + 32T_2) - 8f_1^2 + 3g_2^4 + 2T_4\right] \tag{A.19f}$$

$$\beta_{\lambda_3} = \frac{1}{256\pi^2}\left[\lambda_3(-144g_2^2 + 384\lambda_1 - 512\lambda_2 - 1536\lambda_3 + 16T_2) + 4f_1^2 - 3g_2^4 - T_4\right] \tag{A.19g}$$

$$\beta_{Y_{\mathbb{L}}^-} = \frac{1}{64\pi^2}\left[(-6g_1^2 - 9g_2^2)Y_{\mathbb{L}}^- + Y_{\mathbb{L}}^- T_2 + Y_{\mathbb{L}}^- T_2 + 4Y_{\mathbb{L}}^{+3}\right] \tag{A.19h}$$

$$\beta_{Y_{\mathbb{Q}}^+} = \frac{1}{64\pi^2}\left[(-\frac{2}{9}g_1^2 - 9g_2^2 - 32g_3^2)Y_{\mathbb{Q}}^+ + Y_{\mathbb{Q}}^+ T_2 + 4Y_{\mathbb{Q}}^{+3}\right], \tag{A.19i}$$

where it is used

$$T_2 = \text{Tr}\left[Y_{\underline{L}}^{-2} + 3Y_{\underline{Q}}^{+2}\right] \tag{A.20a}$$

$$T_4 = \text{Tr}\left[Y_{\underline{L}}^{-4} + 3Y_{\underline{Q}}^{+4}\right] \tag{A.20b}$$

And the beta-functions of the gauge couplings are

$$\beta_{g_1} = 3\frac{g_1^3}{16\pi^2} \tag{A.21a}$$

$$\beta_{g_2} = \frac{17}{6}\frac{g_1^3}{16\pi^2} \tag{A.21b}$$

$$\beta_{g_3} = -7\frac{g_1^3}{16\pi^2} \tag{A.21c}$$

104

## A.2.2 Fermionic Singlet

By introduction of the fermionic singlet, discussed in chapter 4, the beta-functions of the model are modified by

$$\Delta_f \beta_{\beta_1} = \frac{1}{16\pi^2}(-4T_f^+ + 4\beta_1 \vec{g}_f^2) \tag{A.22a}$$

$$\Delta_f \beta_{f_1} = \frac{1}{16\pi^2}(-4T_f^- + 4f_1 \vec{g}_f^2) \tag{A.22b}$$

$$\Delta_f \beta_{\kappa_1} = \frac{1}{16\pi^2}[-9\vec{g}_f^2] + 8\kappa_1 \vec{g}_f^2 \tag{A.22c}$$

$$\Delta_f \beta_{\kappa_2} = \frac{1}{16\pi^2}[-7\vec{g}_f^2] + 8\kappa_1 \vec{g}_f^2 \tag{A.22d}$$

with $T_f^+ = \vec{g}_f^{\,T}(\bar{Y}_{\underline{L}}^{+2} + \bar{Y}_{\underline{L}}^{-2})\vec{g}_f$ and $T_f^- = \vec{g}_f^{\,T}(\bar{Y}_{\underline{L}}^{+2} - \bar{Y}_{\underline{L}}^{-2})\vec{g}_f$. And the beta-function corresponding to the Yukawa coupling $g_f$ is

$$\beta_{g_f} = \frac{1}{16\pi^2}(-\frac{7}{2}\vec{g}_f^2 g_f^i - \frac{3}{4}g_1^2 g_f^i - \frac{9}{8}g_2^2 g_f^i) + \left((Y_{\underline{L}}^{+2} + Y_{\underline{L}}^{-2})\vec{g}_f\right)^i \tag{A.23}$$

Note that in the case of a full singlet the running of the gauge couplings is not altered.

## A.2.3 Fermionic Isosinglet Color Triplet

The introduction of the isosinglet representation, discussed in chapter 5, leads to the modifications

$$\Delta_P \beta_{\beta_1} = \frac{1}{16\pi^2}(-12T_P^+ + 12\beta_1 \vec{g}_P^2) \tag{A.24a}$$

$$\Delta_P \beta_{f_1} = \frac{1}{16\pi^2}(-12T_P^+ + 12\beta_1 \vec{g}_P^2) \tag{A.24b}$$

$$\Delta_P \beta_{\kappa_1} = \frac{1}{16\pi^2}[-24\vec{g}_P^2] + 24\kappa_1 \vec{g}_P^2 \tag{A.24c}$$

$$\Delta_P \beta_{\kappa_2} = \frac{1}{16\pi^2}[-24\vec{g}_P^2] + 24\kappa_1 \vec{g}_P^2 \tag{A.24d}$$

with $T_P^+ = \vec{g}_P^T(\bar{Y}_{\underline{Q}}^{+2} + \bar{Y}_{\underline{Q}}^{-2})\vec{g}_P$ and $T_P^- = \vec{g}_P^T(\bar{Y}_{\underline{Q}}^{+2} - \bar{Y}_{\underline{Q}}^{-2})\vec{g}_P$, and since the isosinglet is colored and carries $U(1)$-charge,

$$\Delta_P \beta_{g_1} = \frac{16}{9}\frac{g_3^2}{16\pi^2} \tag{A.24e}$$

*Appendix A  Renormalization Group Functions*

$$\Delta_P \beta_{g_3} = \frac{2}{3} \frac{g_3^2}{16\pi^2} \tag{A.24f}$$

And the beta-function for $g_P$ is

$$g_P = \frac{1}{16\pi^2} \left[ g_P{}^i (8\vec{g_P}^2 - \frac{17}{12}g_1^2 - \frac{9}{8}g_2^2 - 8g_3^2) + \left( (\bar{Y}_{\underline{Q}}^{+2} + \bar{Y}_{\underline{Q}}^{-2})\vec{g_P} \right)^i - \frac{1}{2}\vec{g_P}^2 g_P{}^i \right] \tag{A.25}$$

# Acknowledgements

# Appendix B

# Bibliography

[1] CMS Collaboration, S. Chatrchyan *et al.*, Phys.Lett. **B716**, 30 (2012), 1207.7235.

[2] ATLAS Collaboration, G. Aad *et al.*, Phys.Lett. **B716**, 1 (2012), 1207.7214.

[3] Particle Data Group, K. Nakamura *et al.*, J.Phys. **G37**, 075021 (2010).

[4] R. Mohapatra and P. Pal, World Sci.Lect.Notes Phys. **60**, 1 (1998).

[5] T. Asaka, S. Blanchet, and M. Shaposhnikov, Phys.Lett. **B631**, 151 (2005), hep-ph/0503065.

[6] M. Holthausen, M. Lindner, and M. A. Schmidt, Phys.Rev. **D82**, 055002 (2010), 0911.0710.

[7] M. Sher, Phys.Rept. **179**, 273 (1989).

[8] K. A. Meissner and H. Nicolai, Phys.Lett. **B648**, 312 (2007), hep-th/0612165.

[9] K. A. Meissner and H. Nicolai, Phys.Lett. **B660**, 260 (2008), 0710.2840.

[10] K. A. Meissner and H. Nicolai, Phys.Rev. **D80**, 086005 (2009), 0907.3298.

[11] J. C. Pati and A. Salam, Phys.Rev. **D10**, 275 (1974).

[12] R. Mohapatra and J. C. Pati, Phys.Rev. **D11**, 2558 (1975).

[13] G. Senjanovic and R. N. Mohapatra, Phys.Rev. **D12**, 1502 (1975).

[14] N. Deshpande, J. Gunion, B. Kayser, and F. I. Olness, Phys.Rev. **D44**, 837 (1991).

[15] E. Gildener and S. Weinberg, Phys.Rev. **D13**, 3333 (1976).

[16] S. R. Coleman and E. J. Weinberg, Phys.Rev. **D7**, 1888 (1973).

[17] Y. Zhang, H. An, X. Ji, and R. N. Mohapatra, Nucl.Phys. **B802**, 247 (2008), 0712.4218.

[18] A. Maiezza, M. Nemevsek, F. Nesti, and G. Senjanovic, Phys.Rev. **D82**, 055022 (2010), 1005.5160.

[19] ATLAS Collaboration, G. Aad *et al.*, Eur.Phys.J. **C72**, 2056 (2012), 1203.5420.

[20] CMS Collaboration, S. Chatrchyan *et al.*, Phys.Rev.Lett. **109**, 261802 (2012), 1210.2402.

[21] G. Degrassi *et al.*, JHEP **1208**, 098 (2012), 1205.6497.

[22] W. Rodejohann and H. Zhang, JHEP **1206**, 022 (2012), 1203.3825.

[23] I. Masina, (2012), 1209.0393.

[24] A. Hebecker, A. K. Knochel, and T. Weigand, JHEP **1206**, 093 (2012), 1204.2551.

[25] M. Holthausen, Conformal Symmertry in the Minimal Left-Right Symmetric Model, Diplomarbeit, Ruprecht-Karls-Universität Heidelberg, 2009.

[26] R. Barbieri and G. Giudice, Nucl.Phys. **B306**, 63 (1988).

[27] K. Kannike, Eur.Phys.J. **C72**, 2093 (2012), 1205.3781.

[28] S. R. Coleman, Phys.Rev. **D15**, 2929 (1977).

[29] G. Isidori, G. Ridolfi, and A. Strumia, Nucl.Phys. **B609**, 387 (2001), hep-ph/0104016.

[30] J. Espinosa and M. Quiros, Phys.Lett. **B353**, 257 (1995), hep-ph/9504241.

[31] G. Passarino and M. Veltman, Nucl.Phys. **B160**, 151 (1979).

[32] A. Denner, Fortsch.Phys. **41**, 307 (1993), 0709.1075.

[33] S. Rajpoot, Mod.Phys.Lett. **A2**, 307 (1987).

[34] D. Chang and R. N. Mohapatra, Phys.Rev.Lett. **58**, 1600 (1987).

[35] K. Babu and X. He, Mod.Phys.Lett. **A4**, 61 (1989).

[36] M. E. Peskin and D. V. Schroeder, (1995).

[37] I. Rothstein, Nucl.Phys. **B358**, 181 (1991).

[38] S. Antusch, M. Drees, J. Kersten, M. Lindner, and M. Ratz, Phys.Lett. **B519**, 238 (2001), hep-ph/0108005.

Erklärung:

Ich versichere, dass ich diese Arbeit selbstständig verfasst habe und keine anderen als die angegebenen Quellen und Hilfsmittel benutzt habe.

Heidelberg, den (Datum) . . . . . . . . . . . . . . . . . . . . . . . . . . . . . . . . . . . . . .